TTI-2-10-69-140-8

TEXAS
TRANSPORTATION
INSTITUTE

TEXAS
HIGHWAY
DEPARTMENT

COOPERATIVE
RESEARCH

IMPACT PERFORMANCE AND A SELECTION CRITERION FOR TEXAS MEDIAN BARRIERS

in cooperation with the
Department of Transportation
Federal Highway Administration

RESEARCH REPORT 140-8
STUDY 2-10-69-140
EVALUATION OF THE ROADWAY ENVIRONMENT

TECHN[...] AG[...]

1. Report No.

2. Government Accession No.

3. Re[...]

4. Title and Subtitle
IMPACT PERFORMANCE AND A SELECTION CRITERION FOR TEXAS MEDIAN BARRIERS

5. Report Date
April, 1974

6. Performing Organization Code

7. Author(s)
Hayes E. Ross, Jr.

8. Performing Organization Report No.
Research Report 140-8

9. Performing Organization Name and Address
Texas Transportation Institute
Texas A&M Unicersity
College Station, Texas 77840

10. Work Unit No.

11. Contract or Grant No.
Study No. 2-10-69-140

12. Sponsoring Agency Name and Address
Texas Highway Department
11th and Brazos
Austin, Texas 78701

13. Type of Report and Period Covered
Interim - September, 1968
April, 1974

14. Sponsoring Agency Code

15. Supplementary Notes
Research completed in cooperation with DOT, FHWA.
Study Title: "Evaluation of the Roadway Environment by Dynamic Analysis of the Interaction Between the Vehicle, Passenger, and the Roadway"

16. Abstract
The impact performance of the Texas Metal Beam Guard Fence median barrier (MBGF) was determined and compared with that of the Texas Concrete Median Barrier (CMB). The MBGF consists of two standard W-shaped guardrails mounted back-to-back on a 6 WF 8.5 support post whereas the CMB is a solid concrete barrier.

The impact performance of the MBGF was determined from a combination of crash tests and from crash simulations by the Highway-Vehicle-Object-Simulation-Model (HVOSM). Full-size automobiles (approximately 4,000 lb) were used in both the crash tests and the crash simulations. A close comparison of test and simulated results verified the accuracy of the HVOSM in simulating impacts with the MBGF. The impact performance of the CMB was obtained from another study.

Inspections of 135 median barrier impacts on various urban freeways in Texas were made to determine the distribution of impact angles. These field measurements, supplemented by data from the HVOSM, provided impact angle probabilities as a function of median widths.

The final product of this study was a selection criterion which provides an objective means of comparing the impact severity of the MBGF and the CMB as a function of the median's dimensions. The criterion is based on a design speed of 60 mph, and impacts with a full-size automobile.

17. Key Words
Median Barriers, Crash Tests, Math Simulations, Warrants, Impact Angles, Impact Severity.

18. Distribution Statement

19. Security Classif. (of this report)	20. Security Classif. (of this page)	21. No. of Pages	22. Price
Unclassified	Unclassified	129	

Form DOT F 1700.7 (8-69)

IMPACT PERFORMANCE AND A SELECTION CRITERION FOR TEXAS MEDIAN BARRIERS

by

Hayes E. Ross, Jr.
Associate Research Engineer

Research Report 140-8

Evaluation of the Roadway Environment by
Dynamic Analysis of the Interaction
Between the Vehicle, Passenger,
and the Roadway

Research Study No. 2-10-69-140

Sponsored by

The Texas Highway Department
in cooperation with the
U.S. Department of Transportation, Federal Highway Administration

April 1974

Texas Transportation Institute
Texas A&M University
College Station, Texas

DISCLAIMER

The contents of this report reflect the views of the author who is responsible for the facts and the accuracy of the data presented herein. The contents do not necessarily reflect the official views or policies of the Federal Highway Administration. This report does not constitute a standard, specification, or regulation.

KEY WORDS

Median Barriers, Crash Tests, Math Simulations, Warrants, Impact Angles, Impact Severity.

FOREWORD

The information contained herein was developed on Research Study 2-5-69-140 entitled "Evaluation of the Roadside Environment by Dynamic Analysis of the Interaction Between the Vehicle, Passenger, and Roadway." It is a cooperative research study sponsored jointly by the Texas Highway Department and the U.S. Department of Transportation, Federal Highway Administration.

The basic objective of the study is to develop criteria to aid in the design of a safe highway. This is being accomplished through the application of mathematical simulation techniques and crash tests to determine the dynamic behavior of automobiles and their occupants when in collision with roadside objects or when traversing highway geometric features such as ditches, sloping culvert grates, etc. The study began in September, 1968.

Several significant findings have resulted form the study and these are documented in the following reports:

1. "Documentation of Input for Single Vehicle Accident Computer Program", Young, R.D., et.al., TTI Research Report 140-1, July 1969.

2. "A Three-Dimensional Mathematical Model of an Automobile Passenger", Young, R.D., TTI Research Report 140-2, August 1970.

3. "Criteria for the Design of Safe Sloping Culvert Grates", Ross, H. E., Jr., and Post, E. R., TTI Research Report 140-3, August 1971.

4. "Criteria for Guardrail Need and Location on Embankments", Ross, H. E., Jr., and Post, E. R., TTI Research Report 140-4, April 1972.

5. "Simulation of Vehicle Impact with the Texas Concrete Median Barrier", Young, R.D., et. al., TTI Research Report 140-5, June 1972.

6. "Dynamic Behavior of a Vehicle Traversing Selected Curbs and Medians", Ross, H.E., Jr., and Post, E.R., TTI Research Report 140-6, December 1974.

7. "Comparison of Full-Scale Embankment Tests with Computer Simulations", Ross, H.E., Jr., and Post, E.R., TTI Research Report 140-7, December 1972.

SUMMARY

This study involved the determination of the impact performance of the Texas Metal Beam Guard Fence median barrier (MBGF) and a comparison of its performance with that of the Texas Concerete Median Barrier (CMB). The MBGF consists of two standard W-shaped guardrails mounted back-to-back on a 6 WF 8.5 support post whereas the CMB is a solid concrete barrier.

The impact performance of the MBGF was determined from a combination of crash tests and from crash simulations by the Highway-Vehicle-Object-Simulation-Model (HVOSM). Full-size automobiles (approximately 4,000 lb) were used in both the crash tests and the crash simulations. A close comparison of test and simulated results verified the accuracy of the HVOSM in simulating impacts with the MBGF. The impact performance of the CMB was obtained from another study.

Inspections of 135 median barrier impacts on various urban freeways in Texas were made to determine the distribution of impact angles. These field measurements, supplemented by data from the HVOSM, provided impact angle probabilities as a function of median widths.

The final product of this study was a selection criterion which provides an objective means of comparing the impact severity of the MBGF and the CMB as a function of the median's dimensions. The criterion is based on a design speed of 60 mph, and impacts with a full-size automobile.

IMPLEMENTATION STATEMENT

The results of this study have been used by the Texas Highway Department to establish a policy on the selection of median barriers. This policy will appear in the next publication of the Highway Design Division Operations and Procedures Manual.

The following excerpt, taken from Section 4-302, page 4-93 and 4-94 of the Manual, pertains to median barrier warrants.

> "Medians for urban freeway sections generally are non-depressed and relatively narrow. For new construction, an urban freeway usually includes a 24 foot flush median (see Section 4-301.8 (g)) with either slope faced concrete or double steel beam median barrier. In determining the type of barrier to be used for any project, the primary consideration is safety, both for vehicular impacts and during any subsequent maintenance activities. In this regard, extensive live and simulated crash testing of the two most prominently used median barriers have been conducted, and measurements were made at accident sites to establish frequencies of various angles of encroachment. Analysis of this information indicates that accident severity levels probably will not result in serious injury for unrestrained occupants for the following conditions:
>
> a. For concrete barriers, when installed in median widths of 24 feet (i.e., lateral distance from travel lane edge to centerline of barrier of 12 feet) or less.
>
> b. For double steel beam barriers, when installed in median widths of 30 feet (i.e., lateral distance from travel lane edge to centerline of barrier of 15 feet) or less.
>
> Field experience with concrete median barriers indicates that, unlike the double steel beam system, maintenance operations are not normally required following accidental vehicular encroachment. Accordingly, on new urban freeway sections with narrow medians (18 feet or less), a flexible

median barrier system should not normally be used, since resulting maintenance activities would (a) create unduly hazardous exposure of maintenance crews to high speed and volume traffic, (b) usually necessitate blocking a travel lane thereby significantly disrupting traffic, causing delay, congestion, and a hazardous driving environment, and (c) result in high costs. Therefore, for projects involving new construction or complete reconstruction of a highway section, the determination of median barrier type should be in accordance with the guidelines shown in Figure 4-91A.

Figure 4-91A

Median Width	Barrier Type
Up to 18 feet	Concrete
18 to 24 feet	Concrete or double steel beam
24 to 30 feet	Double steel beam

Where there is a frequent presence of fixed objects such as continuous illumination systems in 18 to 24 foot medians the concrete barrier system offers advantages over double steel beam and should be used. Where the double steel beam barrier system is used, consideration should be given to special design treatments to increase barrier stiffness at fixed object locations. Special circumstances, such as the presence of blowing sand, may dictate deviation from the guidelines shown in Figure 4-91A ..."

ACKNOWLEDGEMENTS

Several people provided valuable input to this study, for which the author is very appreciative. The guidance and suggestions of Mr. John F. Nixon and Mr. Dave Hustace of the Texas Highway Department and Mr. Edward V. Kristaponis of the Federal Highway Administration are acknowledged.

The field data on barrier impacts were collected and synthesized by Mr. Dave Hustace, Mr. Paul Tutt, and other members of Division 10 of the THD. It was reported that measuring skid marks and tire tracks on busy freeways is not a job one should aspire to. Their performance "beyond the call of duty" was appreciated.

Dr. Larry Ringer, Associate Professor of Statistics, Texas A&M University, provided guidance in the statistical analysis of the field data on barrier impacts.

TABLE OF CONTENTS

TABLE OF CONTENTS (cont'd)

LIST OF FIGURES

LIST OF FIGURES (continued)

LIST OF FIGURES (continued)

LIST OF TABLES

I. INTRODUCTION

To prevent median crossover accidents, the Texas Highway Department (THD) uses, in most cases, one of two basic median barriers. These are the concrete median barrier (CMB) and the metal beam guardfence (MBGF). The CMB is for all practical purposes a "rigid" unyielding barrier, while the MBGF is considered to be a "flexible" barrier, one that deforms upon impact.

Several studies have been conducted to determine the impact performance of the CMB (1, 2, 3, 4, 5). It has been shown that for small impact angles the CMB can safely redirect an encroaching vehicle. However, these studies also showed that as the impact angle increases the impact severity increases considerably.

With regard to the MBGF, only a very limited amount of impact performance data existed prior to this study. One of the objectives of this study was therefore to determine its impact performance so that objective comparisons could be made between the CMB and the MBGF. Crash tests and the Texas Transportation Institute's version of the HVOSM* computer program were used to accomplish this objective. Before applying the HVOSM, however, an extensive validation study was performed. Crash test data were compared with the HVOSM predictions. Some modifications were made to the HVOSM in order to achieve an acceptable comparison.

This study also investigated the relationship between median width and the probable angle of impact into a median barrier for errant vehicles.

---

* HVOSM -- Highway-Vehicle-Object-Simulation-Model. Program was developed at CALSPAN Corporation, Buffalo, New York, for the FHWA.

This relationship was needed to develop a selection criterion for the two barrier systems. It has been postulated that the CMB is best for "narrow" medians where high impact angles are improbable and that the MBGF should be used for "wide" medians. However, objective criteria to quantify what "narrow" and "wide" means had to be developed. To accomplish this task, a combination of field measurements and HVOSM computer simulations was used. THD personnel conducted the field measurements. Median barriers on selected urban freeways were inspected for impact damage. Where impacts had occurred, measurements of the angle of impact, median width, etc., were made. These data were then statistically analyzed to determine impact angle probabilities. The HVOSM was used to supplement the field data by defining "upper limits" on impact angles as a function of median widths.

The end result of this study was an objective criterion which can be used in the median barrier selection process. The criterion, which is in the form of a graph, shows the relationship between impact severity and median width, on a probability basis, for the CMB and the MBGF barriers. Other factors, such as installation and maintenance costs, must of course be considered in the selection process. However, an evaluation of these factors was not within the scope of this study.

II. CRASH TESTS OF MBGF

Prior to the tests conducted in this study, only one full-scale crash test had been conducted on the MBGF (3, 4). In that test, an automobile impacted the barrier at 57.3 mph at an encroachment angle of 25 degrees.*

The impact conditions of two tests conducted in this study were 60 mph at 8 degrees, and 63.4 mph at 14.7 degrees. These two tests and the one mentioned above provided considerable insight concerning the impact performance of the MBGF for 60 mph impacts. The tests also provided a data base from which the HVOSM could be validated. After validation, the HVOSM was used to determine the impact performance of the MBGF at speeds below and in excess of 60 mph (see Chapter IV).

This chapter describes the details of the as-tested MBGF, the tests, and the test results.

MBGF Details

The as-tested MBGF barrier is shown in Figure 1. The THD designation of the barrier is MBGF (B)-74. In some installations a 3/8 inch steel wire pedestrian control cable is placed below the guardrail. Also a headlite-barrier fence is sometimes placed on top of the barrier. However, it is assumed that neither of these features will significantly affect the impact performance of the barrier.

---

* That test was denoted "T4-1" in References 3 and 4 and is denoted the same herein.

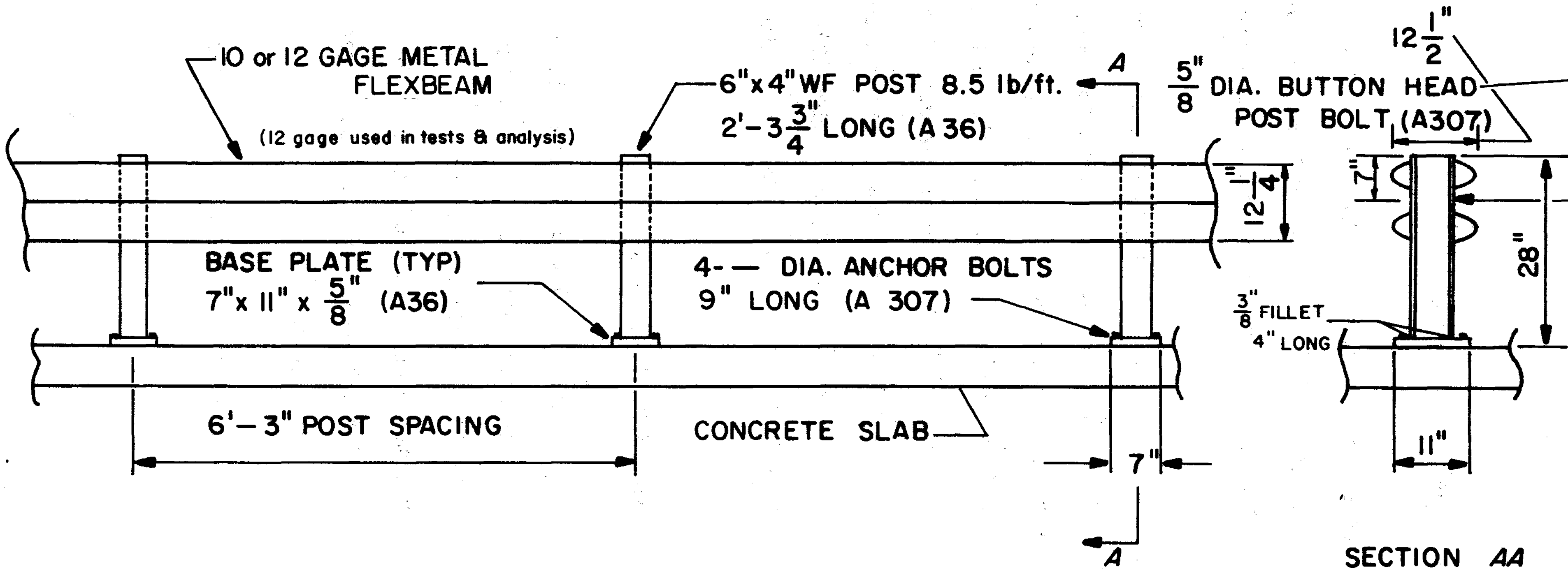

FIGURE 1. TEXAS HIGHWAY DEPT. METAL BEAM GUARD FENCE (BARRIER) MBGF (B) - 74

The MBGF is designed along the "strong beam, weak post" concept. Upon impact the support post breaks away from its base, allowing the back-to-back guardrail to deform. The 3/8 inch fillet welds connecting the outer faces of the two post flanges to the 5/8 inch base plate are designed to fracture at relatively low impact forces. Since the posts shear off at the base at a relatively low impact force, the rail does not rotate significantly, minimizing the possibility of vehicle ramping.

Crash Tests

The two crash tests conducted in the study are referred to herein as MB-1 and MB-2. The MB-1 test refers to the 60 mph/8 degree impact and the MB-2 test refers to the 63.4 mph/14.7 degree impact.

Test vehicles. A 1965 Plymouth, weighing approximately 4200 pounds, was used in Test MB-1. Figure 2 shows the vehicle prior to and after the test. A 1964 Plymouth, weighing approximately 4200 pounds, was used in Test MB-2. Figure 3 shows the vehicle prior to and after the test. Further details of the two test vehicles are given in Appendix A.

Data acquisition. Crash test data were recorded by electronic instrumentation placed in the vehicle and by high speed cameras which photographed the impacts.

Three accelerometers were positioned near the center of gravity of the automobile (see Appendix A for locations). These accelerometers measured the longitudinal, lateral, and vertical accelerations, all with respect to a vehicle-fixed axis. A 50th percentile male dummy was placed in the driver's seat and lap belted. The force in the lap belt during

BEFORE TEST

AFTER TEST

FIGURE 2. MB-I TEST VEHICLE

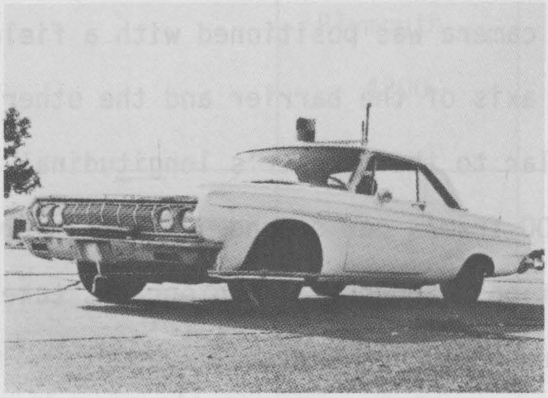

BEFORE TEST

AFTER TEST

FIGURE 3. MB-2 TEST VEHICLE

impact was measured. Also, accelerometers were placed in the dummy's chest to measure accelerations in the fore and aft or longitudinal direction (eyeballs in or out) as well as in the left and right (lateral) direction.

All electronic data were passed through an 80 Hz low-pass active filter for presentation in this report.

One high speed camera was positioned with a field of view parallel to the longitudinal axis of the barrier and the other camera's field of view was perpendicular to the barrier's longitudinal axis. Film speed was approximately 500 frames per second. The film provided a time history of the vehicle's motion. Sequential photographs taken of selected high speed film frames are shown in Chapter III.

Test Results

The results of Tests MB-1 and MB-2 are summarized in Table 1. More detailed results of the tests are given in the next chapter in which the HVOSM is compared with the test results. Vertical accelerations were found to be small in comparison to the longitudinal and lateral accelerations and are therefore not shown herein.

Dummy accelerations and seat belt loads for the two tests are shown in Figures 4 and 5. Peak and average acceleration values are shown in Table 1.

The dynamic performance of the MBGF in these two tests was considered to be good. From a structural standpoint, the barrier contained and redirected the vehicle. From an impact severity standpoint, the

TABLE 1. SUMMARY OF MBGF TESTS

DATA	MB-1		MB-2	
VEHICLE				
Year	1965		1964	
Make	Plymouth		Plymouth	
Weight (lb)	4200		4200	
FILM DATA				
Impact Speed (mph)	60.0		63.4	
Impact Angle (deg)	8.0		14.7	
Dynamic Barrier Deflection (in.)	1.0		12.0	
Departure Angle (deg)	4.0		3.8	
Departure Speed (mph)	47.0		52.0	
ACCELEROMETER DATA	VEHICLE	DUMMY	VEHICLE	DUMMY
Longitudinal				
Peak (G's)	2.0	5.3	5.5	5.4
Highest Average (G's)[1]	0.03	4.2	0.90	4.3
Lateral				
Peak (G's)	5.3	4.0	7.0	8.2
Highest Average (G's)[1]	3.2	2.9	4.7	6.3

[1] Averaged over 50 milliseconds.

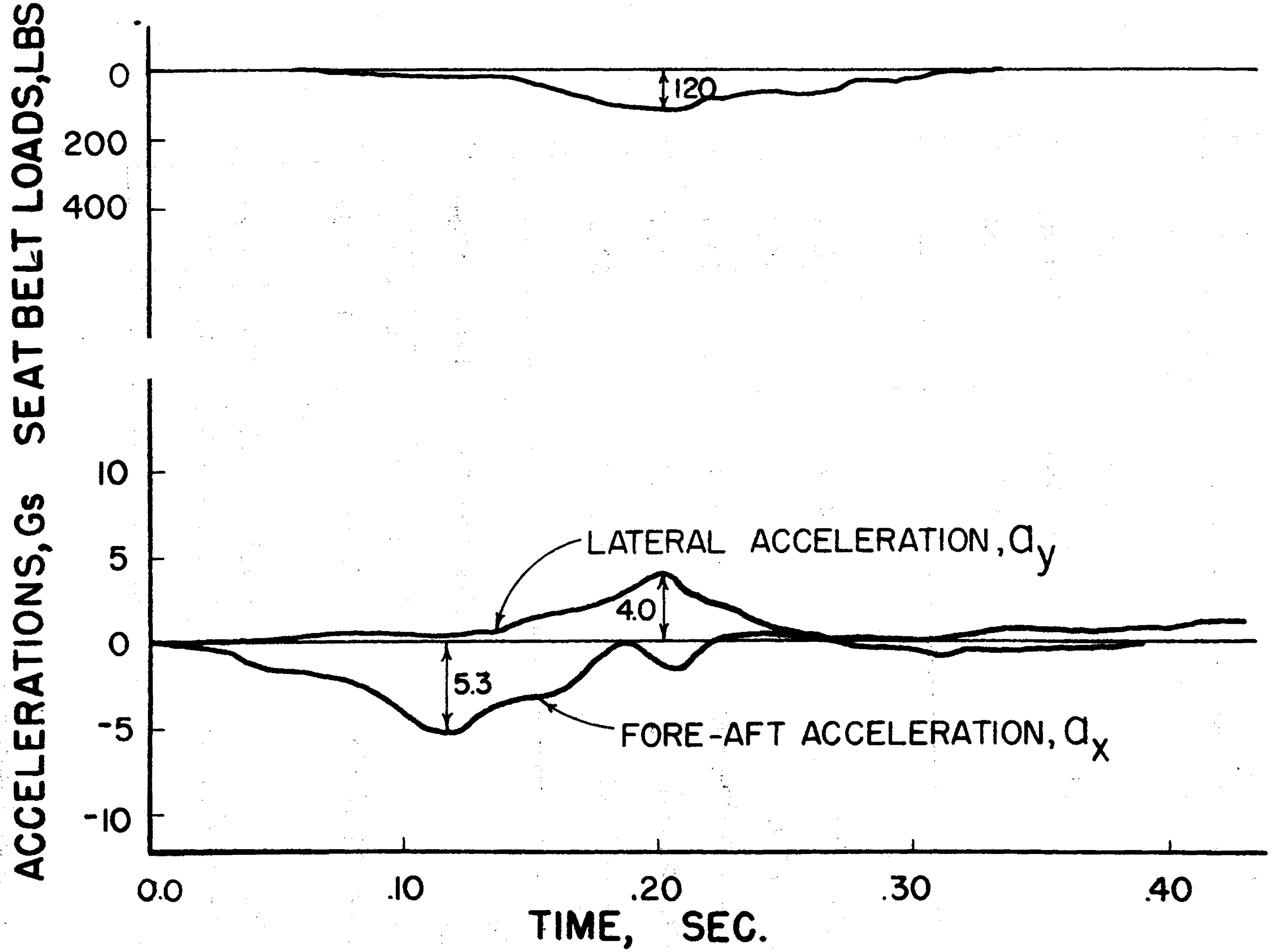

FIG. 4 DUMMY ACCELERATIONS AND SEAT BELT LOADS, MB-1

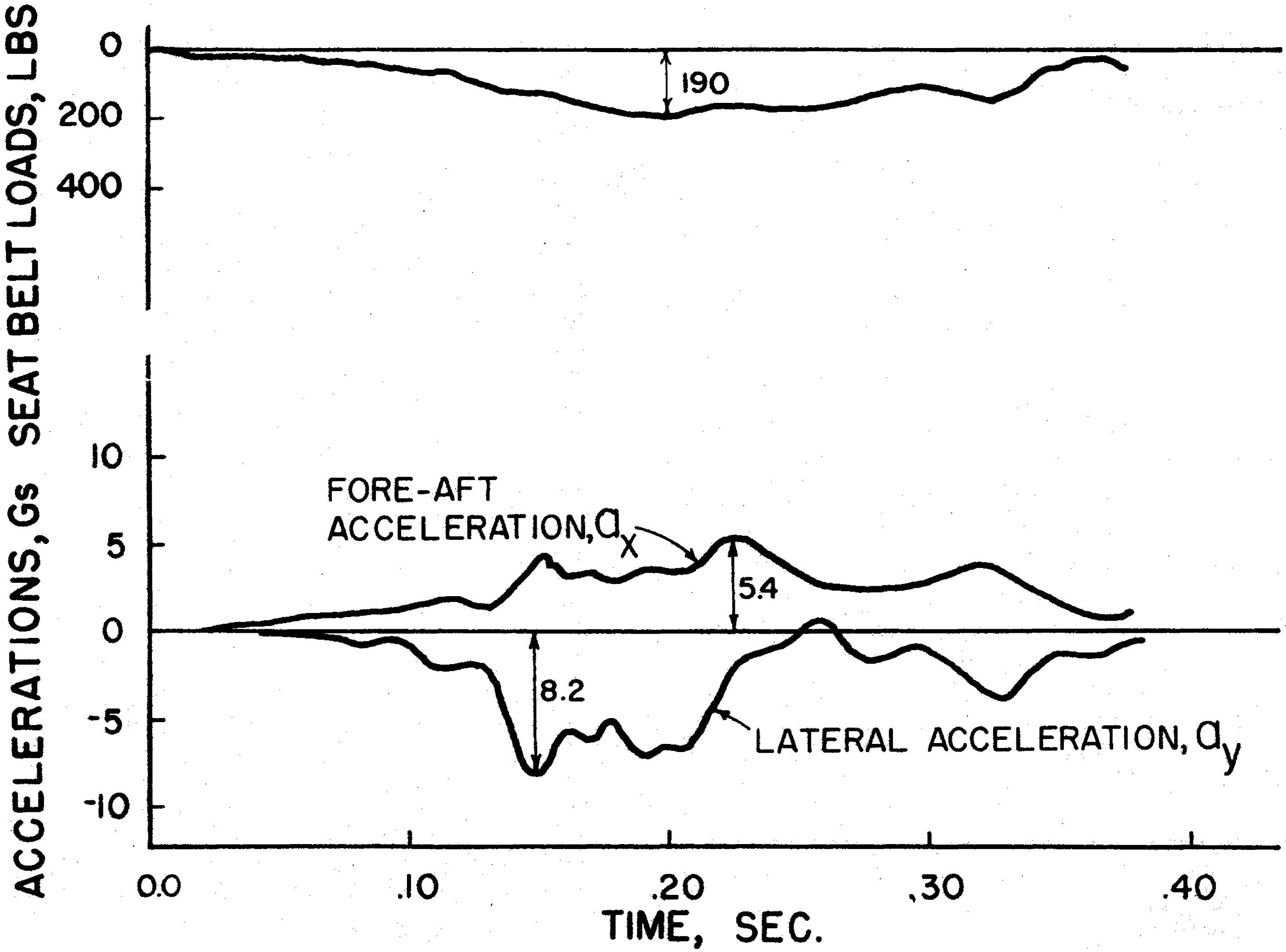

FIG. 5 DUMMY ACCELERATIONS AND SEAT BELT LOADS, MB-2

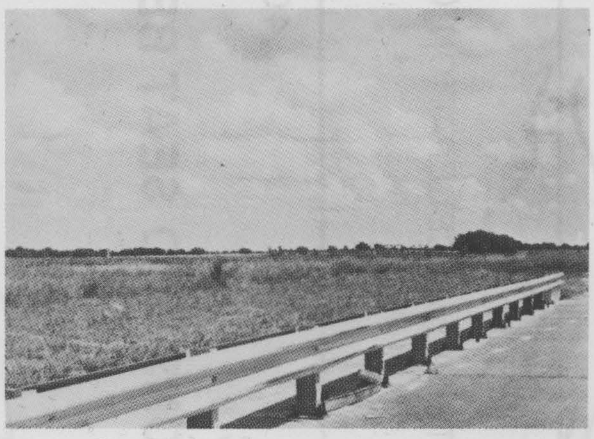

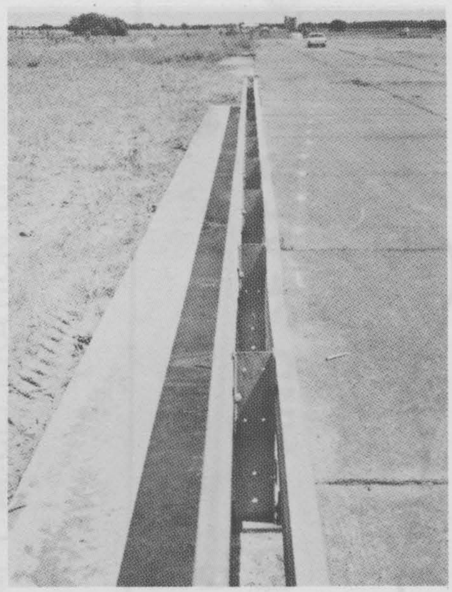

AFTER MB-1 TEST

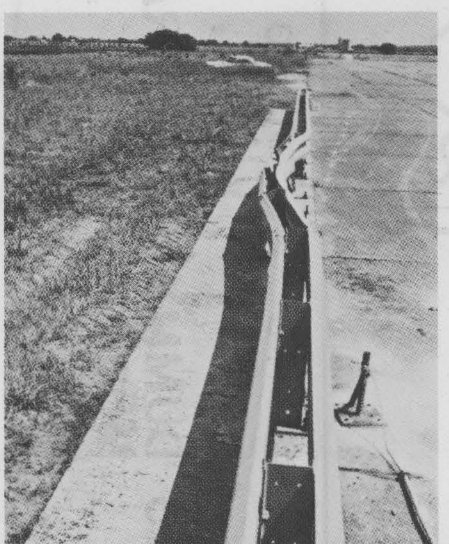

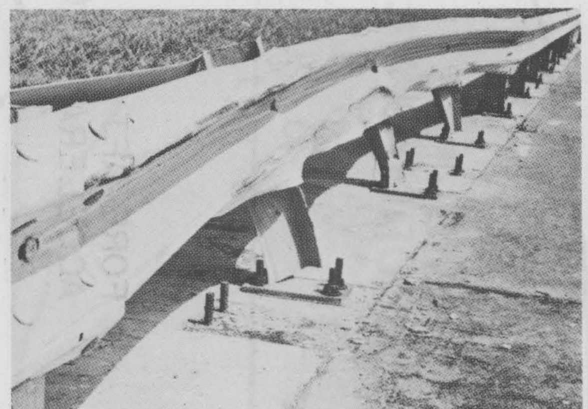

AFTER MB-2 TEST

FIGURE 6. MBGF DAMAGE

accelerations at 7 degrees/60 mph are considered tolerable and no serious injuries are predicted. The impact severity at 15 degrees/60 mph indicates a marginal situation, i.e., the accelerations are near the limits (see Chapter IV) for an unbelted occupant. From a vehicle redirection standpoint, the small departure angles of the two tests are considered to be very good.

Damage to the MBGF after each test is shown in Figure 6. As can be seen, damage to barrier after Test MB-1 was negligible and no repairs are necessary. Repairs to the barrier after Test MB-2 would consist of replacing two 25-foot-W-beam guardrails, three support posts, and the necessary bolts, nuts, etc. Based on previous studies (3), it is estimated that labor and material costs to repair the barrier after the MB-2 test would be $530.00.

Damage to the automobile after each test is shown in Figures 2 and 3. The test car in MB-1 was still operable after the test. However, damage to the left front wheel assembly of the vehicle in Test MB-2 prevented its operation after the impact. It is estimated that the repair costs for the MB-1 vehicle would be $490.00 and that it would cost $1330.00 to repair the MB-2 vehicle. Further discussions of costs are given in Chapter V.

III. VALIDATION OF HVOSM FOR MBGF IMPACT SIMULATIONS

The three full-scale crash tests described in the previous chapter provided impact performance data for the MBGF when impacted by a standard size automobile at approximately 60 mph. It was desirable however, to obtain more data on its performance since impacts in the field could be expected to occur at speeds both below and above 60 mph.

In lieu of additional crash tests (which were not within the budget), it was decided to determine if HVOSM could simulate an automobile impacting the MBGF. To make this determination, the three MBGF crash tests (MB-1, MB-2, and T4-1) were simulated by HVOSM and the results were compared with the test results.

In the initial attempts at simulating the MBGF tests, errors were uncovered in the coding of some of the barrier impact subroutines of HVOSM. These problems and the changes made to the routines to rectify them are discussed in Appendix B.

Validation Process

The validation process actually involved a trial and error procedure. Adjustments were made in the vehicle and barrier stiffness parameters until the HVOSM simulation converged on the results of the MB-2 test. However, these same stiffness parameters were used in the simulation of the other two tests (MB-1 and T4-1) and the resulting comparisons were very good. With the exception of the coefficient of friction between the vehicle and the barrier, it was not necessary to adjust parameters in each test simulation. As a consequence, it was felt that these parameters could be used in HVOSM to simulate impacts with the MBGF at speeds above and below 60 mph.

With regard to the vehicle-barrier friction coefficient, it was found that its value had to be adjusted upward as the angle of impact increased. The reason this adjustment was needed is believed to be as follows. The HVOSM barrier impact subroutines cannot directly account for the effects of a barrier "pocketing" a vehicle. During impacts with the MBGF at relatively large impact angles, a vehicle will deflect the rail considerably but this deflection will occur over a reasonably short length of the rail. For example, in Test T4-1 (57.3 mph/25 degrees), the vehicle deflected the rail 18 inches. However, the deflection occurred over only about 25 feet of the rail. As a result, the barrier tends to pocket the vehicle. The effects of pocketing on vehicle behavior are primarily two-fold: (1) it increases the longitudinal impact force (vehicle axis system) and (2) it decreases the rate at which the vehicle is redirected (yaw rate), at least during the initial phases of the impact. It was found that these effects could be simulated by HVOSM by increasing the vehicle-barrier friction coefficient.

The procedure used to converge on the vehicle and barrier parameters and the value of the parameters themselves are given in Appendix B.

Comparisons Between HVOSM and Tests

Comparisons between HVOSM and the test results were based on two basic types of data. These were accelerations at the vehicle's center of gravity (C.G.) and vehicle motion.

Vehicle motion comparisons. Figures 7, 8, and 9 contain comparisons of vehicle motion for the three tests. The HVOSM perspective drawings were generated by a computer program (6) whose input is the HVOSM output. Hidden lines were removed from the perspective drawings by hand for clarity. The test photos are prints made from selected high speed film frames. It can be seen that the general motion of the HVOSM compares well with the test results. Note that the automobile does not roll appreciably after impact with the MBGF.

Figures 10, 11, and 12 show the path of the vehicle after impact with the MBGF. Very close correlation occurred between HVOSM and the test results for tests MB-1 and MB-2. In test T4-1, considerable damage was done to the left front tire assembly, causing the vehicle to turn more to the left after impact than did the HVOSM (which cannot simulate such a failure).

Acceleration comparisons. Plots of acceleration versus time for the three MBGF tests are shown in Figures 13 through 18. Also shown on each plot are the corresponding HVOSM accelerations. Accelerations in the vertical direction were small in comparison to the lateral and longitudinal components and were therefore omitted from consideration.

In tests MB-1 and MB-2 the accelerometers were located at the C.G. of the vehicle. Location of the accelerometers are given in Appendix A. Longitudinal accelerations refer to the fore-aft direction of the vehicle and lateral accelerations refer to the left-right direction of the vehicle.

In test T4-1 the accelerometers were located on the frame members, near the rear axle. Their position is given in Appendix A. Due to a malfunction, the lateral accelerations in test T4-1 were not recorded.

TEST HVOSM

SEC. 0.000

SEC. .050

SEC. .100

FIGURE 7. TEST VERSUS HVOSM, TEST MB-1
(60 mph/8 degrees)

TEST HVOSM

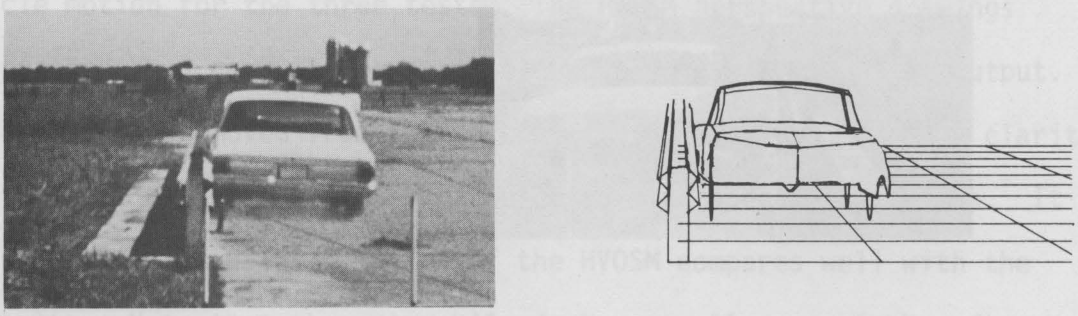

SEC. .150

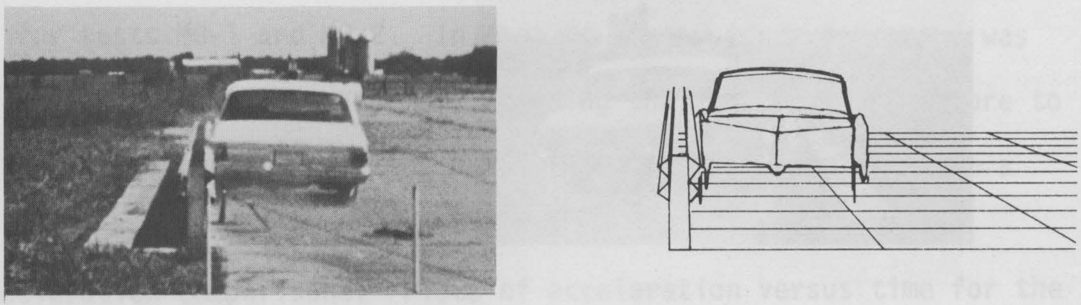

SEC. .200

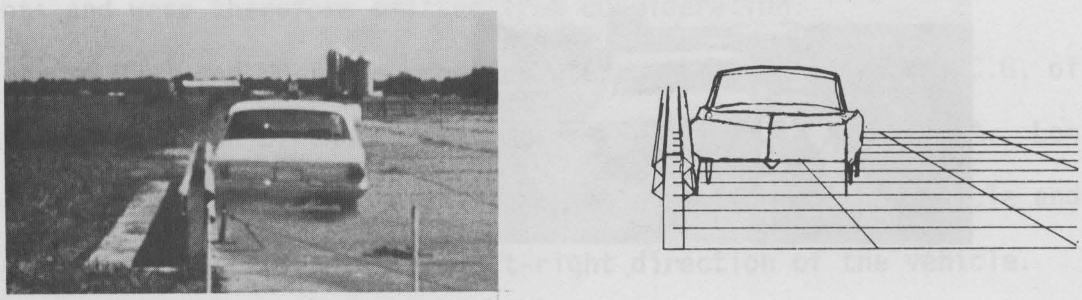

SEC. .250

FIGURE 7. CONTINUED

TEST HVOSM

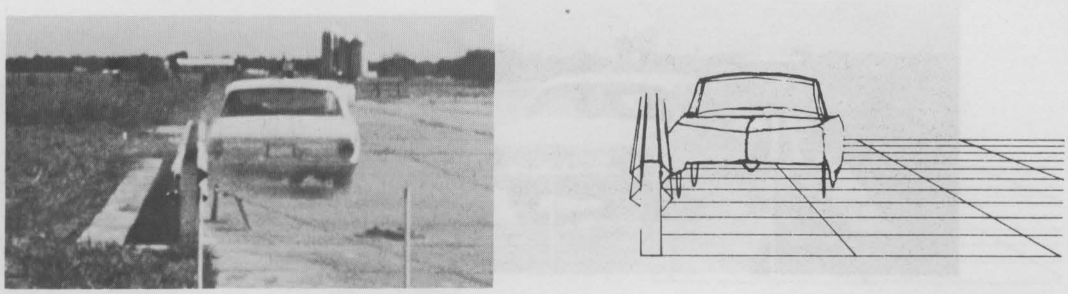

SEC. .300

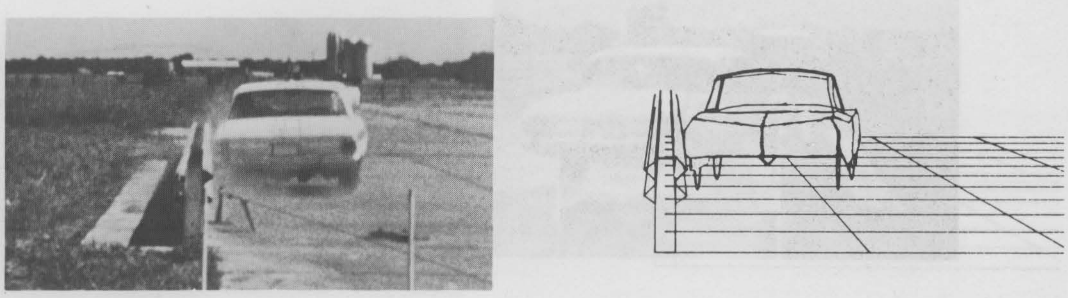

SEC. .350

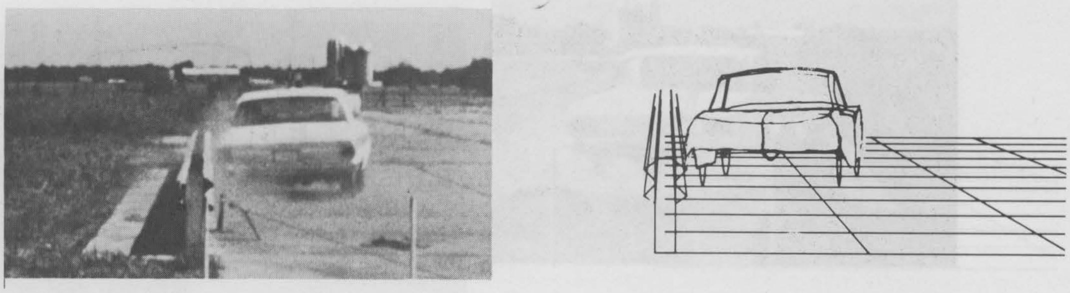

SEC. .400

FIGURE 7. CONCLUDED

TEST HVOSM


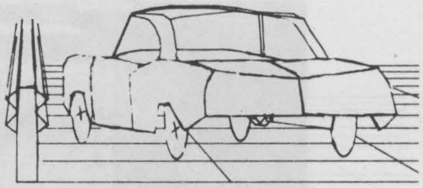

SEC. 0.000


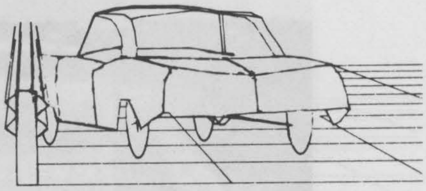

SEC. .050

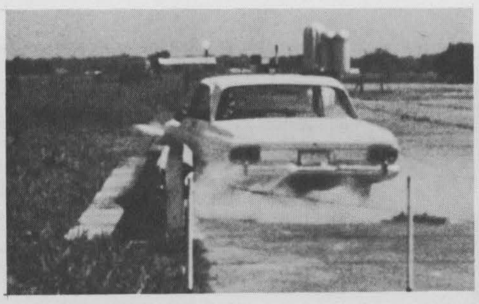
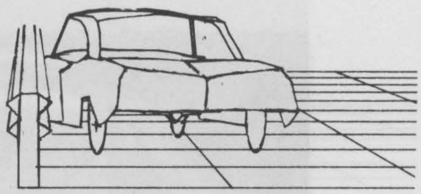

SEC. .100

FIGURE 8. TEST VERSUS HVOSM, TEST MB-2
(63.4 mph/14.7 degrees)

TEST HVOSM


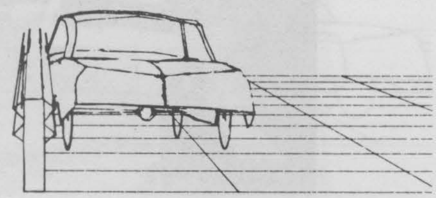

SEC. .150


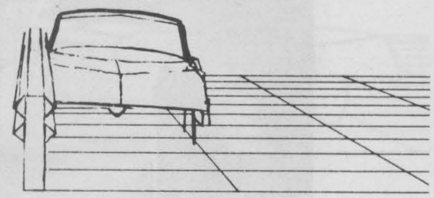

SEC. .200


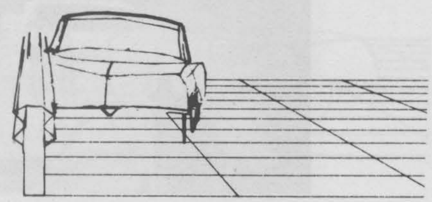

SEC. .250

FIGURE 8. CONTINUED

TEST HVOSM

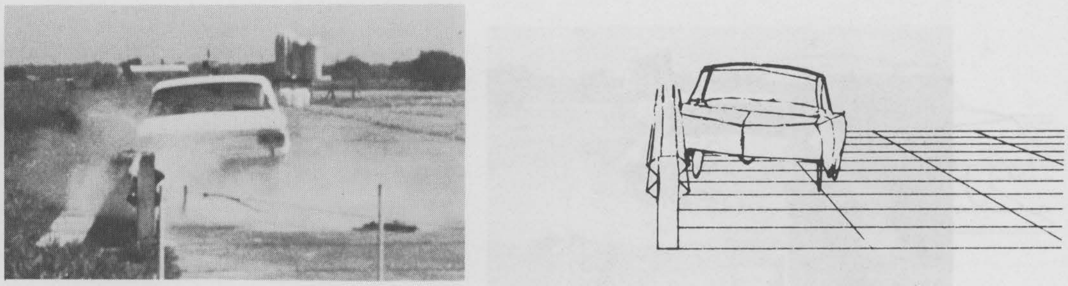

SEC. .300

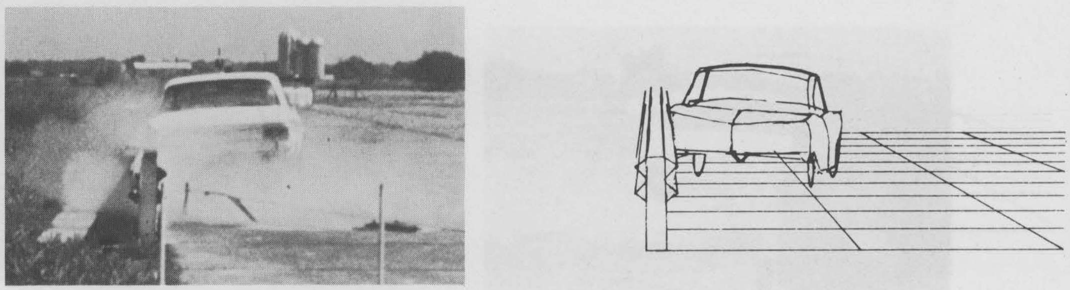

SEC. .350

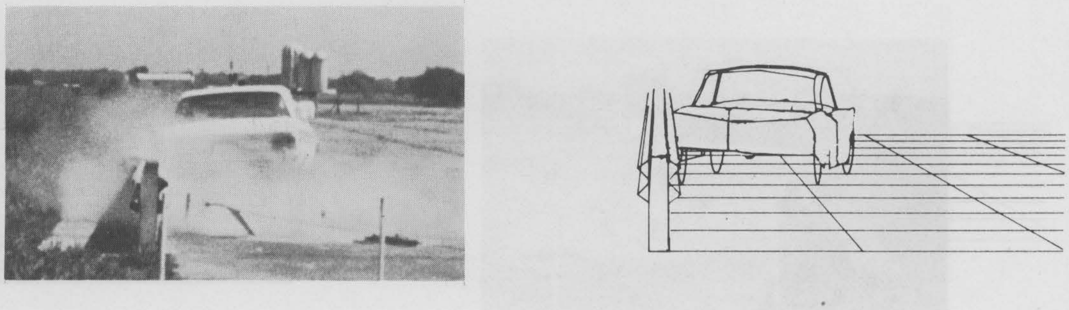

SEC. .400

FIGURE 8. CONCLUDED

TEST HVOSM

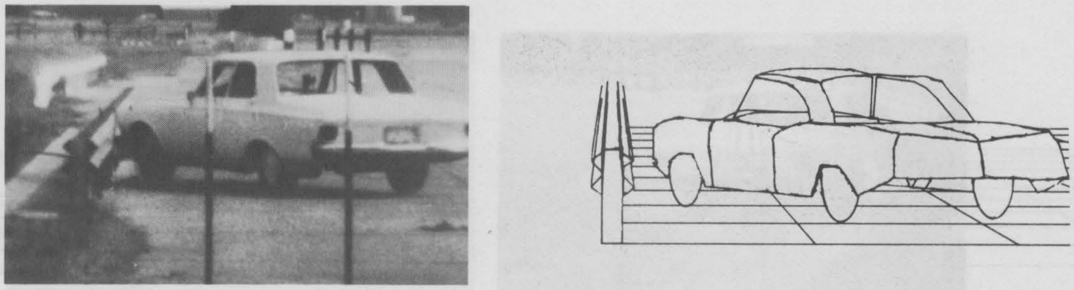

SEC. 0.000

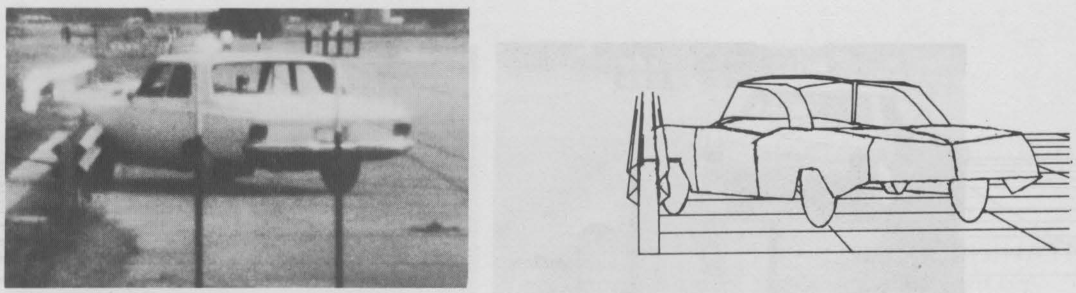

SEC. .050

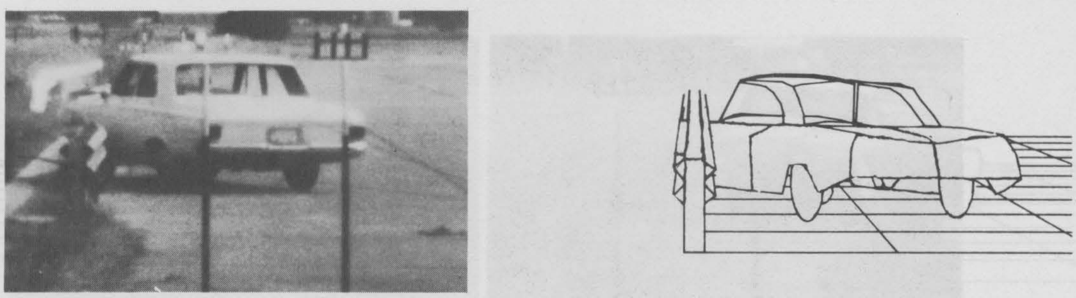

SEC. .100

FIGURE 9. TEST VERSUS HVOSM, TEST T4-1
(57.3 mph/25 degrees)

TEST HVOSM

SEC. .150

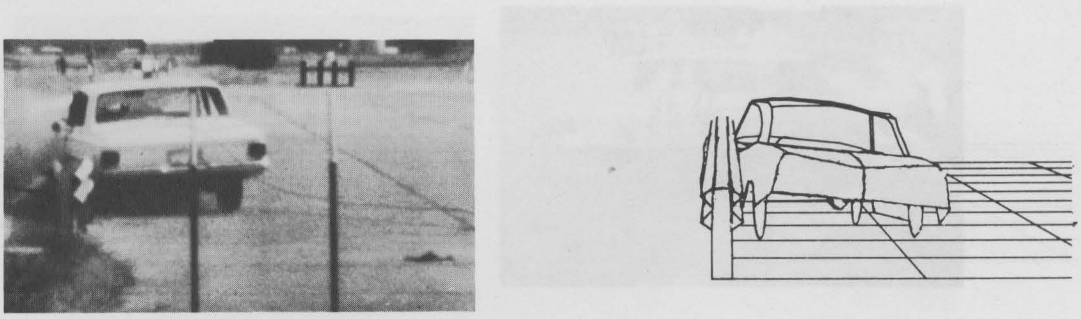

SEC. .200

SEC. .250

FIGURE 9. CONTINUED

TEST HVOSM

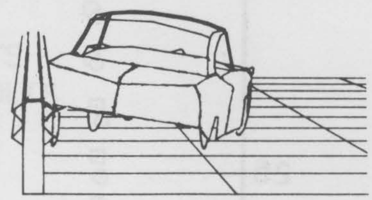

SEC. .300

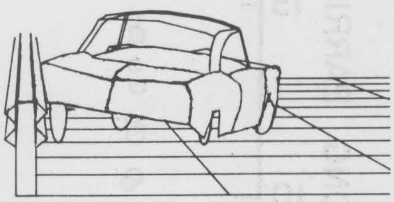

SEC. .350

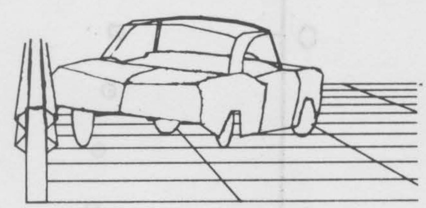

SEC. .400

FIGURE 9. CONCLUDED

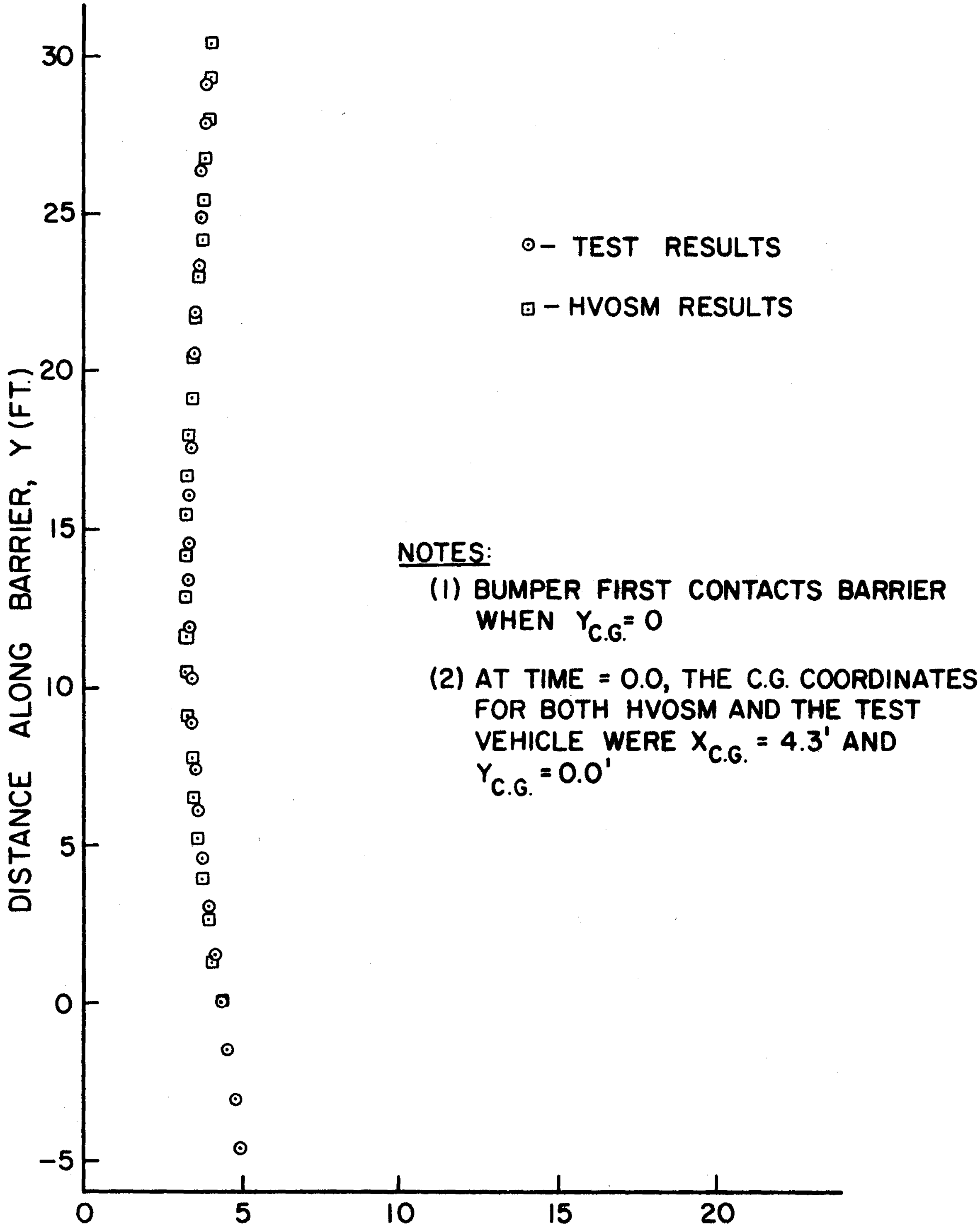

FIGURE 10. C.G. PLOT, TEST MB-1, 60 MPH / 8 DEGREES

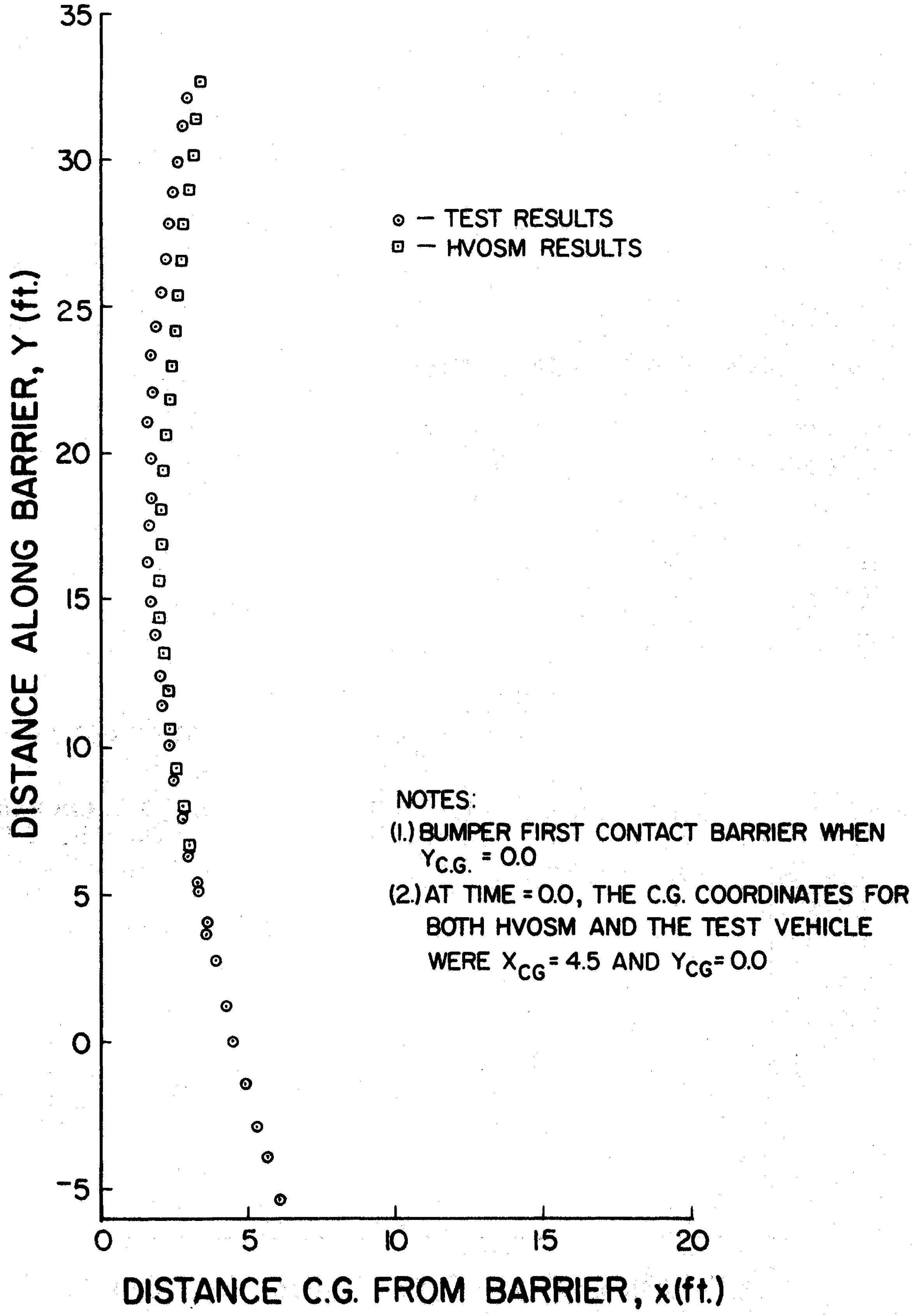

FIGURE 11. C.G. PLOT, TEST MB-2, 63.4 MPH/ 14.7 DEGREES

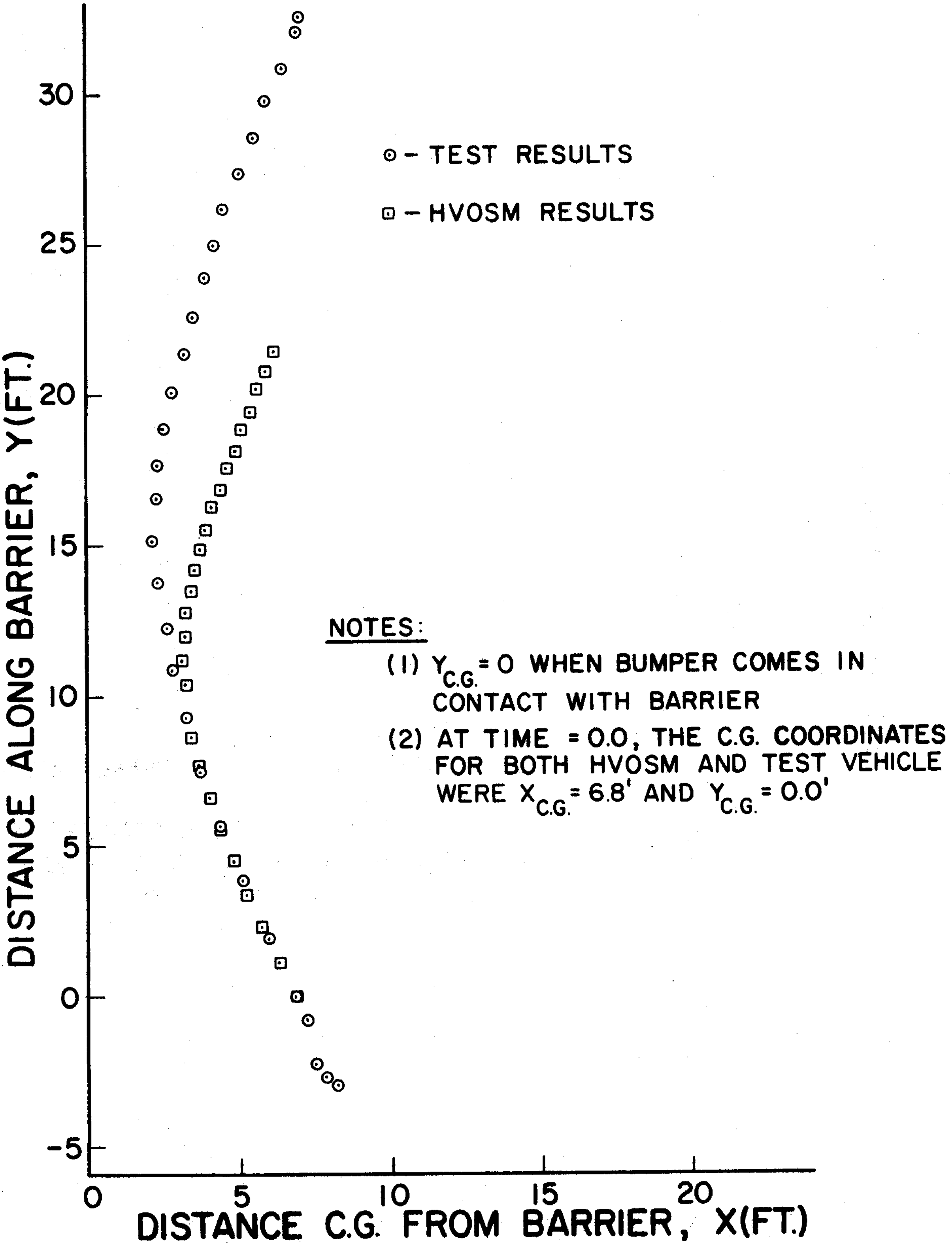

FIGURE 12. C.G. PLOT, TEST T4-1, 57.3 MPH / 25 DEGREE

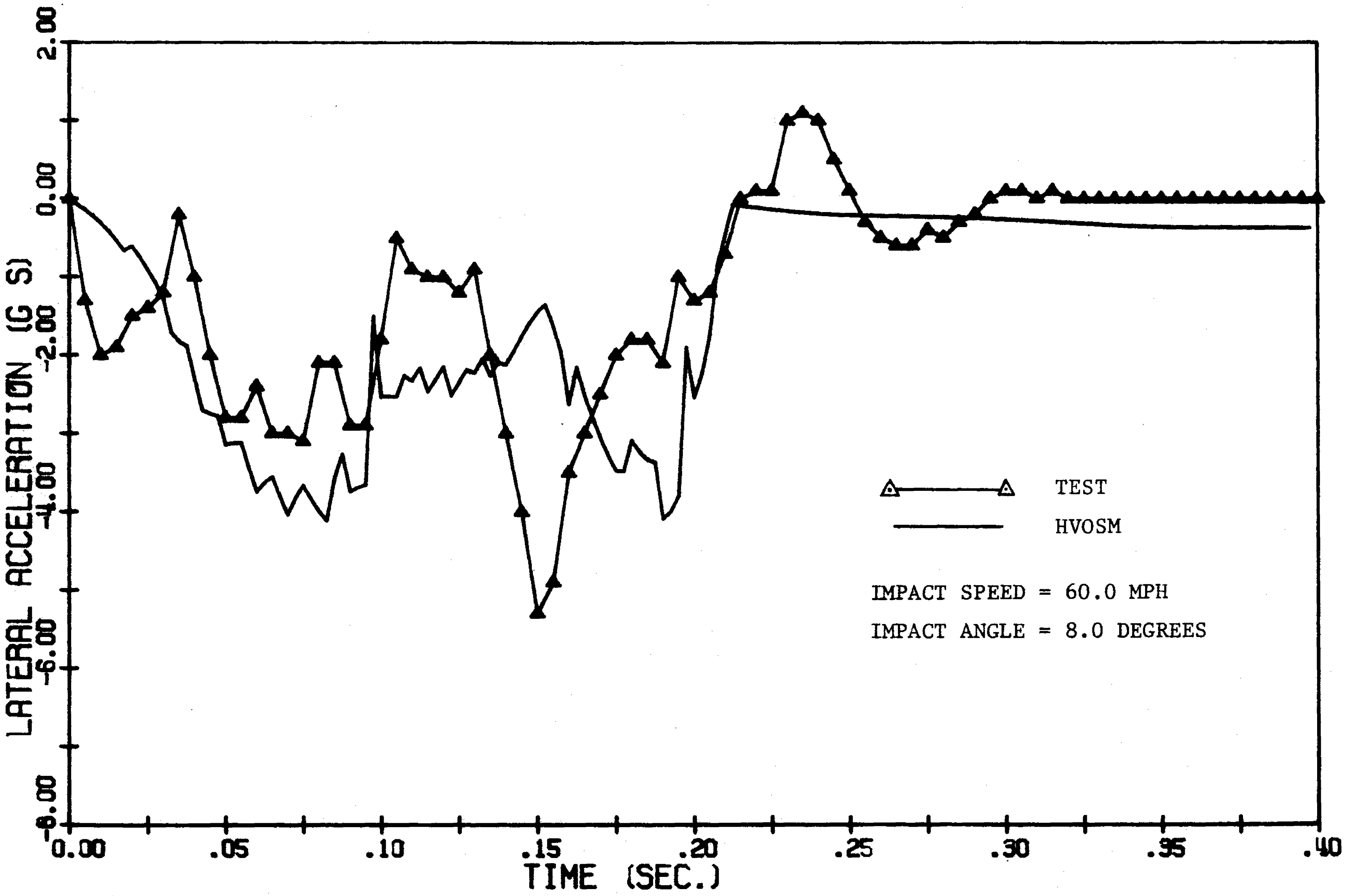

FIGURE 13. LATERAL ACCELERATION, TEST MB-1

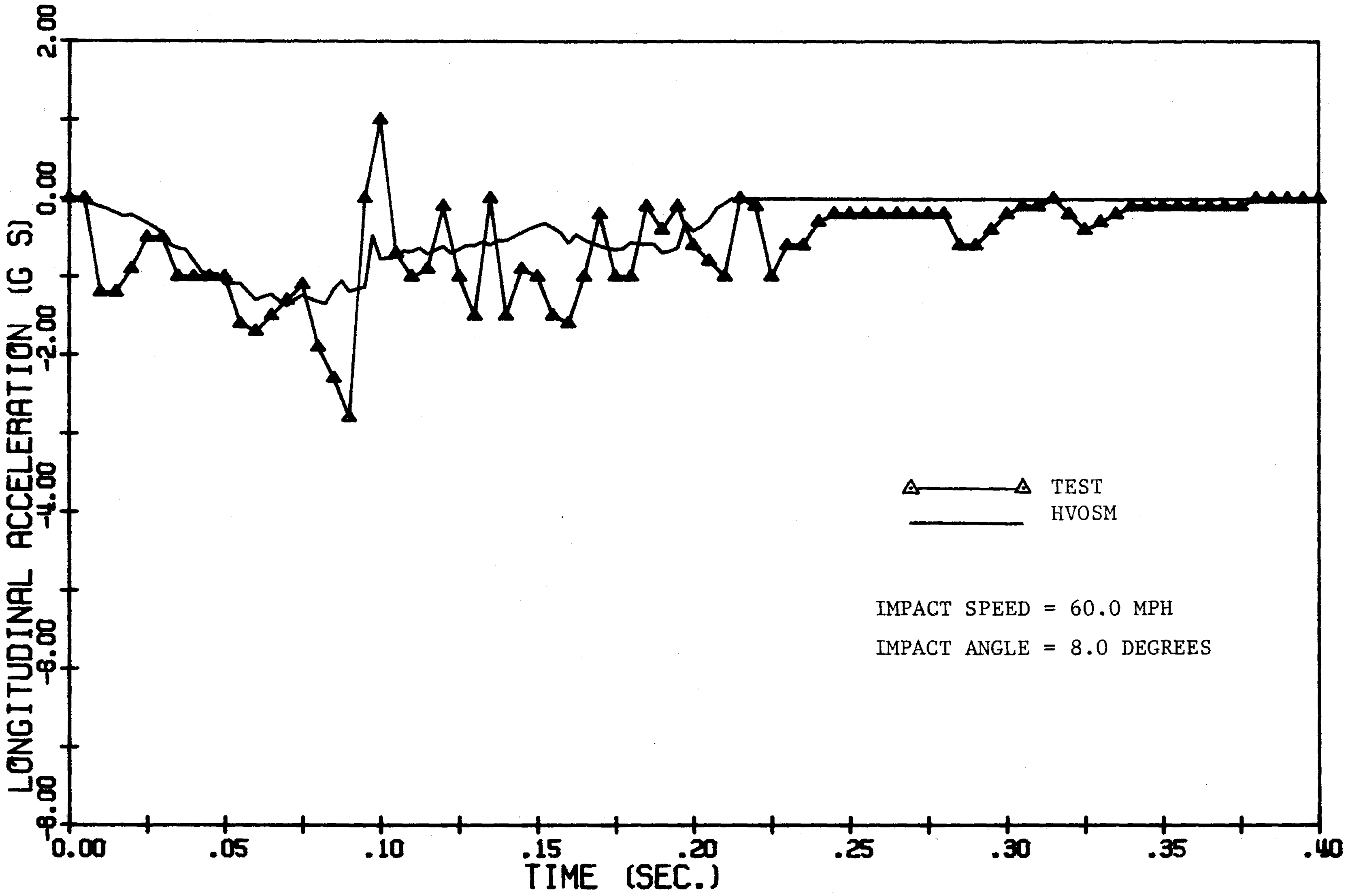

FIGURE 14. LONGITUDINAL ACCELERATION, TEST MB-1

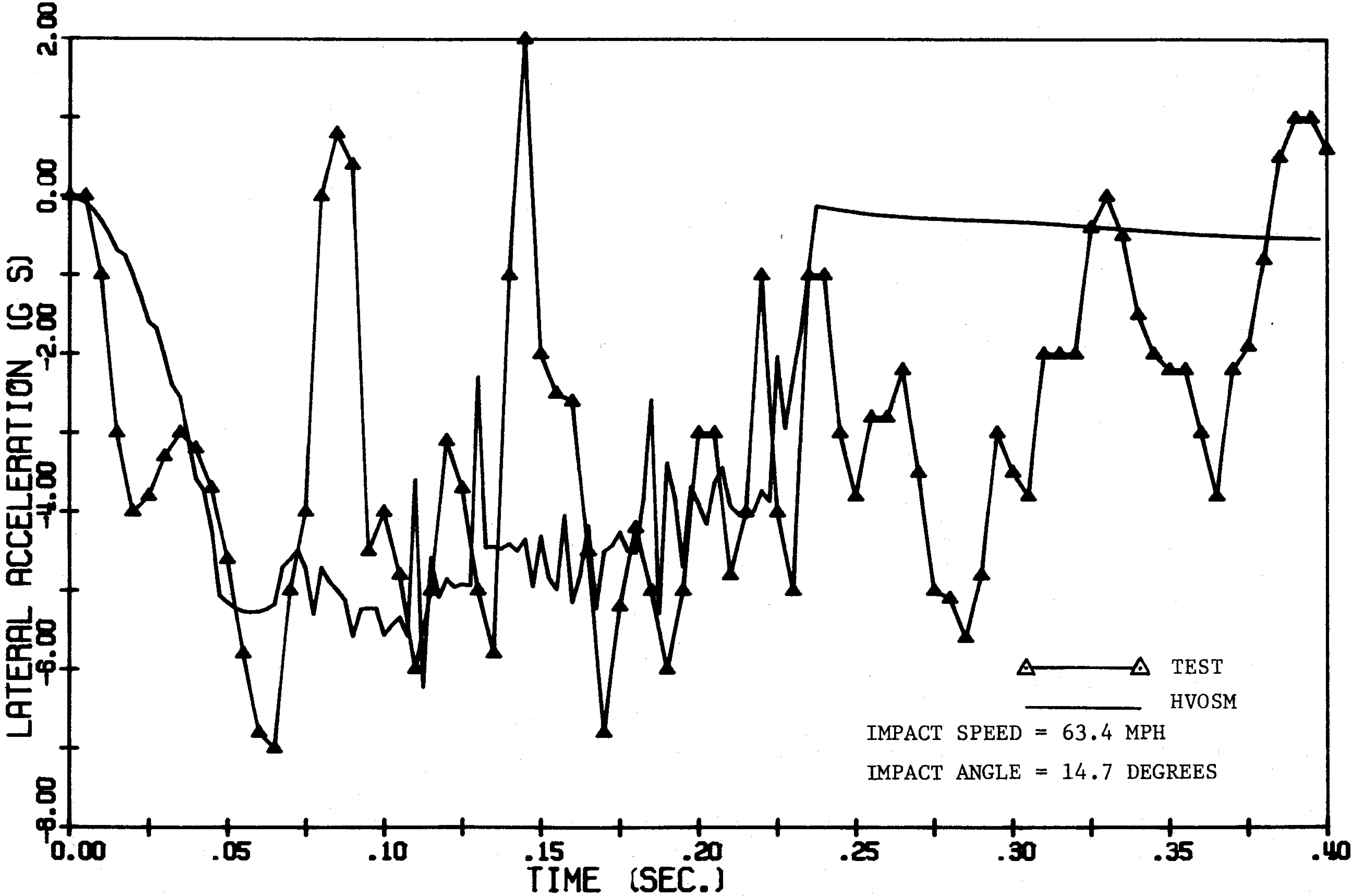

FIGURE 15. LATERAL ACCELERATION, TEST MB-2

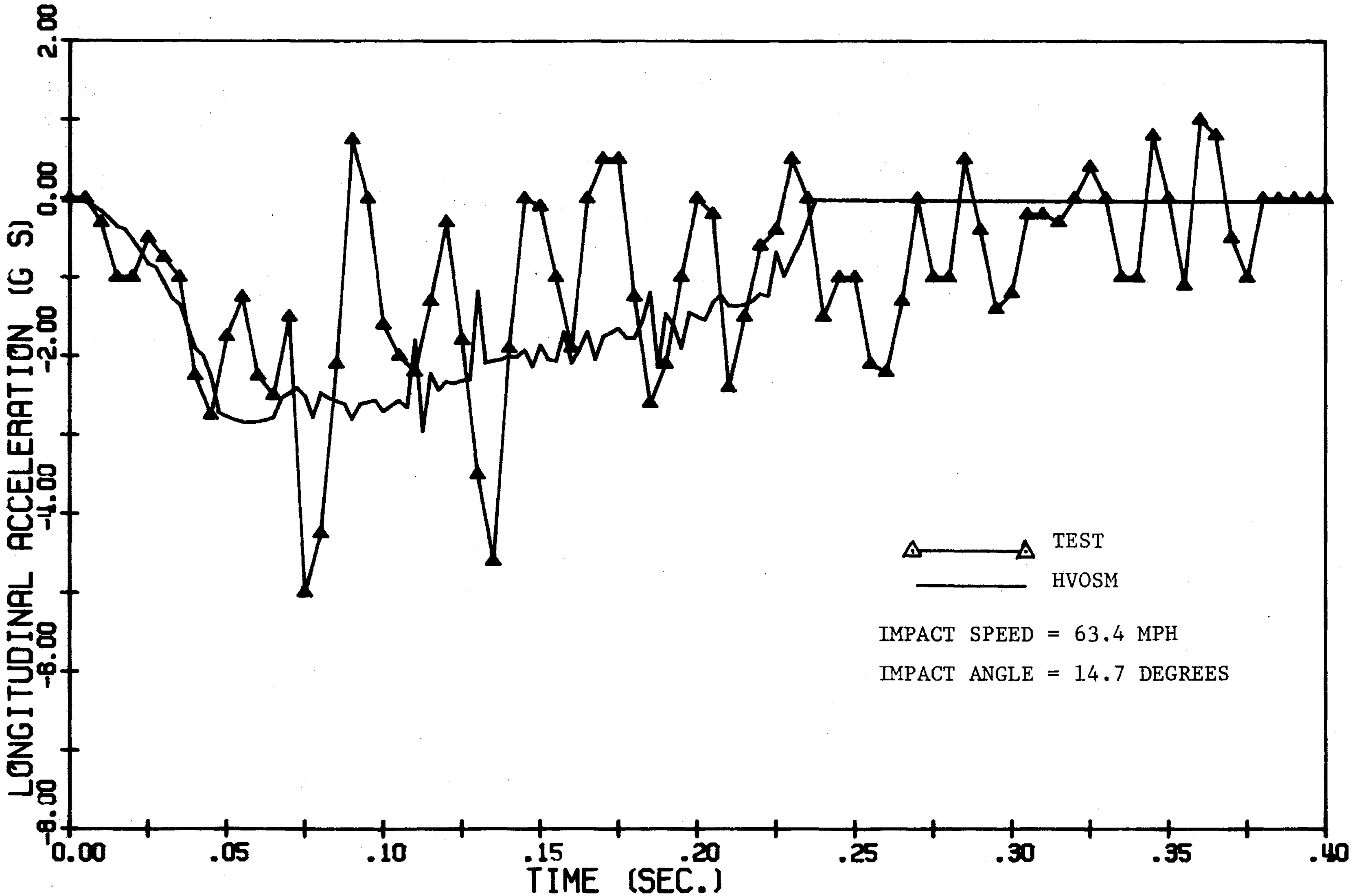

FIGURE 16. LONGITUDINAL ACCELERATION, TEST MB-2

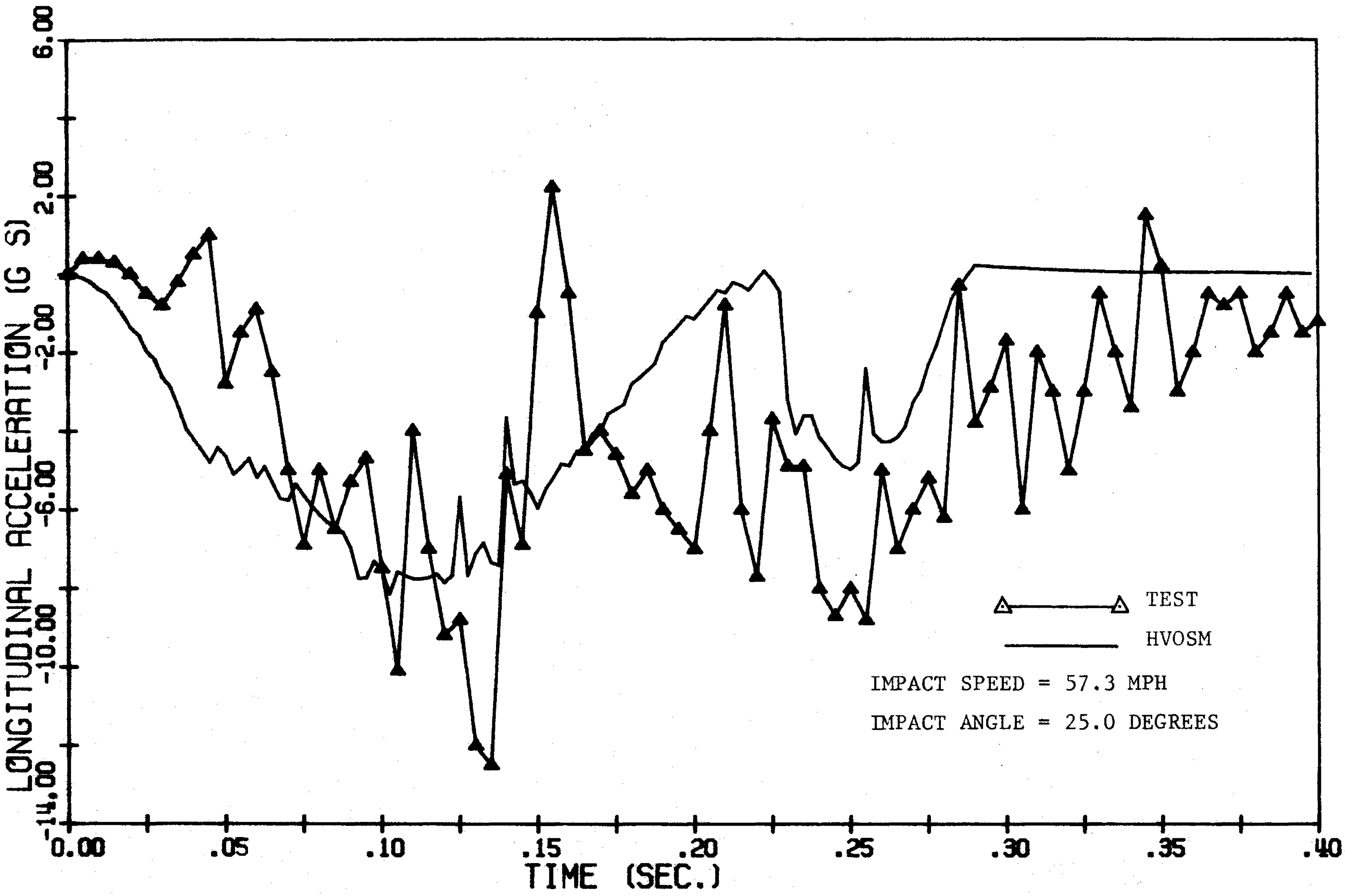

FIGURE 17. LONGITUDINAL ACCELERATION, LEFT FRAME, TEST T4-1

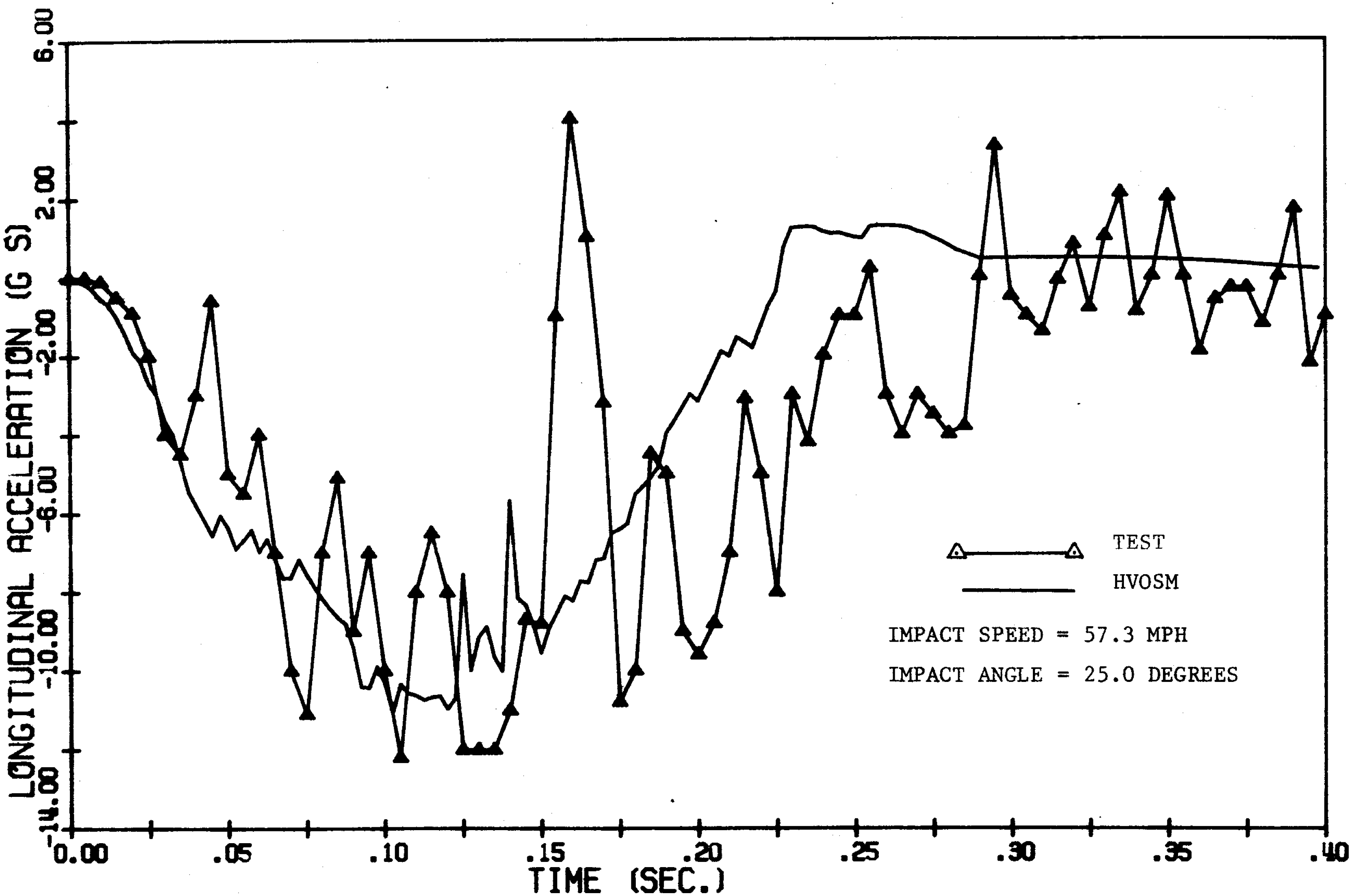

FIGURE 18. LONGITUDINAL ACCELERATION, RIGHT FRAME, TEST T4-1

It can be seen that the HVOSM accelerations generally follow the trend of the test accelerations. In some instances (see Figure 15 for example) the test data are characterized by rapid changes while the HVOSM values are somewhat smoother. This high-frequency vibratory nature of the test data is attributed in part to "ringing" or high-frequency response of the sprung mass of the vehicle. HVOSM does not have the capability to simulate this type of response. However, the contribution of such motion to overall impact severity is not considered significant. Another reason for sudden and large changes in the test values is that as the vehicle crushes, various members of various stiffnesses are encountered. HVOSM can simulate this effect to a small degree by "hard points".

A summary of the acceleration data is given in Table 2. Shown in the table are peak accelerations and the highest average accelerations occurring over any 50 millisecond period. The times at which the peak accelerations occur and the periods over which the highest average accelerations occur are also given in the table.

Although some disparity occurs between test values and the HVOSM values for peak accelerations and the times at which these occur, the average accelerations are in reasonably close agreement. In most cases, more significance is placed on the highest average accelerations rather than the highest peak accelerations. This is especially true when vehicle accelerations are used as a measure of severity (to the occupant/occupants of the vehicle).

After evaluating the validation efforts, it was concluded that HVOSM (as modified) could be used to supplement crash test data for the MBGF.

TABLE 2. ACCELERATION COMPARISONS

	TEST NUMBER					
	MB-1		MB-2		T4-1*	
	Test Results	HVOSM Results	Test Results	HVOSM Results	Test Results	HVOSM Results
Peak Lateral Acceleration (G's)/Time (sec)	5.3 / 0.16	4.1 / 0.19	7.0 / 0.070	6.2 / 0.113	not available	9.4 / 0.25
Peak Longitudinal Acceleration (G's)/Time (sec)	2.8 / 0.08	1.4 / 0.07	5.0 / 0.080	2.8 / 0.058	12.0 / 0.13	11.0 / 0.103
Highest Average Lateral Acceleration (G's)/Time Period (sec)	3.2 / .14-.19	3.6 / .045-.095	4.7 / .17-.22	4.8 / .173-.223	not available	7.2 / 0.23-0.28
Highest Average Longitudinal Acceleration (G's)/Time Period (sec)	1.0 / .045-.095	1.2 / .045-.095	2.5 / .035-.085	2.6 / .048-.098	10.0 / 0.10-0.15	10.0 / .088-.138

* Right frame member

When considering the very complex nature of the MBGF impacts, HVOSM predicted the gross motion of the vehicle and vehicle accelerations quite accurately.

IV. PARAMETRIC STUDIES

Metal Beam Guard Fence

To supplement the MBGF crash test data, nine HVOSM simulations were made. Impacts at speeds of 50 mph, 70 mph, and 80 mph, in combination with impact angles of 5 degrees, 15 degrees, and 25 degrees, were simulated.

Table 3 summarizes the results of these nine simulations (runs 1 through 9). Also shown in Table 3 are the results of the simulations of the three crash tests (runs 10, 11, and 12). The accelerations given in Table 3 are the highest average accelerations occurring over any 50 millisecond period. A small utility computer program was written to compute these maximum averages as well as the maximum severity index (discussed in a following paragraph). The program scanned the data, computed the average accelerations and the severity index for all 50 millisecond periods, and selected and printed the maximums. It is noted that the time period over which the maximum average longitudinal acceleration occurred did not necessarily correspond to that for the average lateral acceleration. Also, the time period over which the maximum severity index occurred did not necessarily correspond to that for the maximum average longitudinal acceleration or to that of the maximum average lateral acceleration.

A severity index (S.I.) was used to quantify the severity (to an occupant) of the vehicle impacts with the MBGF. It is defined as follows (7):

$$S.I. = \sqrt{\left(\frac{G_{Long}}{G'_{Long}}\right)^2 + \left(\frac{G_{Lat}}{G'_{Lat}}\right)^2 + \left(\frac{G_{Vert}}{G'_{Vert}}\right)^2} \qquad (1)$$

TABLE 3. PARAMETRIC STUDY RESULTS, MBGF

RUN NO.	IMPACT CONDITIONS SPEED (mph)	IMPACT CONDITIONS ANGLE (deg)	EXIT ANGLE[1] (deg)	MAXIMUM ROLL ANGLE (deg)	MAXIMUM AVERAGE ACCELERATIONS (G's)[2] G_{Long}	MAXIMUM AVERAGE ACCELERATIONS (G's)[2] G_{Lat}	MAXIMUM SEVERITY[3] INDEX (S.I.)
1	50	5	1.9	1.8	0.56	1.92	0.39
2	50	15	5.1	5.0	2.45	4.14	0.90
3	50	25	12.2	9.6	7.80	5.50	1.57
4	70	5	1.2	1.5	0.76	2.70	0.55
5	70	15	2.9	2.3	2.87	5.51	1.15
6	70	25	7.8	10.1	12.03	8.98	2.49
7	80	5	1.0	1.6	0.88	3.15	0.64
8	80	15	2.7	3.0	3.41	6.60	1.39
9	80	25	7.0	9.7	15.30	11.53	3.17
10	60	8	2.5	1.8	1.20	3.60	0.73
11	63.4	14.7	3.6	5.0	2.59	4.80	0.98
12	57.3	25.0	9.2	8.4	9.03	6.83	1.88

[1] Angle when vehicle lost contact with barrier.

[2] Averaged over 50 milliseconds, at C.G. The maximum average longitudinal and lateral accelerations do not necessarily occur during the same time period.

[3] As computed over 50 milliseconds.

Where

G_{Long} = average longitudinal acceleration;

G_{Lat} = average lateral acceleration;

G_{Vert} = average vertical acceleration;

G'_{Long} = tolerable average longitudinal acceleration;

G'_{Lat} = tolerable average lateral acceleration; and

G'_{Vert} = tolerable average vertical acceleration.

The terms in the numerator of Equation 1 are the average accelerations on the vehicle, and the terms in the denominator are the limiting vehicle accelerations an occupant can withstand without serious or fatal injuries. It is assumed that an S.I. greater than one indicates that an occupant would sustain serious or fatal injuries. A detailed description of the index is given in the literature (7, 8).

Limiting accelerations used in this study were as follows (7):

$$G'_{Long} = 7$$

$$G'_{Lat} = 5$$

$$G'_{Vert} = 6$$

For the MBGF, the vertical accelerations were negligible and therefore only the first two terms of the S.I. were included. However, the severity indices on the CMB (provided in subsequent parts of this report) involved all three terms since all three acceleration components were significant.

Concrete Median Barrier

In the following chapter, the S.I. for the MBGF is compared with that of the CMB. Values of the S.I. for the CMB were obtained from a previous study (1, 2), with two exceptions. To adequately compare the two barriers, it was necessary to simulate two impacts with the CMB which were not in the previous study. Impacts at 50 mph and 25 degrees and at 70 mph and 25 degrees were simulated. The results of these two runs, together with all other CMB data, are given in Table 4.

TABLE 4. PARAMETRIC STUDY RESULTS, CMB (1)

RUN NO.	IMPACT CONDITIONS SPEED (mph)	IMPACT CONDITIONS ANGLE (deg)	EXIT ANGLE[1] (deg)	MAXIMUM ROLL ANGLE (deg)	MAXIMUM AVERAGE ACCELERATIONS (G's)[2] G_{Long}	G_{Lat}	G_{Vert}	MAXIMUM SEVERITY[3] INDEX (S.I.)
1	50.0	5.0	1.1	1.3	0.49	1.61	0.12	0.33
2	70.0	5.0	0.3	2.2	0.72	2.53	0.43	0.52
3	80.0	5.0	0.1	3.3	0.21	2.90	0.54	0.58
4	50.0	10.0	2.5	4.2	1.13	2.99	0.94	0.64
5	70.0	10.0	1.2	19.5	0.16	5.06	2.03	1.07
6	80.0	10.0	1.2	34.6	1.92	6.42	2.61	1.38
7	50.0	15.0	3.6	15.0	0.47	4.29	1.38	0.91
8	70.0	15.0	(4)	(4)	2.81	6.44	3.16	(4)
9	80.0	15.0	(4)	(4)	3.24	7.49	3.29	(4)
10	50.0	25.0	(5)	(5)	4.45	7.41	4.28	1.76
11	63.0	25.0	5.1	37.0	6.47	11.23	4.38	2.54
12	70.0	25.0	(5)	(5)	9.37	12.27	1.78	2.81

[1] Angle when vehicle lost contact with barrier.

[2] Averaged over 50 milliseconds, at C.G. The maximum average longitudinal and lateral accelerations do not necessarily occur during the same time period.

[3] As computed over 50 milliseconds.

[4] Vehicle rolled over upon exiting from barrier. Severity considered intolerable.

[5] Data unavailable.

V. COMPARISON OF CMB AND MBGF IMPACT PERFORMANCE

Impact Severity

Shown in Figure 19 are plots of the S.I. versus impact speed for the CMB and the MBGF for three different impact angles. Data in Figure 19 were taken from Tables 3 and 4.

It can be seen that for small impact angles, the two barriers are approximately equal in impact severity. However, as the impact angle increases, the difference in impact severity of the two barriers is more pronounced, with the MBGF providing the less severe impact. This result was expected since the MBGF does have flexibility and can dissipate a considerable amount of the energy of the impacting vehicle. The CMB is for all practical purposes a rigid barrier.

It can be seen from Table 3 that the MBGF can redirect a vehicle without introducing large roll angles, i.e., the potential for roll over appears to be minimal. This could be a significant factor when comparing the MBGF with the CMB since at high speeds and large impact angles the latter has shown a tendency to cause the impacting vehicle to roll over (2).

Damage Costs

Evaluation of the impact performance of a barrier should include a consideration of repair costs to both the barrier and the vehicle. The following cost figures, which admittedly are based on very limited data, give a quantative measure of the damage costs incurred after impact with the MBGF and the CMB.

With regard to barrier damage, the CMB requires no repair for all practical purposes, at least for the impact conditions investigated.

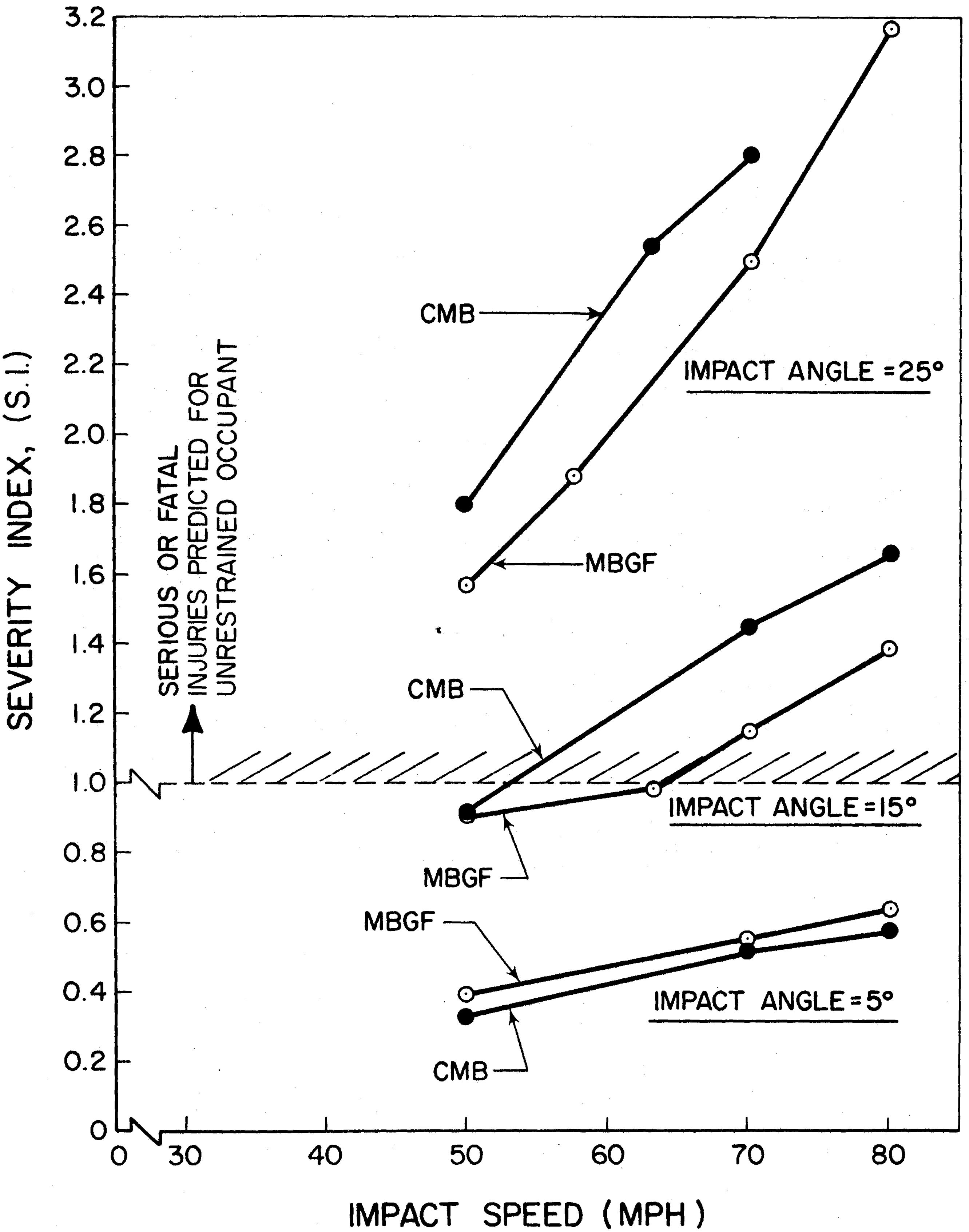

FIGURE 19. S.I. VERSUS IMPACT SPEED

Damage to the MBGF for an impact at 60 mph and an impact angle of 7 degrees was negligible. Damage to the MBGF for 60 mph impacts at impact angles of 15 degrees and 25 degrees is approximately the same. Repair cost in these cases is based on previous estimates (3) with a factor of 1.2 being applied to estimate cost increases since the referenced data were published. The barrier repair costs are shown in Table 5.

Also shown in Table 5 are the estimated costs to repair the automobiles after impact with the respective barriers. Automobile repair costs were obtained in each case from a local auto appraiser. The appraiser's estimates, given in Appendix C, were rounded off to the nearest ten dollars.

Based on the estimates and the corresponding impact conditions, impact with the CMB will cause more damage to the automobile than the MBGF. However, it is pointed out that at impact angles less than 7 degrees, the CMB will redirect an automobile with little or no sheet metal damage, which reduces or eliminates damages. The MBGF does not have this capability and some automobile damage can be expected for any impact.

TABLE 5. ESTIMATES OF DAMAGE COSTS FOR 60 mph IMPACT (DOLLARS)

	IMPACT ANGLE					
	7 Degrees		15 Degrees		25 Degrees	
	MBGF	CMB	MBGF	CMB	MBGF	CMB
Barrier Damage	NIL	NIL	530.00[1]	NIL	530.00[1]	NIL
Vehicle Damage[2]	490.00	615.00	1330.00	1550.00	1430.00	1500.00

---

[1] Taken from reference 3 with a factor of 1.2 being applied for increases in cost.

[2] As obtained from an auto appraiser.

VI. IMPACT ANGLE PROBABILITIES

The study up to this point provided objective criteria for comparing the impact performance of the CMB and the MBGF for a given set of impact conditions, i.e., impact speed and angle. However, data in this form are of limited value if one cannot relate impact conditions (or probability thereof) to the particular median geometry in question. The objective of this phase of the study was therefore to determine the impact condition probability as a function of median width or the distance from the roadway to barrier's face.

To accomplish this objective, the researchers relied on both field data and on data as determined by use of the HVOSM model. A description of each of these two approaches follows.

Field Data on Barrier Impacts

Very valuable work on the nature of vehicle encroachments has been done by Hutchinson and Kennedy (9). However, the referenced work involved all encroachments and there was no apparent way to predict what number of these encroachments would have impacted a barrier, had there been one in the median, and what impact angle. It was decided that a number of field evaluations would be made to determine actual impact angles.

The field data were gathered by members of the THD Research Division. The field sites were urban freeways of several large cities in Texas. The collection procedure involved the location of sites where median barrier accidents had occurred (as judged by barrier damage) in which impact angles could be measured, either through skid marks or tire tracks. In some cases, the barrier deflection (permanent set) was measured. However, there was no attempt to relate barrier damage to any other parameters, such as vehicle speed.

Median widths investigated ranged from 13 feet to 56 feet. A total of 135 cases were recorded. However, a large portion of these (111) fell in the 22-foot to 26-foot median width range. In a few instances, the barrier was located on a raised median. However, in such cases a roll curb was used (5-3/4 inch height or less) and as a consequence it is doubtful that the curb would have a significant effect on the vehicle's path, at least for the short distance between the curb and the barrier.

Inspections of impacts with barriers on narrow raised medians were also made by the THD investigation team. The following statement by Hustace of the THD concerns this phase of the inspection.

> "The narrow median, although sustaining numerous impacts, had frequently not provided tire tracks due to the airborne tire after having struck the curb face. Although curb scuff marks and barrier damage is usually readily apparent, the nearness of the barrier face and overhang of the vehicle would normally result in an over conservative angle from a calculated value. This factor, combined with the extreme hazard of angle measurements on narrow medians, leads me to feel that the data generated by Hutchinson and Kennedy for vehicle departure angles should be adequate to represent the narrow median situations since vehicle-driver recovery-response would be minimum due to the close proximity of the barrier. Also, in turn, the absence of wide median barrier sites and the lack of serious consideration for median barrier installations in the wide median does not demand the same urgent attention as does the barrier installation for the medium and narrow width medians."

A statistical analysis of the 135 cases led to the following conclusions:

(a) There was enough data to determine a relation between impact angle and probability of occurrence for median widths between

22 feet and 26 feet. The relation is shown in Figure 20. Note that the data from the 22-foot, 24-foot, 25-foot, and 26-foot medians were combined to develop this curve. There was not a significant variation in the distribution to warrant a curve for each of these four widths.

(b) There was not enough data to develop distributions of impact angles as a function of median widths. This was due to the fact that most of the data was for median widths between 22 feet and 26 feet.

(c) Based on the data for the 22-foot to 26-foot medians, it appears that the distribution of impact angles for a given median width can be approximated by the "normal distribution". The mean impact angle for the data was 10.8 degrees with a standard deviation of 6.2 degrees. It can be seen in Figure 20 that a normal distribution having a mean impact angle of 10.8 degrees and a standard deviation of 6.2 degrees correlates well with the field data.

HVOSM Simulations of Encroachment Angles

A series of HVOSM runs were conducted to supplement the field data. The objective of these runs was to develop relationships between encroachment angle and median width for different probability levels.

The research approach and its rationale were as follows:

(a) The HVOSM was used to establish extreme encroachment angles (95th percentile values) for any given median width. Further details of the procedure used to determine these angles are given in a subsequent part of this chapter.

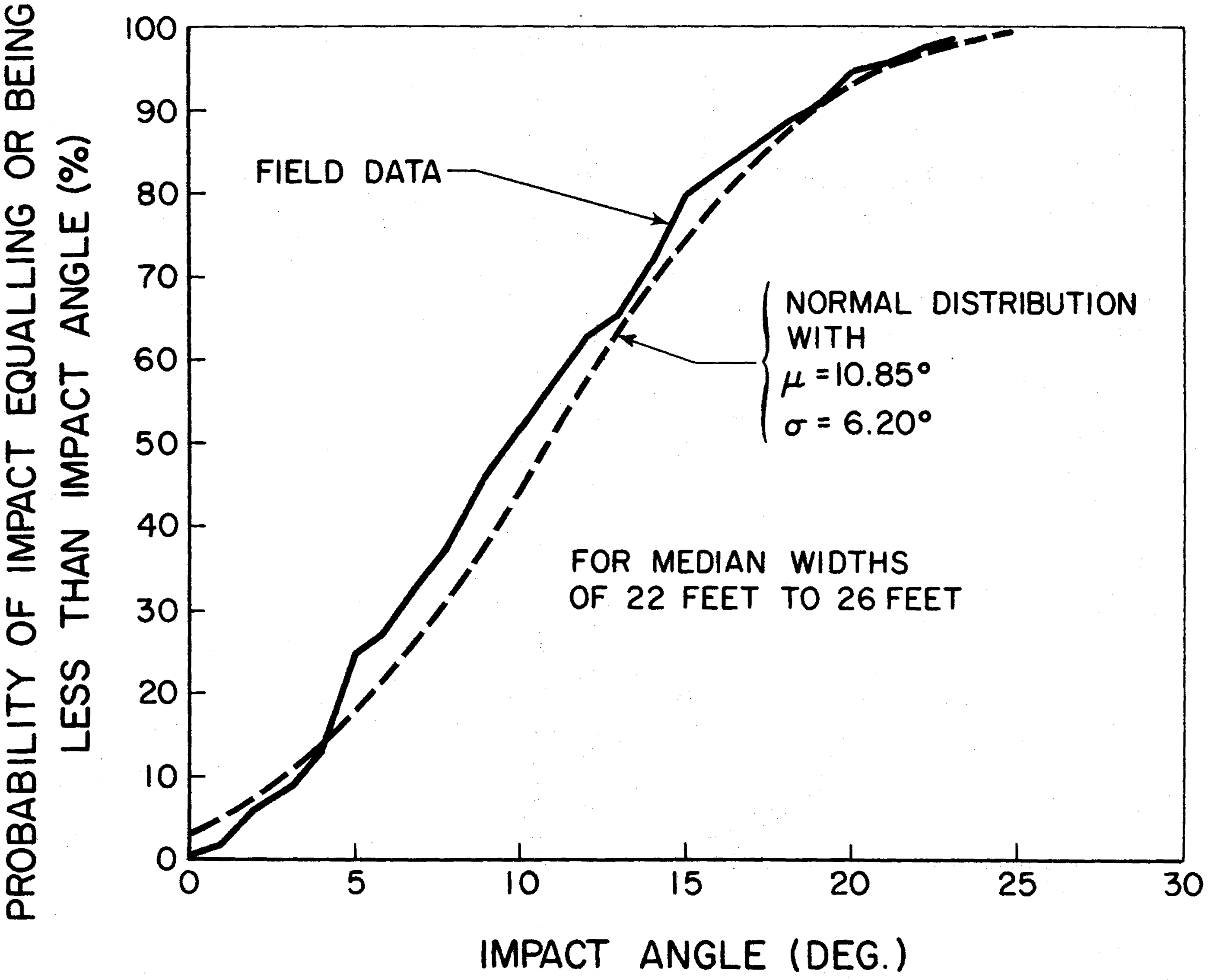

FIGURE 20. DISTRIBUTION OF IMPACT ANGLES FOR FIELD DATA

(b) Using the extreme angles from part "a" and assuming a zero impact angle at the 5th percentile, a normal distribution was constructed for various median widths (a normal distribution is uniquely defined, given any two points on the curve). Use of the normal distribution in this manner appears reasonable due to its close correlation with field data (see Figure 20).

(c) From the data generated in part "b", curves were drawn depicting impact angle versus median width for different levels of probability.

It is important to note that the ability of the HVOSM to simulate an automobile during steering maneuvers has been demonstrated by other researchers (11). The referenced validation studies involved sinusoidal steering inputs.

Extreme encroachment angles. Much speculation has occurred concerning the highest angle an automobile can impact a barrier located a given distance from the roadway. This investigation did not provide data to end all speculations, nor did it purport to, but it did shed some light on the problem.

Basically, the HVOSM was used to determine the response and the encroachment angle of a standard automobile with standard tires as it was suddenly steered off the roadway while travelling at 60 mph. The automobile was assumed to be in a "coast" mode, i.e., with no traction after the steering maneuver began. The steering maneuver was an attempt to simulate an emergency avoidance maneuver. It consisted of steering from a zero steer angle to a prescribed angle in a prescribed time at a uniform rate. The turning rate was determined by observing the highest rates at which drivers had performed similar maneuvers in full-scale tests at TTI.

Figure 21 shows the four steering conditions which were input to the HVOSM. As shown, the steer angle was increased up to a selected value at a constant rate and then held constant. It is noted that most automobiles have a steering wheel angle to steer angle ratio between 20 and 25. For example, an eight-degree steer angle would require between 160 and 200 degrees of steering wheel turn.

A total of 12 simulation runs were made. For each of the four steering conditions shown in Figure 21, three tire-pavement friction coefficients were simulated, namely 1.0, 0.75, and 0.5. The results are presented in two basic forms; plots of the vehicle path and plots of encroachment angle versus lateral distance.

Figure 22 shows plots of the path of the center of gravity of the vehicle for a tire-pavement friction coefficient of 1.0 for four steering maneuvers. The "lateral distance" is a distance from the roadway tangent on which the steering maneuver began (roadway parallel to "longitudinal distance" axis). The four HVOSM plots are the paths of the vehicle for each of the four steering maneuvers of Figure 21. Note that an increase in the steer angle does not result in a proportionate increase in the path curvature, especially beyond steer angles of eight degrees. This is due primarily to the saturation of the side force capabilities of the front tires after the steer angle exceeds approximately eight degrees. It is conjectured that the curvature approaches a limiting value for steer angles of 16 degrees. It is possible that other forms of steering input (e.g., non-linear rates of steer application) could result in paths of larger curvature, but it is doubtful that the differences would be significant.

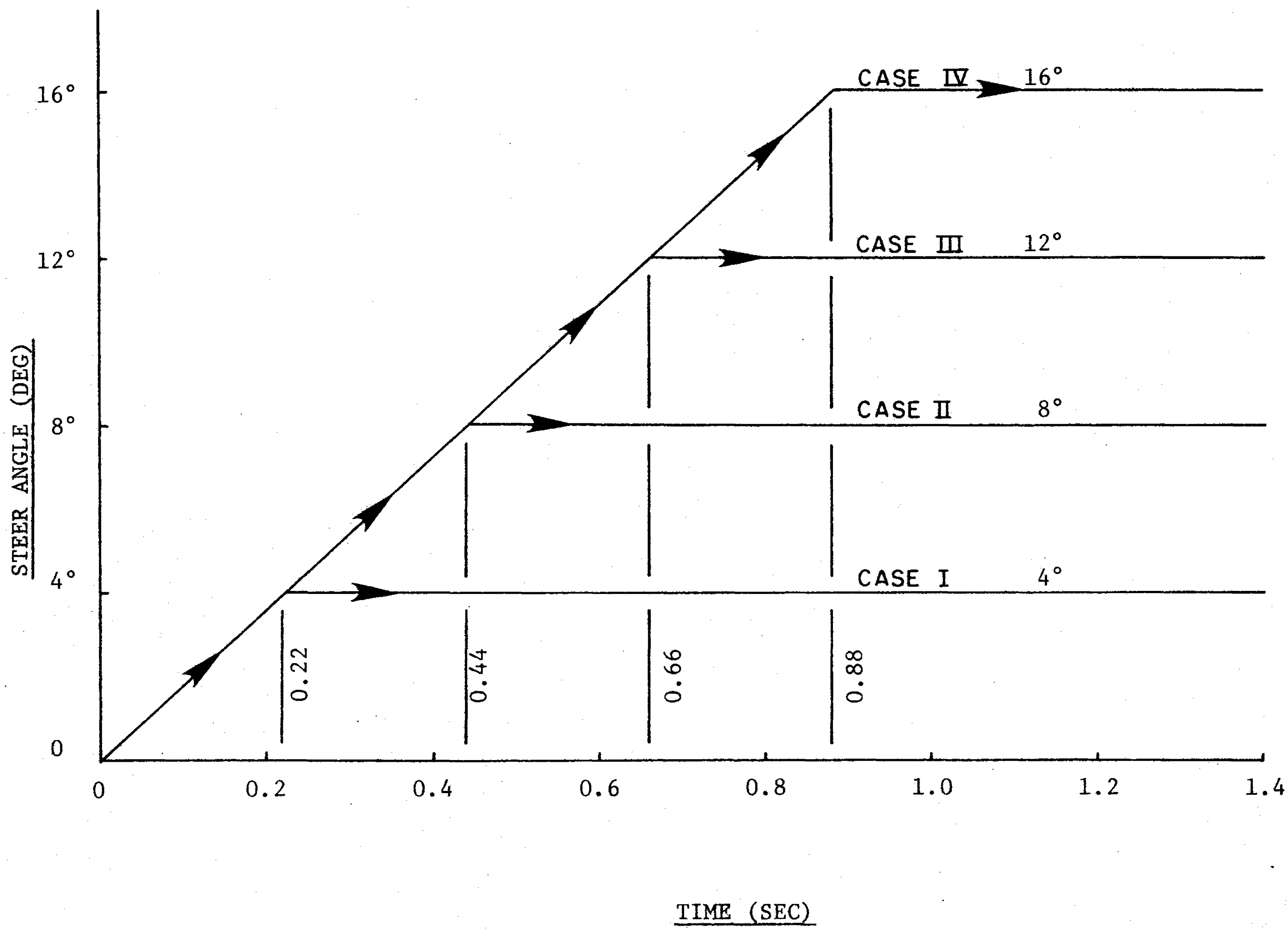

FIGURE 21. STEERING INPUT VERSUS TIME

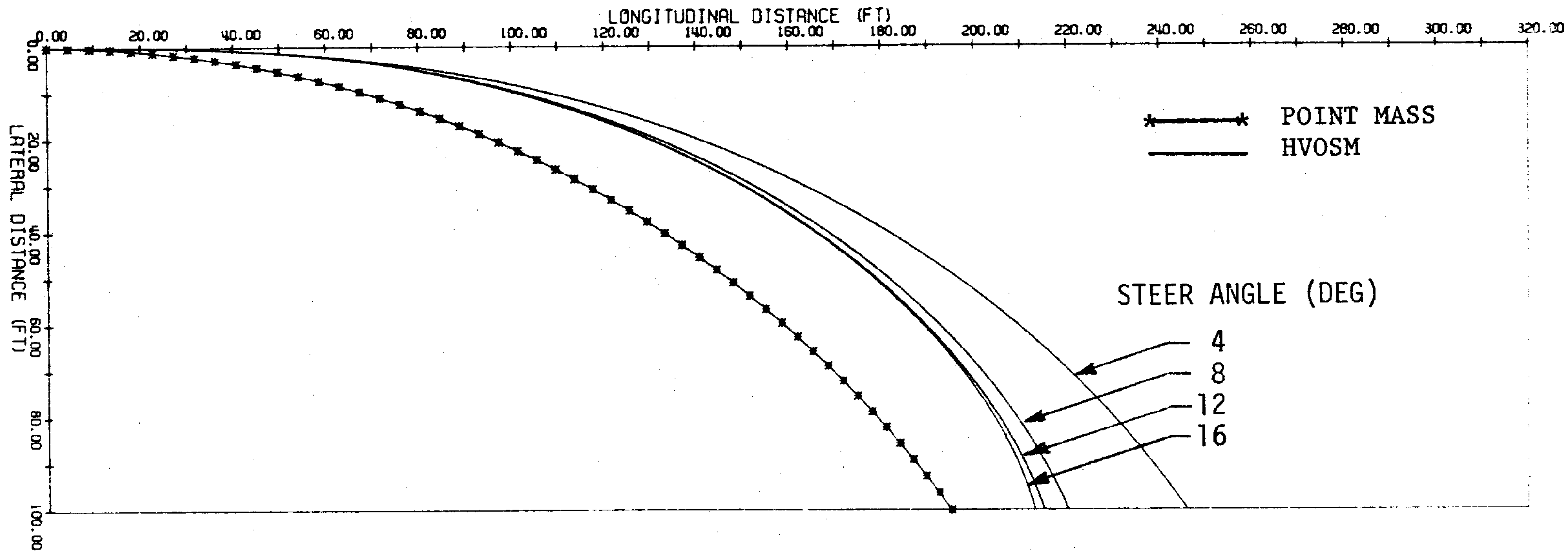

FIGURE 22. VEHICLE PATH, $\mu = 1.0$

Also shown on Figure 22 is a path plot of the vehicle as simulated by a simple "point mass" model. For a point mass the maximum available side force, F_f, is computed as follows:

$$F_f = \mu W \tag{2}$$

where

μ = friction coefficient, and

W = weight of vehicle.

As the point mass vehicle corners in a circular turn (with no pavement superelevation) its centrifugal force, F_c, is determined as follows:

$$F_c = \frac{Wv^2}{gr} \tag{3}$$

where

v = vehicle velocity,

g = gravitational acceleration, and

r = radius of turn.

The minimum radius the point mass can follow is computed by equating F_f and F_c, and then solving for r_{min} as follows:

$$\frac{Wv^2}{gr} = \mu W \tag{4}$$

and

$$r_{min} = \frac{v^2}{g\mu} \tag{5}$$

From Figure 22, it can be seen that the actual paths (as determined by HVOSM) differ considerably from that of the point mass. This is due to the inability of the point mass model to accurately represent the transient nature of vehicle handling. Whereas the point mass model assumes an instantaneous steady state turn once the turn has been initiated, the HVOSM accounts for the transient period of the vehicle's response. Plots similar to those of Figure 22 for values of μ of 0.75 and 0.5 are included in Appendix D.

Figure 23 shows plots of vehicle path for a steer angle of 16 degrees as a function of the friction coefficient. Similar plots for steer angles of 4 degrees, 8 degrees, and 12 degrees, are included in Appendix D. ,

Shown in Figure 24 are encroachment angles as a function of lateral distance. Coordinates of each of these curves were determined by computing the arctangent of the slope of the appropriate curve in Figure 22 as a function of lateral distance. The encroachment angle is the angle between a tangent to the C.G.'s path and the roadway tangent.

It is interesting to note that although the point mass model does not accurately simulate the vehicle's path, it does predict the encroachment angle quite accurately, at least for the extreme steering maneuvers and for lateral distances up to about 40 feet. For lower friction coefficients, the comparison is even better (see Appendix D). It is also interesting to note that many people felt that the point mass representation gave very excessive encroachment angles, i.e., the vehicle could not attain the angles predicted by the point mass model. Such is not the case. In fact, for high skid-resistant pavements where large lateral distances are accessible e.g., a wide median, the point mass predictions are too low.

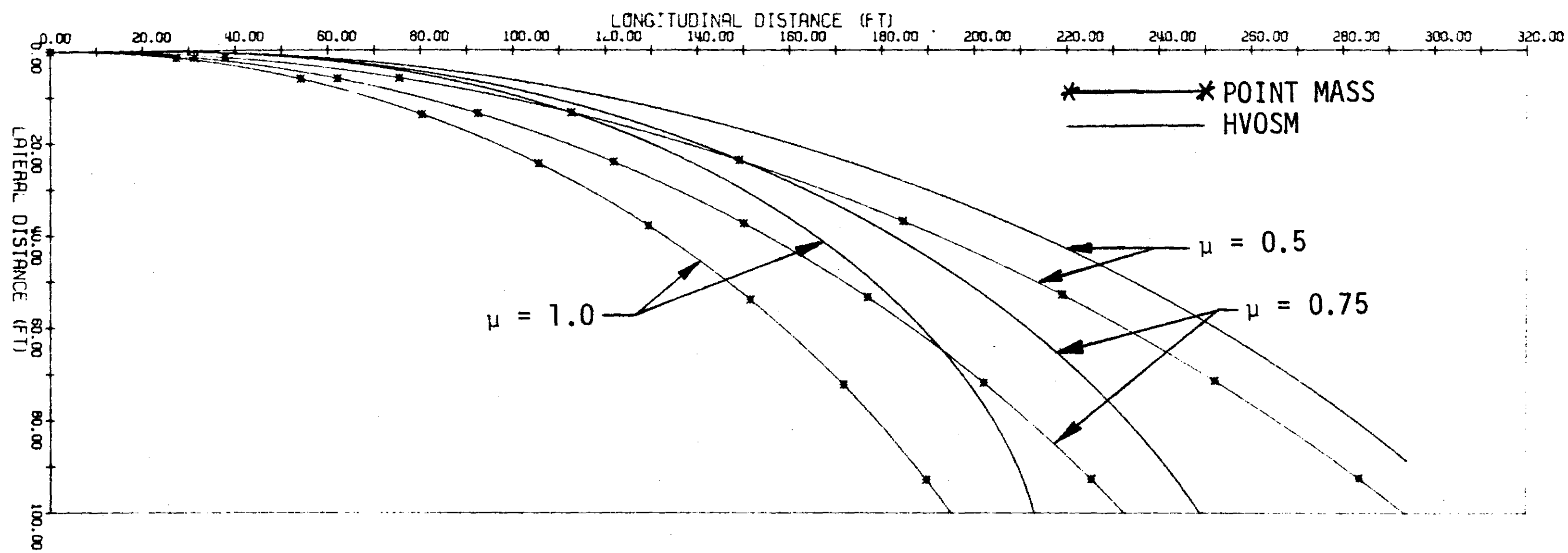

FIGURE 23. VEHICLE PATH, STEER ANGLE = 16 DEGREES

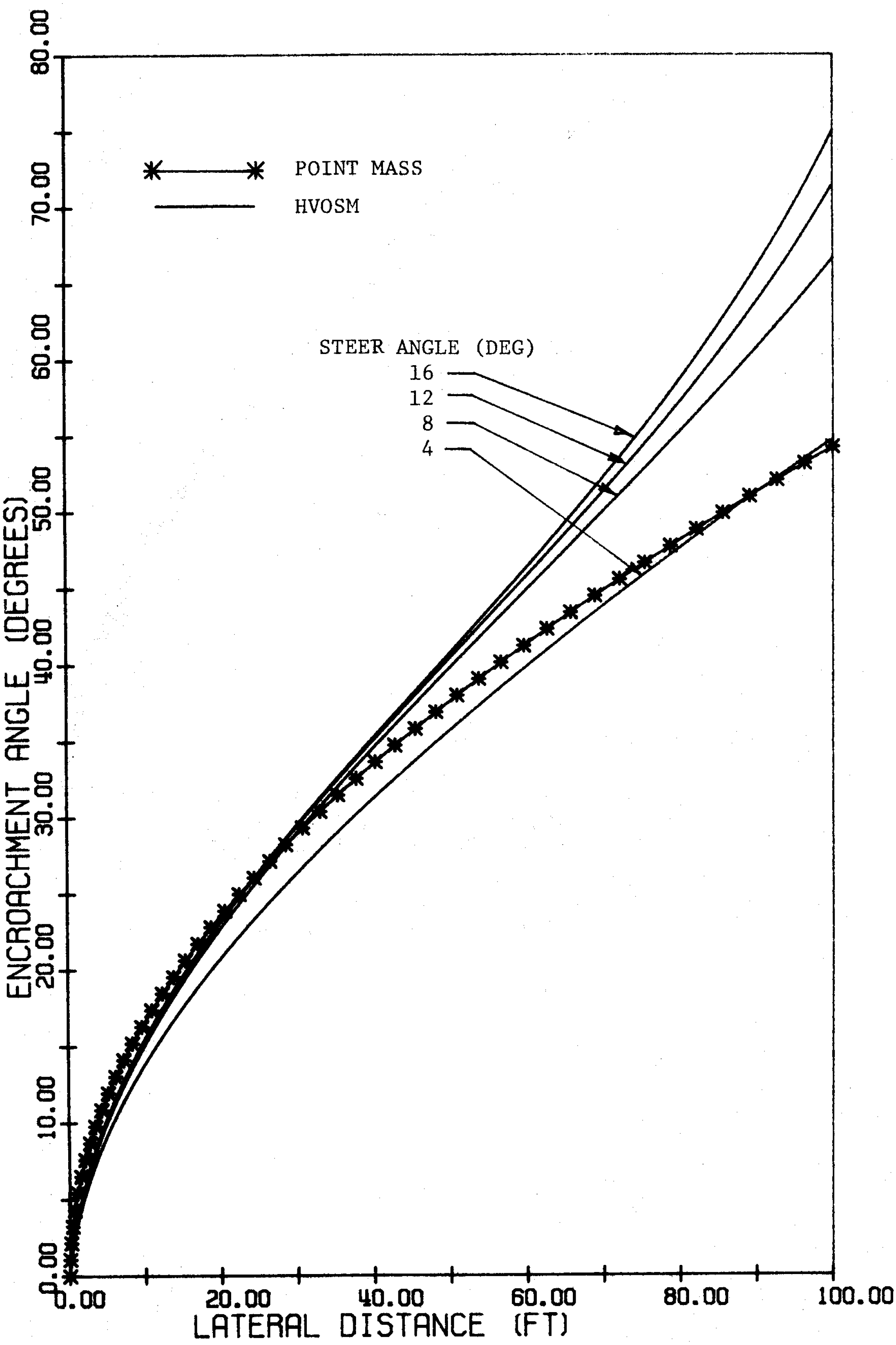

FIGURE 24. ENCROACHMENT ANGLES, $\mu = 1.0$

Figure 25 is a plot of encroachment angles for the three friction coefficients and for a steer angle of 16 degrees. Similar plots are given in Appendix D for steer angles of 4 degrees, 8 degrees, and 12 degrees.

To arrive at a relationship between extreme encroachment angle and median width (lateral distance), the values as determined for a steer angle of 16 degrees and a friction coefficient of 1.0 were selected. In most cases these conditions would be extreme and as such they represent what is considered to be limiting values.

To compute actual impact angles it was necessary to account for the dimensions of the automobile. With reference to Figure 26, it is obvious that the vehicle will impact the barrier before the C.G. crosses the barrier plane. The vehicle dimensions given in Figure 26 are typical of a medium-weight sedan. From geometry,

$$\alpha = \mathrm{TAN}^{-1} \frac{36}{88.5} \tag{6}$$

or α = 22.13 degrees.

Thus,

$$L_T - L_{CG} = (95.54)[\mathrm{SIN}(\alpha + \theta)] \tag{7}$$

or

$$L_T = \frac{(95.54)}{12.0}[\mathrm{SIN}(22.13 + \theta)] + L_{CG} \tag{8}$$

with L_T and L_{CG} in feet.

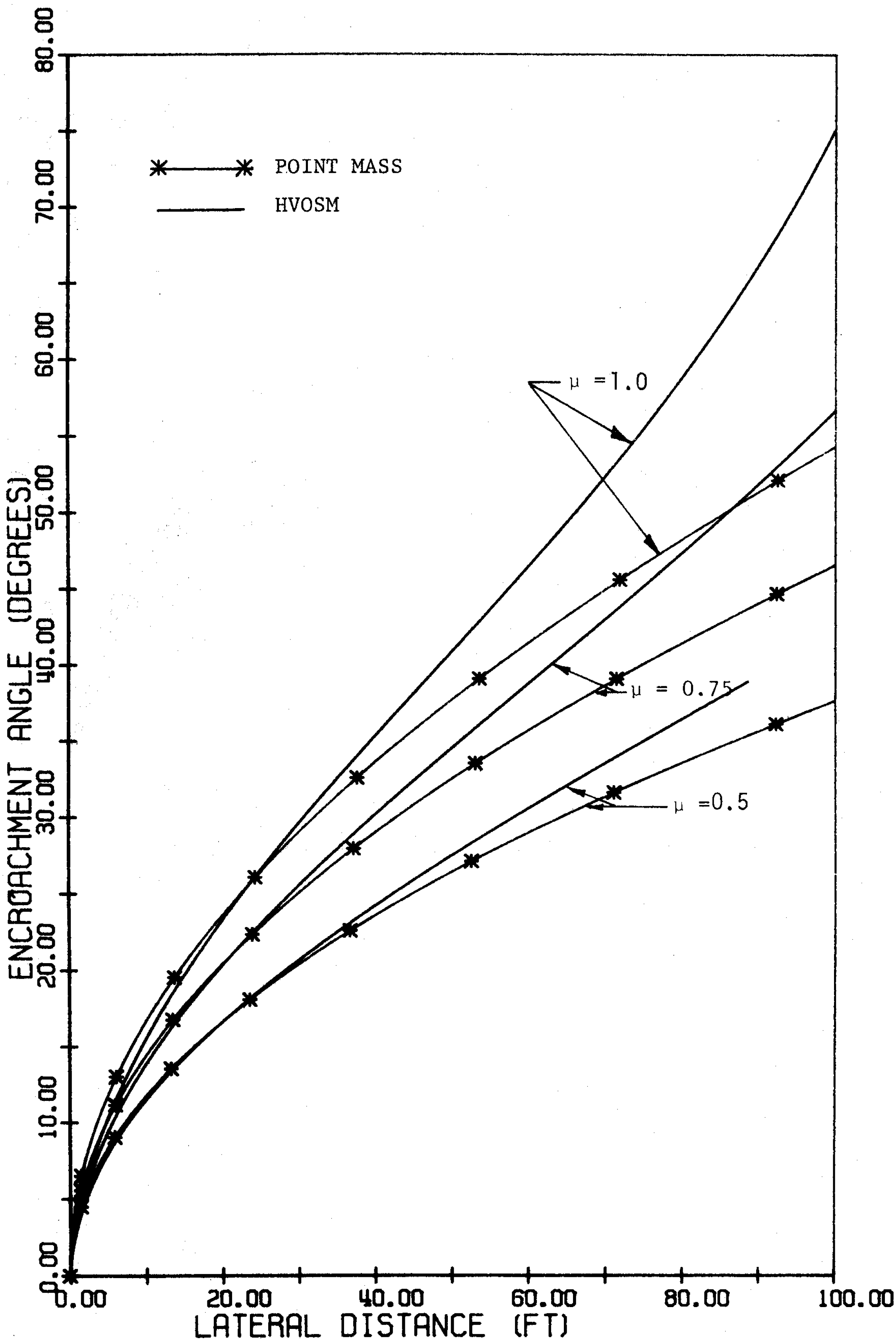

FIGURE 25. ENCROACHMENT ANGLES, STEER ANGLE = 16 DEGREES

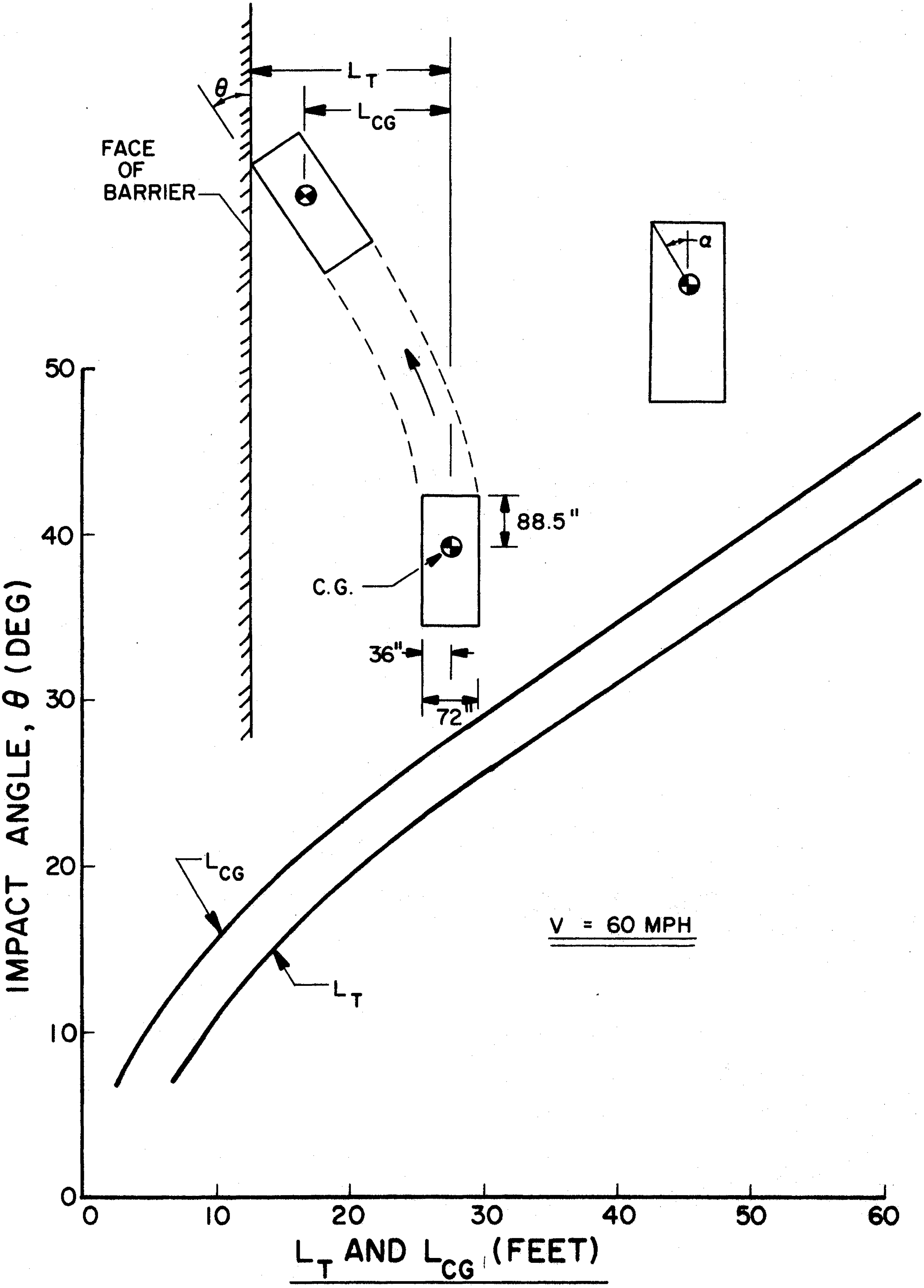

FIGURE 26. IMPACT ANGLE DATA

The "L_{CG}" curve of Figure 26 is identical to the curve of Figure 24 for a steer angle of 16 degrees. The "L_T" curve is a plot of Equation 8, with θ and L_{CG} determined from the "L_{CG}" curve.

Figure 27 shows the relationship between the extreme impact angle and the median distance, D, for two conditions; impact from lane 1 and impact from lane 2. Note the median distance, D, is not the half-median width but rather is the distance from the edge of the roadway to the barrier face. It was assumed that the vehicle was in the center of the 12-foot lane when the emergency steering maneuver began. The curves of Figure 27 are simply an application of the "L_T" curve of Figure 26. For example, for a median distance of 10 feet and an encroachment from lane 1,

$$L_T = 10 + 3 + \frac{6}{2} = 16 \text{ feet}$$

From Figure 26,

$$\theta = 16.3 \text{ degrees.}$$

Note that the "impact from lane 1" curve will intersect the vertical axis above zero for a zero median distance, i.e., there can be an impact angle even though there is no median distance. This is due to the assumed three-foot gap between the vehicle and the face of the barrier for a vehicle travelling in the center of the lane.

<u>Impact angle probabilities</u>. The probability distribution of impact angles for a given median distance was assumed to be a normal distribution, as has been discussed earlier in this report. To determine the distribution for a given median distance, the 95th percentile value of the impact

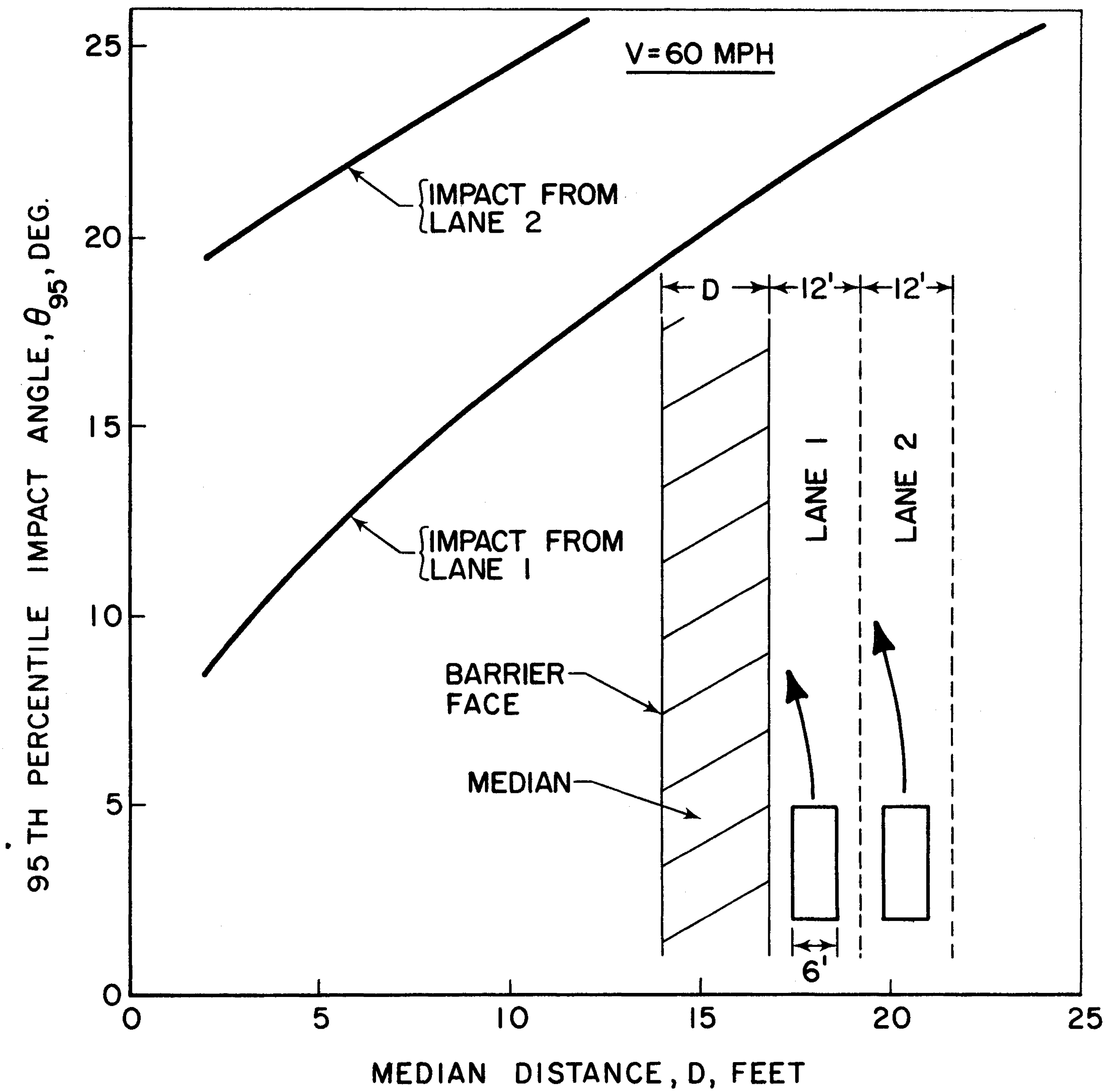

FIGURE 27. NINETY-FIFTH PERCENTILE IMPACT ANGLE VERSUS MEDIAN DISTANCE

angle was assumed to be that as determined from the "lane 1" curve of Figure 27 and the 5th percentile impact angle was assumed to be zero. These two points uniquely defined the distribution.

For a normal distribution,

$$\theta_p = \sigma X_p + \beta \tag{9}$$

Where

θ_p = impact angle for probability "p";

σ = standard deviation;

X_p = a parameter determined from tables of normal distribution function, for given probability "p"; and

β = mean of distribution.

As assumed,

$$\theta_5 = 0$$

From the tables (10),

$$X_5 = -1.65$$

Therefore,

$$0 = -1.65(\sigma) + \beta$$

or

$$\sigma = \frac{\beta}{1.65} \tag{10}$$

From the tables (10),

$$X_{95} = +1.65$$

Thus,

$$\theta_{95} = 1.65(\sigma) + \beta \tag{11}$$

Substituting σ from Equation 10 into Equation 11 gives

$$\theta_{95} = 1.65(\frac{\beta}{1.65}) + \beta$$

So,

$$\beta = \frac{\theta_{95}}{2.0} \qquad (12)$$

Thus, for known values of θ_{95}, β and σ can be determined from Equations 12 and 10, respectively.

For example, the distribution of impact angles for a median distance of 12 feet (or a median width of approximately 24 feet) is computed as follows. From Figure 27,

θ_{95} = 17.8 degrees ("impact from lane 1" curve).

From Equation 12,

$$\beta = \frac{17.8}{2.0} = 8.9$$

and from Equation 11,

$$\sigma = \frac{8.9}{1.65} = 5.39$$

Therefore,

$$\theta_p = 5.39(Z_p) + 8.9$$

Values of θ_p are shown in Table 6 as a function of p, and Figure 28 shows a plot of p versus θ_p. Also shown on the figure is a plot of the field data (same as shown in Figure 20) which has been discussed earlier. The field data was gathered on medians ranging in width between 22 feet

TABLE 6. IMPACT ANGLE DISTRIBUTION FOR 12 FOOT MEDIAN DISTANCE

PERCENTILE, p (percent)	Zp	IMPACT ANGLE θ_p (degrees)
0	-4.00	-12.66
5	-1.65	0.00
10	-1.28	2.00
20	-0.84	4.40
30	-0.52	6.10
40	-0.25	7.60
50	0.00	8.90
60	0.25	10.20
70	0.52	11.70
80	0.84	13.40
90	1.28	15.80
95	1.65	17.80
100	4.00	30.50

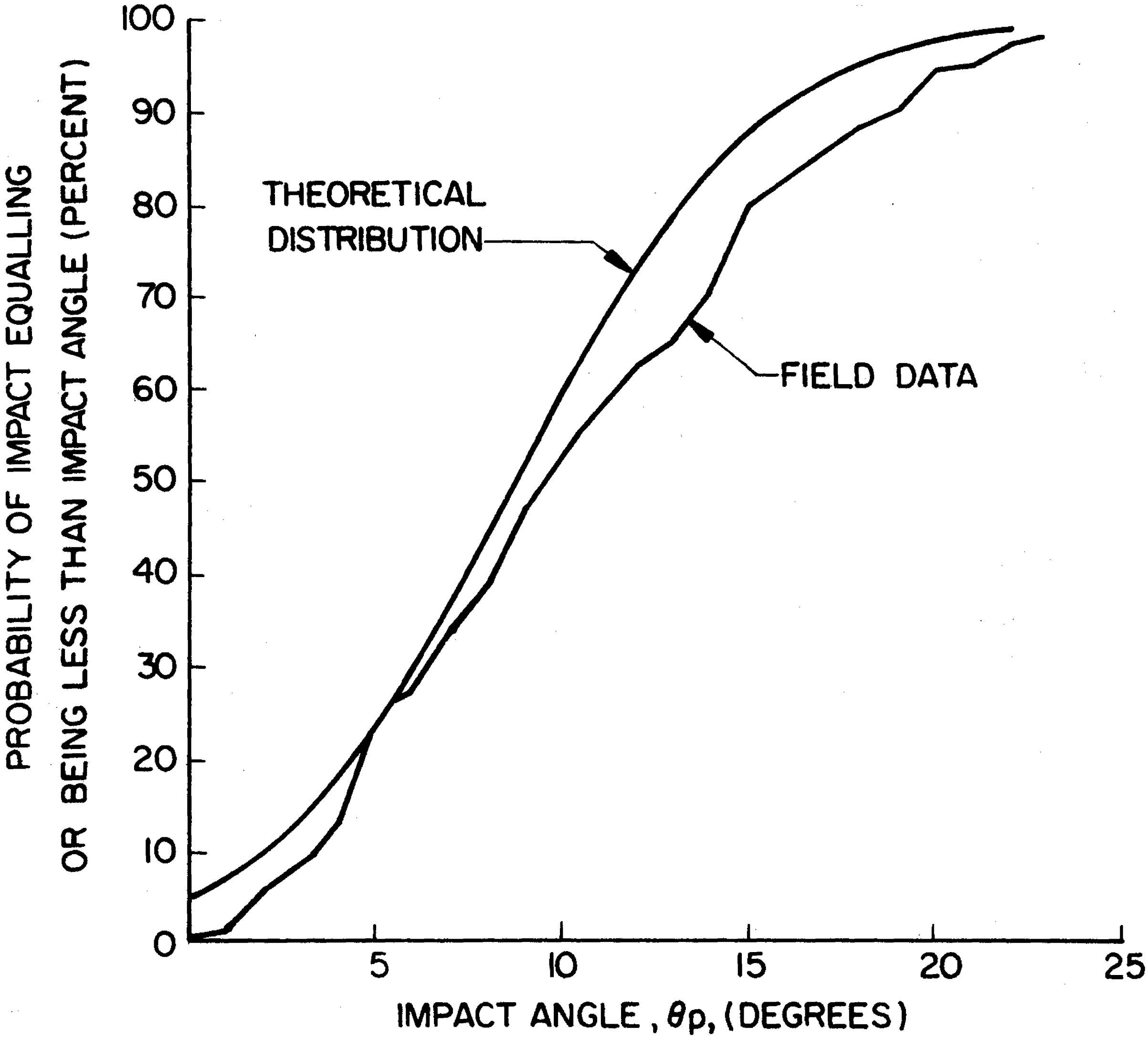

FIGURE 28. IMPACT ANGLE VERSUS PROBABILITY OF IMPACT, MEDIAN DISTANCE = 12 FEET

and 26 feet, or an average median distance of approximately 12 feet. Although there are some differences in these two curves, the degree of correlation is considered to be good.

There are several factors which likely contributed to the differences that did occur in the curves of Figure 28. The first of these, and probably the most significant one, is the speed of the impacting vehicle. Unfortunately, there was no way to determine impact speeds from the field measurements. It is conjectured that the low angle impacts occurred at speeds higher, on an average, than did the higher angle impacts. It is also conjectured that most of the impacts occurred at speeds less than 60 mph. The theoretical distribution is based on an initial encroachment speed of 60 mph. Some slight decrease in speed occurred in the HVOSM simulations during the encroachment, but it was not considered significant (less than 2 mph).

Another factor which could cause differences is that some of the barrier impacts likely occurred after the vehicle impacted another vehicle or object. Actions of the driver during the encroachment, such as braking, could also have a significant effect on vehicle path.

The number of lanes can also have an effect on the distribution of encroachment angles. The field data were taken on urban freeways having various numbers of lanes. As assumed, the theoretical distributions were based on encroachments from the inside lane.

It was concluded, however, that the effect of the combination of these factors can be represented by the as-formulated theoretical distribution. Figure 29 shows the theoretical impact angles as a function of median distance for various percentiles, where the 95th percentile curve is the

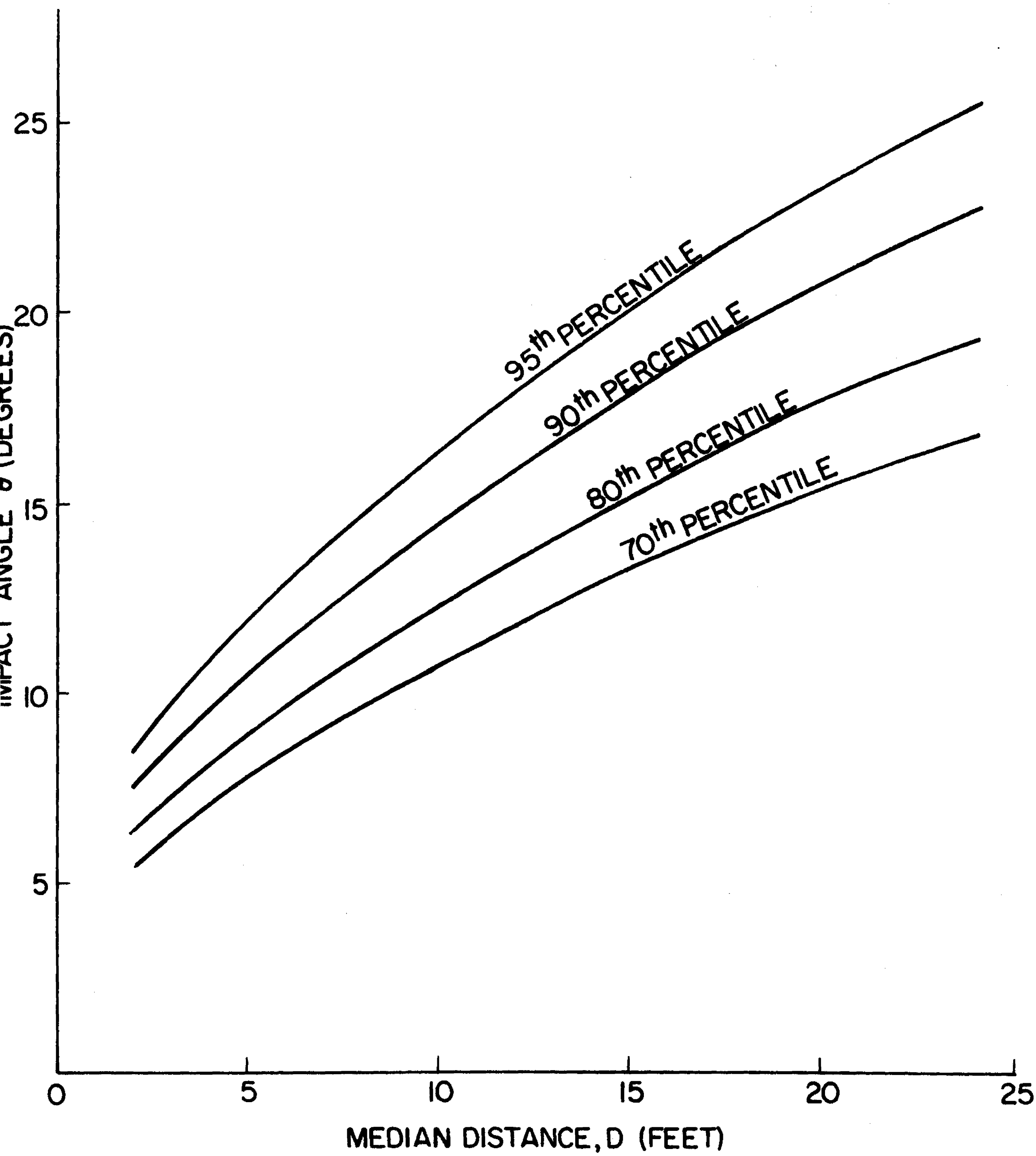

FIGURE 29. IMPACT ANGLE VERSUS MEDIAN DISTANCE

same as the "impact from lane 1" curve of Figure 27. Coordinates of the 90th percentile, the 80th percentile, and the 70th percentile curves are given in Table 7.

TABLE 7. COORDINATES OF VARIOUS PERCENTILE CURVES

MEDIAN DISTANCE, D (ft)	MEAN IMPACT ANGLE, β (Deg)	STANDARD DEVIATION, σ (Deg)	IMPACT ANGLE (Deg)		
			θ_{70}	θ_{80}	θ_{90}
2	4.20	2.55	5.53	6.34	7.46
3	4.85	2.94	6.38	7.32	8.61
4	5.35	3.24	7.03	8.07	9.50
5	5.95	3.61	7.83	8.98	10.57
7	6.90	4.18	9.07	10.41	12.25
9	7.75	4.70	10.19	11.70	13.77
10	8.15	4.94	10.72	12.30	14.47
12	8.90	5.39	11.70	13.43	15.80
14	9.70	5.88	12.76	14.64	17.23
16	10.40	6.30	13.68	15.69	18.46
18	11.10	6.73	14.60	16.75	19.71
20	11.70	7.09	15.39	17.66	20.78
22	12.25	7.42	16.11	18.48	21.75
24	12.80	7.76	16.84	19.32	22.73

VII. SELECTION CRITERION

Impact performance data and impact angle data needed to formulate a selection criterion were now available. Impact severity of the two barriers was presented in Chapter V, and impact angle data were presented in the preceding chapter.

The criterion is based on a design speed of 60 mph and relates to full-size automobiles. Shown in Table 8 are values of the severity index as related to impact angle. These values were obtained from Figure 19. The criterion is presented graphically in Figure 30. Coordinates of the S.I. versus impact angle curves were taken from Table 8 and the plots of median distance versus impact angle were taken from Figure 29.

It is pointed out that the criterion referred to is based on safety considerations only and does not include cost and maintenance factors. It is also pointed out that the criterion is dependent on the design speed. For example, if the design speed were 50 mph, the severity curves of Figure 30 for the two barriers would have been much closer together. It may be desirable to develop a different criterion in such a case.

Figure 30 allows one to objectively compare the impact severity of the two barriers as a function of the median distance. For example, assume that one is interested in the impact severities of the two barriers when placed 12.5 feet from the roadway (a median width of approximately 25 feet), for the 80th percentile impact. Application of the curves is as shown on Figure 30. The results are as follows:

	S.I.
MBGF	0.90
CMB	1.09

TABLE 8. SEVERITY INDEX OF BARRIERS AT 60 mph IMPACT SPEED

IMPACT ANGLE (deg)	SEVERITY INDEX	
	MBGF	CMB
5	0.47	0.42
15	0.96	1.18
25	2.00	2.39

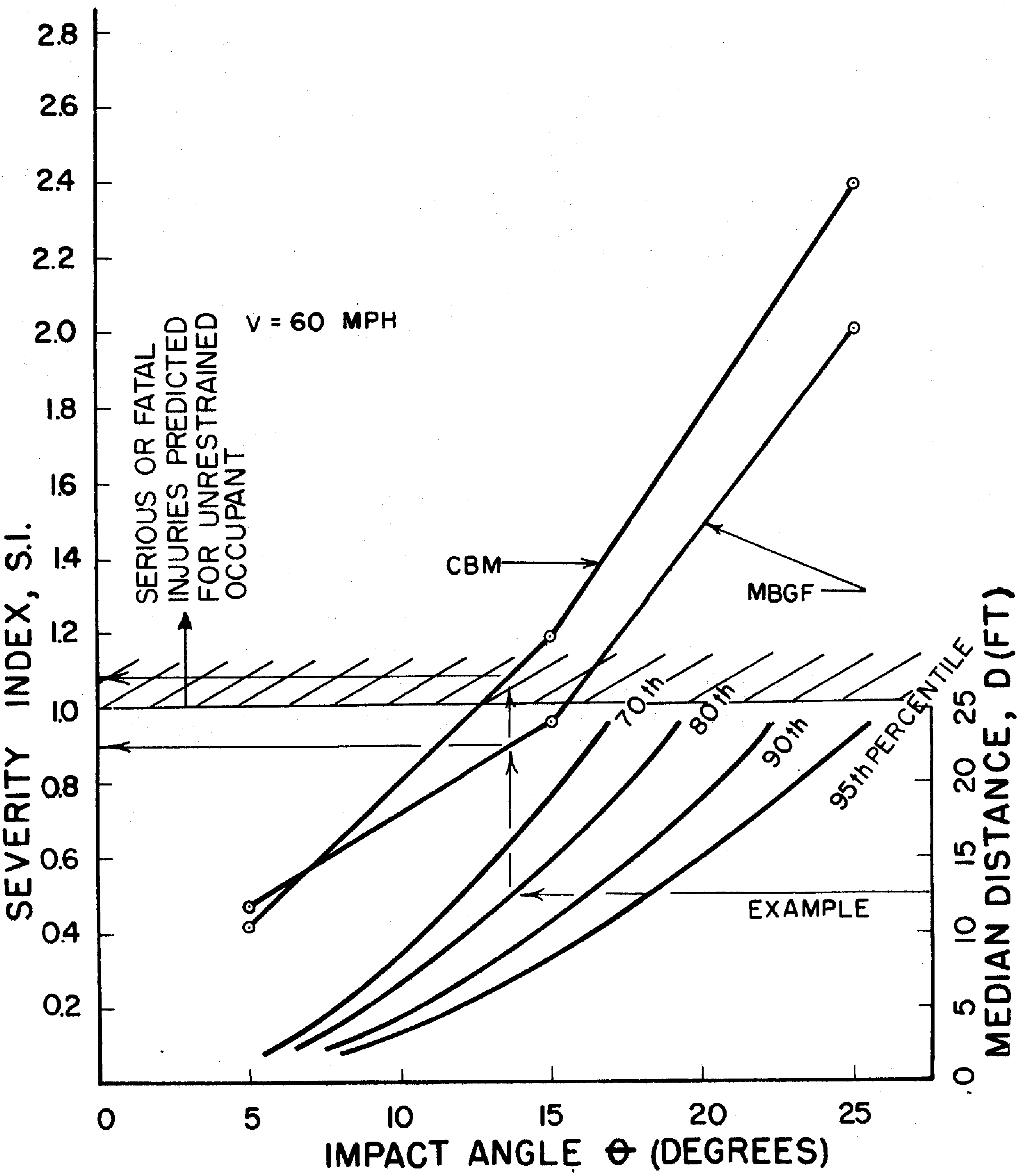

FIG. 30. SELECTION CRITERION

The results indicate the MBGF to be about 21 percent less severe for the given conditions.

As mentioned previously, the selection process involves the consideration of other factors, such as initial and maintenance costs of the barrier and the hazard to repair crews and motorists while the barrier is being serviced. It is the author's belief that a selection procedure based on a "cost-effective" analysis can be formulated which incorporates the effects of all these factors. Such a formulation, however, was not within the scope of this work.

VIII. CONCLUSIONS

The following conclusions were drawn as a result of this study:

1. The Texas standard metal beam guardfence will contain and redirect an automobile impacting at 60 mph at impact angles of 7 degrees, 15 degrees, and 25 degrees. There is no tendency for the automobile to become unstable after impact with the MBGF and the exit angle of the vehicle is not large. Serious or fatal injuries are not predicted for impacts at angles less than 15 degrees and speeds less than 60 mph.
2. The as modified version of HVOSM can be used to simulate automobile impacts with the MBGF. Close correlations between test and simulated results forms a basis for this conclusion.
3. The severity of impact with the Texas standard concrete median barrier is approximately equal to that of the MBGF for angles of impact of 7 degrees or less. However, as the angle of impact increases, impacts become progressively more severe with the CMB than with the MBGF.
4. The CMB is practically maintenance free whereas it costs approximately $500 to repair the MBGF after a 60 mph, 15 degree, impact. Based on gross estimates, automobile repair costs resulting from an impact with the CMB are slightly higher than that for the MBGF at an impact speed of 60 mph and an impact angle in excess of 7 degrees.

5. Sufficient field data was obtained to determine the percentile distribution of impact angles for a barrier placed in the center of a 24-foot median. A theoretically derived distribution, obtained by application of the HVOSM, compared favorably with the field data. Percentile distributions of impact angles as a function of median distance (distance from roadway edge to barrier face) were obtained by the theoretical analysis.
6. An objective barrier selection criterion was developed from which the impact severity of the MBGF and the CMB can be determined for any given median distance. The criterion is based on a design speed of 60 mph and impacts with a full-size automobile. The Texas Highway Department used this criterion to develop warrants for the use of these two barriers.

REFERENCES

1. Young, R. D., Post, E. R., Ross, Jr., H. E., and Holcomb, R. M., "Simulation of Vehicle Impact with the Texas Concrete Median Barrier-Volume One, Test Comparisons and Parameter Study", TTI Research Report 140-5, Texas A&M University, College Station, Texas, June 1972.

2. Young, R. D. Post, E. R., and Ross, Jr., H. E., "Simulation of Vehicle Impact with Texas Concrete Median Barrier: Test Comparisons and Parameter Study", Highway Research Record No. 460, HRB, 1973, pp. 61-72.

3. Hirsch, T. J., Post, E. R., and Hayes, G. G., "Vehicle Crash Test and Evaluation of Median Barriers for Texas Highways", TTI Research Report 146-4, Texas A&M University, College Station, Texas, September 1972.

4. Post, E. R., Hirsch, T. J., Hayes, G. G., and Nixon, J. F., "Vehicle Crash Test and Evaluation of Median Barriers for Texas Highways", Highway Research Record No. 460, HRB, 1973, pp. 97-113.

5. Lundstrom, L. C., Skeels, P. C., Englund, B. R., and Rogers, R. A., "A Bridge Parapet Designed for Safety," Highway Research Record No. 83, HRB, 1965, pp. 169-183.

6. Theiss, C. M., "Perspective Picture Output for Automobile Dynamic Simulation", CAL Report No. VJ-2251-V-2R, Cornell Aeronautical Laboratory, December 1968.

7. Weaver, G. D., and Marquis, E. L., "The Relation of Side Slope Design to Highway Safety (Combination of Slopes)", Final Report on NCHRP Project 20-7, Task Order No. 2/2, Report RF 626B, Texas Transportation Institute, Texas A&M University, October, 1973.

8. Ross, H. E. Jr., and Post, E. R., "Criteria for Guardrail Need and Location on Embankments, Volume I: Development of Criteria" Research Report 140-4, Texas Transportation Institute, Texas A&M University, April 1972.

9. Hutchinson, J. W. and Kennedy, T. W., "Medians of Divided Highways - Frequency and Nature of Vehicle Encroachments", Univ. of Ill. Engineering Experiment Station Bulletin 487, Urbana (1966).

10. Selby, S. M., "Standard Mathematical Tables" (CRC), Student Edition, 17th Edition, The Chemical Rubber Company, 1969, pages 581-588.

11. McHenry, R. R., and Deleys, N. J., "Vehicle Dynamics in Single-Vehicle Accidents-Validation and Extension of a Computer Simulation", Cornell Aeronautical Laboratory Report No. VJ-2251-V-3, December, 1968.

APPENDIX A. TEST VEHICLE DATA

TABLE A1. TEST VEHICLE PARAMETERS

ITEM	TEST NUMBER MB-1	MB-2	T4-1
Make	'65 Plymouth	'64 Plymouth	'63 Plymouth
Model	2 dr Hardtop	2 dr Hardtop	4 dr Sedan
Total Weight (lb)	4200	4200	3640
Wheel Weights (lb):			
Left Front	1100	1150	970
Right Front	1130	1090	900
Left Rear	990	970	870
Right Rear	970	990	900
Dimensions (in)[1]			
L_1	32.0	34.0	35.6
L_2	54.5	44.75	N.A.
L_3	55.0	53.0	52.4
L_4	21.0	21.0	N.A.
L_5	8.0	8.0	8.0
L_6	26.0	27.0	26.0
L_7	N.A.	N.A.	25.0
L_8	72.0	72.0	72.0
L_9	117.0	117.0	116.0
L_{10}	36.0	36.0	N.A.
L_{11}	N.A.	N.A.	15.0

[1] See Figure A1.

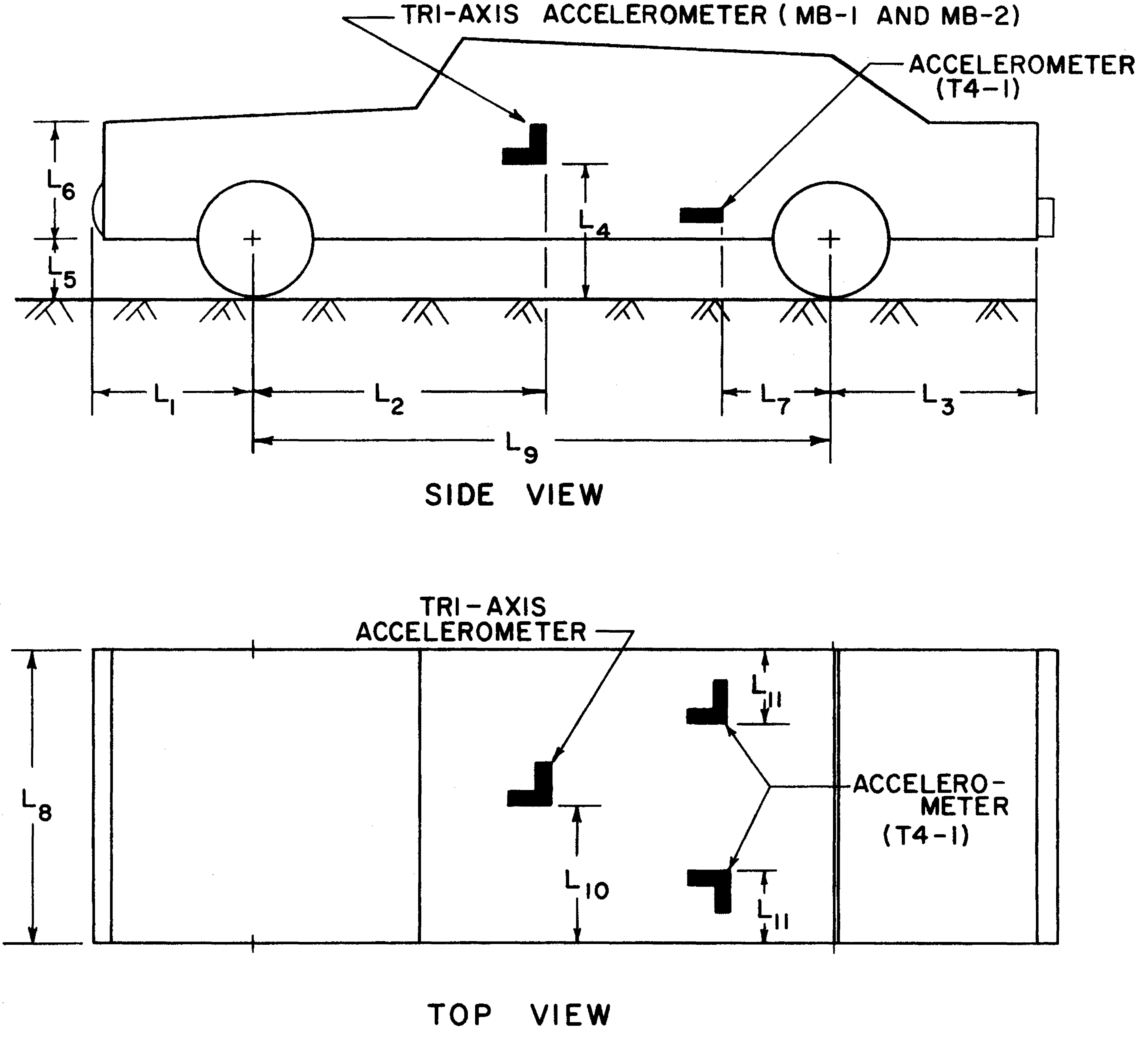

FIGURE A1 - TEST VEHICLE DIMENSIONAL PARAMETERS

APPENDIX B. MODIFICATIONS TO HVOSM

APPENDIX B

MODIFICATIONS TO HVOSM

Initial attempts at simulating Crash Test MB-2 were unsuccessful. After the program reached a certain point in the simulation, the solution process would enter an endless loop. Write statements were placed in the program to isolate the problem, which was found to be in subroutine SFORCE.

A listing of the as modified subroutine SFORCE is given in Figure B1. The problem and its correction was as follows.

The problem occurred when the barrier started to reload, after it had been initially loaded and then partially unloaded. At this point, the values of EPSL and DELX*SET were such that loop 38 became endless. The value of YBP in card 250 was always such that the solution would go to statement number 40 (card 404), bypassing the calculations of the vehicle crush force FNX. As a consequence, the force balance was never satisfied (card 407). Upon leaving loop 38, the logic would result in the solution being sent to statement number 250 and thence back to loop 38.

The modification to correct this problem is given in cards 462A, 462B, 462C and 462D. Statement number 100 limits the values of YBP, i.e., the position of the barrier can never be less than YPBO (its initial position).

Another modification to subroutine SFORCE concerned the computation of the hardpoint forces. Previously the hardpoint forces were computed at the beginning of loop 38 (see Appendix B of reference 2). The computation, done in loop 91, is now done just prior to the computation of the vehicle crush force (just after card 399). The hardpoint force computation involves cards 245 through 249 (moved without re-numbering). Note that in addition to the previous limitation, the hardpoint force is not computed if the lateral velocity of the hardpoint (VPT) is negative (see card 247). To accommodate this change, the value of VPT in SFORCE was brought, through the common block HARDPT, from subroutine RESFRC.

Upon completion of the above changes, simulation test MB-2 was again attempted. Various combinations of barrier and vehicle stiffness parameters were used in an attempt to simulate the crash test results. The results, however, were still not satisfactory. Since the problem appeared to involve the non-linear force-deflection algorithm used in the program, it was decided to use a simplified version of the algorithm. In effect, the algorithm assumed that the barrier was completely elastic, although the non-linear force-deflection relationship (5th order polynominal) was retained. A listing of the simplified NLDFL subroutine is given in Figure B2.

As a result of this modification, the researchers were able to converge on a set of vehicle and barrier parameters which resulted in good correlation between HVOSM and test results.

The values of the pertinent vehicle and barrier parameters were as given in Table B1.

TABLE B1. VEHICLE AND BARRIER STIFFNESS PARAMETERS

```
                          SPRUNG MASS-BARRIER IMPACT DATA
 BARRIER DIMENSIONS                                                   BARRIER LOAD DEFLECT.
(YB')0 =2400.000 INCHES    KV        =     2.000 LB/IN**3             SIGMAR 0 =      0.0
DELYB'  =    0.500   ''    SET       =     0.900 DEFL.RATIO           SIGMAR 1 =13466.0000
ZBT'    =  -27.000   ''    CONS      =     0.100 ENERGY RATIO         SIGMAR 2 =-2763.0000
ZBB'    =  -14.750   ''    MUB       =     0.300                      SIGMAR 3 =  250.8900
 VEHICLE DIMENSIONS        EPSILON V=      1.000 IN/SEC               SIGMAR 4 =   -9.8195
XVF     =   88.500 INCHES  EPSILON B=    500.000 LB                   SIGMAR 5 =    0.140230
XVR     = -115.500   ''    DELTB     =     0.0025 SEC                 SIGMAR 6 =      0.0
YV      =   36.000   ''                         (INTEG.INCR)          SIGMAR 7 =      0.0
ZVT     =  -14.000   ''                                               SIGMAR 8 =      0.0
ZVB     =   13.750   ''                                               SIGMAR 9 =      0.0
INDB =   3 (=1 RIGID BARRIER, FINITE VERT. DIM.)                      SIGMAR10 =      0.0
            =2  ''     ''   INFINITE  ''   ''  )
            =3 DEFORM.BARRIER,FINITE  ''   ''  )
            =4  ''     ''   INFINITE  ''   ''  )
                          STRUCTURAL HARDPOINTS RELATIVE TO C. G.
                                    X        Y         Z    STIFFNESS
                                         (INCHES)              LB/IN
                          POINT   1  81.000   16.500    5.000    2500.000
                          POINT   2  54.500   34.000    0.0      2500.000
                          POINT   3 -62.500   34.000    0.0      2500.000
```

It is important to note that, with the exception of the barrier to vehicle friction coefficient MUB, these same values were also used in the simulation of tests MB-1 and T4-1 and all runs described in Chapter IV. In both MB-1 and T4-1, correlation between HVOSM and test results were considered good.

As has been discussed in Chapter III, the value of MUB was different in each of the three test simulations. Those values were as follows:

TEST	MUB
MB-1	0.2
MB-2	0.3
T4-1	0.6

In the parametric studies of Chapter IV, the value of MUB was as follows:

RUNS*	MUB
1, 4, 7	0.2
2, 5, 8	0.3
3, 6, 9	0.6

* See Table 3.

```
C     SINGLE VEHICLE ACCIDENT SIMULATION - SUBROUTINE UPFRCE              SFOR
C     SINGLE VEHICLE ACCIDENT SIMULATION - SUBROUTINE SFORCE              SFOR
      SUBROUTINE SFORCE                                                   SFOR
      COMMON/INPT/PHI0,THETA0,PSI0,P0,Q0,R0,XCOP,YCOP,ZCOP,U0,V0,W0,A,B,SFOR
     1            DEL10,DEL20,DEL30,PHIR0,DEL10D,DEL20D,DEL30D,PHIR0D,TFSFOR
     2           ,TR,ZF,ZR,RHO,RW,AKT,SIGT,XLAMT,A1,A2,A3,AKRS,AMU,XMUR,SFOR
     3            XMS,XMUF,XIX,XIY,XIZ,XIXZ,CF,AKF,XLAMF,OMEGF,CFP,EPSF,SFOR
     4            RF,CR,AKR,XLAMR,OMEGR,CRP,EPSR,RR,TS,THMAX,DTCOMP,TO,  SFOR
     5            T1,DTCMP1,DTPRNT,MODE,FBAR,FM,AAA,HMAX,HMIN,BET,G,     SFOR
     6            HED(36),DADE(3),XIR,X1,Y1,Z1,X2,Y2,Z2,PHIC(50),DELR,   SFOR
     7            DELE,DDEL,NDEL,PSIF(50),TOF(50),TOR(50),TR,TF,TINCR,   SFOR
     8            XBDRY(10),YBDRY(10),ZGP(21,21),THG(21,21),PHIG(21,21),SFOR
     9            XB,XE,XINCR,NX,YB,YE,YINCR,NY,NBX,NBY,UVWMIN,PQRMIN    SFOR
      COMMON/INPT1/YC1P,YC2P,ZC2P,DELTC,PHIC1,PHIC2,AMUC,FJP(35),XIPS,   SFOR
     1            EPSP,OMGPS,AKPS,EPSPS,XPS,RWHJP,RWHJF,DRWHJ,INDCRB,    SFOR
     2            PSIFI0,PSIFD0                                          SFOR
      COMMON /INTG/NEQ,T,DT,VAR(50),DER(50)                              SFOR
      COMMON /DIMV/X1P,X2P,X3P,X4P,Y1P,Y2P,Y3P,Y4P,Z1P,Z2P,Z3P,Z4P,PHI1,SFOR
     1             PHI2,PHI3,PHI4,PSI1,PSI2,PSI3,PSI4,CAYW(4),CBYW(4),   SFOR
     2             CGYW(4),ZPGI(4),THGI(4),PHGI(4),CPG(4),SPG(4),CTG(4),SFOR
     3             STG(4),CAGZ(4),CBGZ(4),CGGZ(4),D1(4),D2(4),D3(4),     SFOR
     4             XLM1(4),XLM2(4),XLM3(4),AMTX(3,3),CMTX(3,4),XGPP(4),  SFOR
     5             YGPP(4),ZGPP(4),DMATX(10,11),DELTA(4),CAR(4),CBR(4),  SFOR
     6             CGR(4),FR(4),HI(4),FC(4),TI(4),AX(4),BX(4),CX(4),     SFOR
     7             CTXG(4),UG(4),STXG(4),AY(4),BY(4),CY(4),CPYG(4),      SFOR
     8             SPYG(4),VG(4),PSIIP(4),PHICI(4),CAC(4),CBC(4),CGC(4),SFOR
     9             FCXU(4),FCYU(4),FCZU(4),FS(4),CAXW(4),CBXW(4),CGXW(4)SFOR
      COMMON /DIMV/AS(4),BS(4),CS(4),CAS(4),CBS(4),CGS(4),BETP(4),       SFOR
     1             BETBR(4),FSXU(4),FSYU(4),FSZU(4),FRXU(4),FRYU(4),     SFOR
     2             FRZU(4),FXU(4),FYU(4),FZU(4),SI(4),F1FI(2),F1RI(2),   SFOR
     3             F2FI(2),F2RI(2),CAH(4),CBH(4),CGH(4)                  SFOR
      COMMON /COMP/SUMM,THETN,PHIN,PSIN,PI,RAD,GAM1,GAM2,GAM3,GAM4,GAM5,SFOR
     1             GAM6,GAM7,GAM8,GAM9,THETT,PHIT,PSIT,A12,A23,ZRC,TRC2,SFOR
     2             TFC2,TIZ,RHO2,RHOMUR,AMUF,RMUR,ZPR,TM4,RHMR2,AO2APB,  SFOR
     3             BO2APB,RETF,TSC2,RRTS,RROMUF,XMUFO2,AXMFO2,XMTFO4,    SFOR
     4             XIZR,RTR,RHMR2I,XIXP,XIZP,XIXZP,XIYZP,D1PD2,D1MD2,    SFOR
     5             ZRD3,ZRD3P,ZFD3P,ZFD12,TIZ2,TG61,DD1P2,DD1M2,RPR,PHRPSFOR
     6            ,TANTP,SPHTP,CPHTP,SECTP,SFXS,SFYS,SFZS,SNPS,SNTS,     SFOR
     7             SNPSS,TPR,CAY,CBY,CGY,CAX,CBX,CGX,SFYU,SFXU,SFYUF,    SFOR
     8             SFYUR,SFZU,COSTH,SINTH,COSPS,SINPS,COSPH,SINPH,ANG1,  SFOR
     9             ANG2,CPHI,SPHI,CPSI,SPSI,P1,P7,P3,P4,P5,P6,TX,TY,TZ   SFOR
      COMMON /COMP/TRH,DISTX,DISTY,DISTD,DISTS,D21,ZETA4,ZETA4D,ZETA3,   SFOR
     1             ZETA3D,SFZ1,SNPU,SNTU,HCGH1,HCGH2,HCGH3,HCGH4,TERM1,  SFOR
     2             TERM2,SNPSU,SNPR,HCBH1,HCBH2,HCBH3,HCBH4,HCAH1,HCAH2,SFOR
     3             HCAH3,HCAH4,UQ,WP,UR,QR,VP,PR,P2,Q2,R2,VR,WQ,PQ,PHIR2SFOR
     4            ,PHIRD2,RPHRD,GCTH,GSTH,GCTSP,GCTCP,XXX,YYY,IX,IY,XX1,SFOR
     5             XX2,YY1,YY2,THG1,THG2,PHG1,PHG2,ZZ1,ZZ2,LLL           SFOR
      COMMON /COMPN/ OMT2M1,FRSP(4),FRCP(4),OMEGT,ICBHIT,JCBHIT,         SFOR
     1               DPSINT,TANPC1,TANPC2,PHIC1P,PHIC2R,AMUCMP,PHI1D,    SFOR
     2               PHI2D,LCB1(4),LCB2(4),IHIT,AJMTX(3,3),BMTX(3,3),    SFOR
     3               SFRX(4),SFRY(4),SFRZ(4),T1PSI,T2PSI,XMU             SFOR
      COMMON/ADTNL/U1,U2,U3,U4,V1,V2,V3,V4,W1,W2,W3,W4,XTRA(300)         SFOR
      DIMENSION XP(4),YP(4),ZP(4),PHII(4),PSII(4),UI(4),VI(4),WI(4)      SFOR
      EQUIVALENCE (XP,X1P),(YP,Y1P),(ZP,Z1P),(PHII,PHI1),(PSII,PSI1),    SFOR
     1            (UI,U1),(VI,V1),(WI,W1)                                SFOR
      EQUIVALENCE (U,VAR(1)),(V,VAR(2)),(W,VAR(3)),(P,VAR(4)),(Q,VAR(5))SFOR
     1           ,(R,VAR(6)),(DEL1,VAR(7)),(DEL1D,VAR(8)),(DEL2,VAR(9)),SFOR
     2            (DEL2D,VAR(10)),(DEL3,VAR(11)),(DEL3D,VAR(12)),        SFOR
     3            (PHIR,VAR(13)),(PHIRD,VAR(14)),(THETTP,VAR(15)),       SFOR
```

FIGURE B1. LISTING OF AS-MODIFIED SUBROUTINE SFORCE

```
          (PHITP,VAR(16)),(PSITP,VAR(17)),(XCP,VAR(18)),
          (YCP,VAR(19)),(ZCP,VAR(20)),(PSIFI,VAR(21)),
          (PSIFID,VAR(22))
EQUIVALENCE (DU,DER(1)),(DV,DER(2)),(DW,DER(3)),(DP,DER(4)),
          (DQ,DER(5)),(DR,DER(6)),(DDEL1,DER(7)),(DDEL1D,DER(8))
         ,(DDEL2,DER(9)),(DDEL2D,DER(10)),(DDEL3,DER(11)),
          (DDEL3D,DER(12)),(DPHIP,DER(13)),(DPHIPD,DER(14)),
          (DTHTTP,DER(15)),(DPHITP,DER(16)),(DPSITP,DER(17)),
          (DXCP,DER(18)),(DYCP,DER(19)),(DZCP,DER(20)),
          (DPSIFI,DER(21)),(DDPSFI,DER(22))
DIMENSION YCIP(2)
LOGICAL LCB1,LCB2
COMMON/INPT2/A4,Y3P0,ZBTP,ZBBP,XVF,XVR,YV,ZVT,ZVB,AKV,SIGR(11),SFT
          ,CONS,AMUR,EPSV,EPSP,XM,EPST,DDD,INDB,DELYBP,
          DELTP, AU, DATDRV(9), XINPT(100)
COMMON/BARIER/FN,IBHIT,JBHIT,XCPNP(3),YCPNP(3),ZCPNP(3),XCPN(3),
             YCPN(3),ZCPN(3),AA1(17),BB1(17),CC1(17),RR1(17),
             AA2(17),BB2(17),CC2(17),RR2(17),CAB,CBB,CGB,CABT,
             CBBT,CGBT,RB,XBT,YBT,ZBT,XBB,YBB,ZBB,RR2P(17),
             YBPT,XNN(17),YNN(17),ZNN(17),XMTX(3,4),IDPT(17),IPT
             ,ININD,UNP(17),VNP(17),WNP(17),VMAX(4),I1,I2,I3,I4,
             XCPTP,YCPTP,ZCPTP,XCPBP,YCPBP,ZCPBP,YCPMP,AINTI,
             AINTP,SXR,SYR,SZR,SDEN,XRI,YRI,ZRI,FRICT,DFLBB,VTAN,
             FNP,FR,UPP,VRP,WRP,EPSL,XLDP,DELX,VL,NCYC,EEE,ENRGY,
             SWORK,SPENGY,DISS,IPLN,ILOAD
DIMENSION INDXPT(4)
EQUIVALENCE(INDXPT,I1)
EQUIVALENCE (YCIP,YC1P)
EQUIVALENCE (XIYP,XTRA(1)),(SPHIC,XTRA(2)),(CPHIC,XTRA(3))
EQUIVALENCE(NSEG,XTRA(4))
EQUIVALENCE (YBPTP,XTRA(7)),(PCAB,XTRA(8)),(PCBB,XTRA(9)),
          (PCGB,XTRA(10)),(PPRB,XTRA(11)),(CAB1,XTRA(12)),
          (CBB1,XTRA(13)),(CGB1,XTRA(14)),(RB1,XTRA(15))
EQUIVALENCE(NUNLD,XTRA(16))
EQUIVALENCE(NLDCTR,XTRA(17))
EQUIVALENCE (VDEF,XTRA(18)),(PVDEF,XTRA(19))
EQUIVALENCE(PSZR,XTRA(20))
COMMON/BARSTR/ XSTIO(3),YSTIO(3),ZSTIO(3),XSTI(3),YSTI(3),ZSTI(3),
            YSTIPO(3),XSTIP(3),YSTIP(3),ZSTIP(3),FNSTI(3),AKST(3)
COMMON/HAFOPT/ FRICF(4),UPT(4),VPT(4),WPT(4)
SFXS = 0.0
YBP = 0.0
SFYS = 0.0
SFZS = 0.0
SNPS = 0.0
SNTS = 0.0
SNPSS = 0.0
FN = 0.0
IBHIT = 0
IPLN = 0
NAXIS = 0
FRICT = 0.0
VTAN = 0.0
VMAX(1) = 0.0
NSLCF = 0
NUNLD=0
NUNLD2=0
YB1VF = 0.0
IF(INDB.EQ.0) RETURN
IB = (INDB+1)/2
```

FIGURE B1. CONTINUED

```
2 DO 3  I=1,3
  XCPNP(I) = XCP+AMTX(1,1)*XCPN(I)+AMTX(1,2)*YCPN(I)+AMTX(1,3)*
 1            ZCPN(I)
  YCPNP(I) = YCP+AMTX(2,1)*XCPN(I)+AMTX(2,2)*YCPN(I)+AMTX(2,3)*
 1            ZCPN(I)
  ZCPNP(I) = ZCP+AMTX(3,1)*XCPN(I)+AMTX(3,2)*YCPN(I)+AMTX(3,3)*
 1            ZCPN(I)
  YSTIPG(I)=YCP+AMTX(2,1)*XSTIG(I)+AMTX(2,2)*YSTIG(I)+AMTX(2,3)*ZSTI
 1G(I)
3 CONTINUE
  YPMAX = -1.0E30
4 DO 5  I=1,3
  IF(YCPNP(I).LT.YPMAX) GO TO 5
  YPMAX = YCPNP(I)
  NDX = I
5 CONTINUE
  XCPTP = XCP+AMTX(1,1)*XCPN(NDX)+AMTX(1,2)*YCPN(NDX)+AMTX(1,3)*ZVT
  YCPTP = YCP+AMTX(2,1)*XCPN(NDX)+AMTX(2,2)*YCPN(NDX)+AMTX(2,3)*ZVT
  ZCPTP = ZCP+AMTX(3,1)*XCPN(NDX)+AMTX(3,2)*YCPN(NDX)+AMTX(3,3)*ZVT
  XCPBP = XCP+AMTX(1,1)*XCPN(NDX)+AMTX(1,2)*YCPN(NDX)+AMTX(1,3)*ZVB
  YCPBP = YCP+AMTX(2,1)*XCPN(NDX)+AMTX(2,2)*YCPN(NDX)+AMTX(2,3)*ZVB
  ZCPBP = ZCP+AMTX(3,1)*XCPN(NDX)+AMTX(3,2)*YCPN(NDX)+AMTX(3,3)*ZVB
6 YCPMP = AMAX1(YCPTP,YCPBP)
  IF(YPPO-YCPMP.LT.5.0) IBHIT=1
  VDEF = AMAX1(YCPMP-YBPTP,0.0)
  IF(VDEF.LT.2.0*DELYBP) GO TO 41
  IF(MOD(INDP,2).EQ.0) GO TO 8
7 CABT = AMTX(3,1)
  CBBT = AMTX(3,2)
  CGBT = AMTX(3,3)
  TMP = ZPTP-ZCP
  XBT = -AMTX(1,1)*XCP-AMTX(2,1)*YCP+AMTX(3,1)*TMP
  YBT = -AMTX(1,2)*XCP-AMTX(2,2)*YCP+AMTX(3,2)*TMP
  ZBT = -AMTX(1,3)*XCP-AMTX(2,3)*YCP+AMTX(3,3)*TMP
  RBT = XBT*CABT+YBT*CBBT+ZBT*CGBT
  TMP = ZPBP-ZCP
  XBB = -AMTX(1,1)*XCP-AMTX(2,1)*YCP+AMTX(3,1)*TMP
  YBB = -AMTX(1,2)*XCP-AMTX(2,2)*YCP+AMTX(3,2)*TMP
  ZBB = -AMTX(1,3)*XCP-AMTX(2,3)*YCP+AMTX(3,3)*TMP
  RBB = XBB*CABT+YBB*CBBT+ZBB*CGBT
8 CAB = AMTX(2,1)
  CBB = AMTX(2,2)
  CGB = AMTX(2,3)
  TMP = YPPTP-YCP
  IF(ININD.LT.2.OR.CGB*PCBB.EQ.CBB*PCAB) GO TO 80
  XBPP = -AMTX(1,1)*XCP+AMTX(2,1)*TMP-AMTX(3,1)*ZCP
  YBPP = -AMTX(1,2)*XCP+AMTX(2,2)*TMP-AMTX(3,2)*ZCP
  ZBPP = -AMTX(1,3)*XCP+AMTX(2,3)*TMP-AMTX(3,3)*ZCP
  RBPP = XBPP*CAB+YBPP*CBB+ZBPP*CGB
  XMTX(1,1) = CAB
  XMTX(1,2) = CBB
  XMTX(1,3) = CGB
  XMTX(1,4) = RBPP
  XMTX(2,1) = PCAB
  XMTX(2,2) = PCBB
  XMTX(2,3) = PCGB
  XMTX(2,4) = PPBB
  XMTX(3,1) = 0
  XMTX(3,2) = 0
  XMTX(3,3) = 1
```

FIGURE B1. CONTINUED

```
      XMTX(3,4) = PS/P
      CALL SIMSOL(XMTX,4,3,I)
      XB1 = XMTX(1,4)
      YB1 = XMTX(2,4)
      ZB1 = XMTX(3,4)
      IF (XVR.LE.XB1.AND.XB1.LE.XVF.AND.ABS(YB1).LT.YV.AND.ZVT.LE.ZB1
     1.AND.ZB1.LE.ZVB) NAXIS = 1
      IF(NAXIS.EQ.0.AND.VDEF.LT.PVDEF.AND.XB1.LT.XVR) GO TO 41
      TMPA = CBB*PCGB-CGB*PCBB
      TMPB = CGB*PCAB-CAB*PCGB
      TMPC = CAB*PCBB-CBB*PCAB
      TMPAP = TMPB*CGB-TMPC*CBB
      TMPBP =-TMPC*CAB-TMPA*CGB
      TMPCP =-TMPA*CBB-TMPB*CAB
      TMPD = SQRT(TMPAP**2+TMPBP**2+TMPCP**2)
      CAB1 = TMPAP/TMPD
      CBB1 = TMPBP/TMPD
      CGB1 = TMPCP/TMPD
      RB1 = XB1*CAB1+YB1*CBB1+ZB1*CGB1
      YB1VF = 1.0E6
      IF(CBB1.NE.0.) YB1VF=(RB1-XVF*CAB1)/CBB1
   78 DO 79 I=12,17
      AA2(I) = CAB1
      BB2(I) = CBB1
      CC2(I) = CGB1
      RR2(I) = RB1
   79 CONTINUE
C PRESENT LOCATION OF HARDPOINTS IN SPACE FIXED COORDINATES
80    DO 81 I=1,3
      XSTIP(I)=XCP+AMTX(1,1)*XSTI(I)+AMTX(1,2)*YSTI(I)+AMTX(1,3)*ZSTI(I)
      YSTIP(I)=YCP+AMTX(2,1)*XSTI(I)+AMTX(2,2)*YSTI(I)+AMTX(2,3)*ZSTI(I)
      ZSTIP(I)=ZCP+AMTX(3,1)*XSTI(I)+AMTX(3,2)*YSTI(I)+AMTX(3,3)*ZSTI(I)
81    CONTINUE
      XRI=0.
      YRI = 0.0
      ZRI = 0.0
      AINTI = 0.0
      SXR = 0.0
      SYR = 0.0
      SZR = 0.0
      SDEN = 0.0
      FNX=0.
      FNX1=0.
      FB=0.
      FBFN=0.
      SFNST=0.
      NSEG = (YCPMP-YBPTP)/DELYBF+1.0
      IPLN=NSEG
      YBP=YBPTP+IPLN*DELYBP
      NSG111 = NSEG+1
      I111 = 1
    9 DO 38 I=I111,NSG111
      IPLNP=IPLN
      PYBP=YBP
      PDELBB=DELBB
      PPSXR=SXR
      PPSYR=SYR
      PPSZR=SZR
      PSDEN=SDEN
      PFNX=FNX
```

FIGURE B1. CONTINUED

```
      PENX1=ENX1
      PEB=EB
      PEBEN=EBEN
      PSENST=SENST
      SENST=0.
      IPLN = NSEG-I+1
      YBP = YBPTP+IPLN*DELYBP
      IF(YBP.LT.YBPO+EPSL+SET*DELX)GO TO 40
      TMP = YBP-YCP
      XBI = -AMTX(1,1)*XCP+AMTX(2,1)*TMP-AMTX(3,1)*ZCP
      YBI = -AMTX(1,2)*XCP+AMTX(2,2)*TMP-AMTX(3,2)*ZCP
      ZBI = -AMTX(1,3)*XCP+AMTX(2,3)*TMP-AMTX(3,3)*ZCP
      RBI = XBI*CAB+YBI*CBB+ZBI*CGB
      IPT = 0
   10 DO 15 J=1,17
      IDPT(J) = 0
      IF(PSIT.LE.0.0.AND.J.LE.2)GO TO 15
      IF(ININD.LT.2.AND.J.GT.11) GO TO 15
      IF(CAB.EQ.0..AND.(J.EQ.4.OR.J.EQ.5.OR.J.EQ.10.OR.J.EQ.11))GO TO 15
      IF(CBB.EQ.0..AND.(J.LE.2.OR.J.EQ.7.OR.J.EQ.8)) GO TO 15
      IF(CGB.EQ.0..AND.(J.EQ.3.OR.J.EQ.6.OR.J.EQ.9)) GO TO 15
      IF(CAB1*CBB.EQ.CBB1*CAB.AND.(J.EQ.12.OR.J.EQ.13)) GO TO 15
      IF(CBB1*CGB.EQ.CGB1*CBB.AND.(J.EQ.14.OR.J.EQ.15)) GO TO 15
      IF(CGB1*CAB.EQ.CAB1*CGB.AND.J.GE.16) GO TO 15
      IF(NAXIS.EQ.0.AND.J.GT.11) GO TO 15
   11 XMTX(1,1) = CAB
      XMTX(1,2) = CBB
      XMTX(1,3) = CGB
      XMTX(1,4) = RBI
   12 XMTX(2,1) = AA1(J)
      XMTX(2,2) = BB1(J)
      XMTX(2,3) = CC1(J)
      XMTX(2,4) = RR1(J)
   13 XMTX(3,1) = AA2(J)
      XMTX(3,2) = BB2(J)
      XMTX(3,3) = CC2(J)
      XMTX(3,4) = RR2(J)
14    CALL SIMSOL(XMTX,3,3,2)
      XNN(J) = XMTX(1,4)
      YNN(J) = XMTX(2,4)
      ZNN(J) = XMTX(3,4)
      IF(XNN(J).LT.XVP.OR.XNN(J).GT.XVF) GO TO 15
      IF(ABS(YNN(J)).GT.YV) GO TO 15
      IF(ZNN(J).LT.ZVT.OR.ZNN(J).GT.ZVB) GO TO 15
      IDPT(J) = 1
      IPT = IPT+1
      IPPT = J
   15 CONTINUE
      IF(IPPT.LE.11.AND.(NAXIS.EQ.1.AND.YB1VE.GT.YV.AND.ININD.EQ.2))
     1 GO TO 38
      IF(MOD(INDB,2).EQ.0) GO TO 23
      IF(CGB.EQ.0.0.AND.CGBT.EQ.0.0)GO TO 23
      RR2P(1) = RBT
      RR2P(2) = RBB
      RR2P(4) = RBT
      RR2P(5) = RBB
      RR2P(7) = RBT
      RR2P(8) = RBB
      RR2P(10) = RBT
      RR2P(11) = RBB
```

FIGURE B1. CONTINUED

```
      RR2P(12) = RBT
      RR2P(13) = RBP
      RR2P(14) = RBT
      RR2P(15) = RBP
      RR2P(16) = RBT
      RR2P(17) = RBP
   16 DO 22  J=1,17
      IF(PSIT.LE.0.0.AND.J.LE.2)GO TO 22
      IF(J.EQ.3.OR.J.EQ.6.OR.J.EQ.9) GO TO 22
      IF(CAB*CGBT.EQ.CGB*CABT.AND.(J.EQ.4.OR.J.EQ.5.OR.J.EQ.10.OR.
     1   J.EQ.11)) GO TO 22
      IF(CGB*CBBT.EQ.CBB*CGBT.AND.(J.LE.2.OR.J.EQ.7.OR.J.EQ.8)) GO TO 22
      IF(CAB*(CBB1*CGBT-CBBT*CGB1)-CAB1*(CBB*CGBT-CBBT*CGB)+CABT*(CBB*
     1   CGB1-CBB1*CGB).EQ.0.0.AND.J.GE.12) GO TO 22
      IF(J.GE.12.AND.IDPT(J).NE.1) GO TO 22
      IF(IDPT(1).EQ.1.AND.IDPT(2).EQ.1.AND.J.EQ.14) GO TO 173
      IF(IDPT(7).EQ.1.AND.IDPT(8).EQ.1.AND.J.EQ.15) GO TO 173
      IF(IDPT(4).EQ.1.AND.IDPT(5).EQ.1.AND.J.EQ.16) GO TO 173
      IF(IDPT(10).EQ.1.AND.IDPT(11).EQ.1.AND.J.EQ.17) GO TO 173
      XMTX(1,1) = CAB
      XMTX(1,2) = CBB
      XMTX(1,3) = CGB
      XMTX(1,4) = RBT
      IF(J.GE.12) GO TO 170
      XMTX(2,2) = BB1(J)
      XMTX(2,3) = CC1(J)
   17 XMTX(2,1) = AA1(J)
      XMTX(2,4) = RR1(J)
      GO TO 18
  170 XMTX(2,1) = AA2(J)
      XMTX(2,2) = BB2(J)
      XMTX(2,3) = CC2(J)
      XMTX(2,4) = RR2(J)
   18 XMTX(3,1) = CABT
      XMTX(3,2) = CBBT
      XMTX(3,3) = CGBT
      IF((IDPT(1).EQ.1.AND.J.EQ.14).OR.(IDPT(4).EQ.1.AND.J.EQ.16))
     1 GO TO 171
      IF((IDPT(8).EQ.1.AND.J.EQ.15).OR.(IDPT(11).EQ.1.AND.J.EQ.17))
     1 GO TO 172
      XMTX(3,4) = RR2P(J)
      GO TO 19
  171 XMTX(3,4) = RBB
      GO TO 19
  172 XMTX(3,4) = RBT
19    CALL SIMSOL(XMTX,3,3,3)
      IF(XMTX(1,4).LT.XVR.OR.XMTX(1,4).GT.XVF) GO TO 22
      IF(ABS(XMTX(2,4)).GT.YV) GO TO 22
      IF(XMTX(3,4).LT.ZVT.OR.XMTX(3,4).GT.ZVB) GO TO 22
      IF(IDPT(J).NE.0) GO TO 20
      IDPT(J) = 1
      GO TO 21
   20 IF(ABS(XMTX(3,4)).GE.ABS(ZNN(J)))GO TO 22
   21 XNN(J) = XMTX(1,4)
      YNN(J) = XMTX(2,4)
      ZNN(J) = XMTX(3,4)
      GO TO 22
  173 IDPT(J) = 0
      IPT = IPT-1
   22 CONTINUE
```

FIGURE B1. CONTINUED

```
   23 IF(IPT.LT.3) GO TO 28
   24 DO 25  J=1,17
      IF(IDPT(J).EQ.0) GO TO 25
      TMPU = U-YNN(J)*R +ZNN(J)*Q
      TMPV = V+XNN(J)*R -ZNN(J)*P
      TMPW = W+YNN(J)*P -XNN(J)*Q
      UNP(J)  =  AMTX(1,1)*TMPU+AMTX(1,2)*TMPV+AMTX(1,3)*TMPW
      VNP(J)  =  AMTX(2,1)*TMPU+AMTX(2,2)*TMPV+AMTX(2,3)*TMPW
      WNP(J)  =  AMTX(3,1)*TMPU+AMTX(3,2)*TMPV+AMTX(3,3)*TMPW
   25 CONTINUE
   26 DO 27  J=1,4
      VMAX(J)  =  -1.0E30
      INDXPT(J)  =  0
   27 CONTINUE
   28 DO 34  J=1,17
      IF(IDPT(J).EQ.0) GO TO 34
   29 DO 33  K=1,4
      IF(VNP(J).LT.VMAX(K)) GO TO 33
      IF(K.EQ.4) GO TO 32
      K1  =  K+1
   30 DO 31  L=K1,4
      M  =  4-L+K1
      VMAX(M)  =  VMAX(M-1)
      INDXPT(M)  =  INDXPT(M-1)
   31 CONTINUE
   32 VMAX(K)  =  VNP(J)
      INDXPT(K)  =  J
      GO TO 34
   33 CONTINUE
   34 CONTINUE
      IPT  =  4
      IF(INDXPT(4).EQ.0) IPT  =  3
   37 J3  =  I3
      J1  =  I1
      J2  =  I2
      J4  =  I4
      CALL AREA
      DO 91 IJ=1,3
      FNSTI(IJ)=0.
      IF(VPT(IJ+1).GE.0.0.AND.YSTIPO(IJ).GE.YBP) FNSTI(IJ) =
     1 AKST(IJ)*(YSTIPO(IJ) - YBP)
      SFNST=SFNST+FNSTI(IJ)
91    CONTINUE
      IF(IB.EQ.1) GO TO 38
      FNX1=AKV*DELYBP*SCBN
      FNX=FNX1+SFNST
      IF(NSLCE.NE.0) GO TO 38
   40 DELBB = AMAX1(YBP-YBPO,EPSL+SET*DELX)
      CALL NLDFRC
      FBFN=FB-FNX
      IF(EPSB.LT.FBFN)GOTO38
      IF(I.EQ.1)GOTO105
      IF(FBFN.GE.0.)GOTO105
      IF(ABS(FBFN).LT.ABS(PFBFN))GOTO105
      PRINT 1001,T,I,YBP,PYBP,FNX,PFNX
1001  FORMAT(T2,' T=',F7.4,' I=',I3,' YBP=',F10.4,' PYBP=',F10.4,' FNX='
     1,G13.5,' PFNX=' ,G13.5,' EQUILIB AT PREV SLICE RESET')
      IPLN=IPLNP
      YBP=PYBP
      DELBP=PDELBP
```

FIGURE B1. CONTINUED

```
      SXR=PPSXR
      SYR=PPSYR
      SZR=PPSZR
      SDEN=PSDEN
      FNX=PFNX
      FNX1=PFNX1
      FB=PFB
      SFNST=PSFNST
105   YBPT=AMAX1(YBP,YBP0+EPSL+SFT*DELX)
      NSLCE = NSLCE+1
      IF(NLDCTR.EQ.3)CALL NLDEL
      NUNLD2=0
      IF(NUNLD.EQ.0)GOTO38
      NUNLD2=1
      GOTO110
38    CONTINUE
110   DO 111 IJ=1,3
      IF(YSTIP(IJ).GT.YBPT)YSTIP(IJ)=YBPT
      AA=XSTIP(IJ)-XCP
      BB=YSTIP(IJ)-YCP
      CC=ZSTIP(IJ)-ZCP
      XSTI(IJ)=AMTX(1,1)*AA+AMTX(2,1)*BB+AMTX(3,1)*CC
      YSTI(IJ)=AMTX(1,2)*AA+AMTX(2,2)*BB+AMTX(3,2)*CC
      ZSTI(IJ)=AMTX(1,3)*AA+AMTX(2,3)*BB+AMTX(3,3)*CC
111   CONTINUE
      IF(NUNLD2.NE.0)GOTO103
      IF(NUNLD.NE.0) GO TO 100
      IF( IB .NE. 1)  GO TO 50
   45 NEGPT=0
      DO 46  J=1,IPT
      IF( VMAX(J) .LT.  0.0 )  NEGPT=NEGPT + 1
   46 CONTINUE
      IF( NEGPT .GE. IPT) GO TO 41
50    FN =AKV*DELYBP*SDEN
      FN1=FN +SFNST
      IF(ININD.EQ.0) ININD = 1
      IF(ABS(FN1).GT.10.0.AND.NUNLD.EQ.0) CALL RESFRC
      IF(NSLCE.EQ.0.AND.IB.EQ.1) GO TO 103
      IF(NSLCE.EQ.0) GO TO 100
  103 TMP = YBPT-YCP
      NUNLD2=0
      XBPP = -AMTX(1,1)*XCP+AMTX(2,1)*TMP-AMTX(3,1)*ZCP
      YBPP = -AMTX(1,2)*XCP+AMTX(2,2)*TMP-AMTX(3,2)*ZCP
      ZBPP = -AMTX(1,3)*XCP+AMTX(2,3)*TMP-AMTX(3,3)*ZCP
      FB = XBPP*CAB + YBPP*CBB + ZBPP*CGB
      GO TO 39
  100 IF(YBP.GT.YBP0) GO TO 250
      YBPT = YBP0
      FB = 0.0
      GO TO 103
  250 NUNLD = NUNLD+1
      NSG111 = NSG111+1
      I111 = NSG111
      GO TO 9
   39 NUNLD = 0
   41 IF(NLDCTR.EQ.3.AND.IPT.GE.3)WRITE(6,1000)T,XB1,YB1,IPT,J1,J2,J3,
     1         J4,XNN(J1),YNN(J1),ZNN(J1),XNN(J2),YNN(J2),ZNN(J2),
     2              XNN(J3),YNN(J3),ZNN(J3),XNN(J4),YNN(J4),ZNN(J4)
 1000 FORMAT(F7.4,2F7.1,5I3,12F8.1)
      NLDCTR = NLDCTR+1
      RETURN
      END
```

FIGURE B1. CONCLUDED

```
C     SINGLE VEHICLE ACCIDENT SIMULATION - SUBROUTINE NLDFL              NL
      SUBROUTINE NLDFL                                                   NL
      COMMON/INPT/PHIO,THETAO,PSIO,PO,QO,RO,XCOP,YCOP,ZCOP,UO,VO,WO,A,B,NL
     1            DEL10,DEL20,DEL30,PHIRO,DEL10D,DEL20D,DEL30D,PHIROD,TFNL
     2           ,TR,ZF,ZR,RHO,RW,AKT,SIGT,XLAMT,A1,A2,A3,AKRS,AMU,XMUR,NL
     3            XMS,XMUF,XIX,XIY,XIZ,XIXZ,CF,AKF,XLAMF,OMEGF,CFP,EPSF,NL
     4            RF,CR,AKR,XLAMR,OMEGR,CRP,EPSR,RR,TS,THMAX,DTCOMP,TO, NL
     5            T1,DTCMP1,DTPRNT,MODE,CBAR,EM,AAA,HMAX,HMIN,BET,G,     NL
     6            HED(36),DATE(3),XIR,X1,Y1,Z1,X2,Y2,Z2,PHIC(50),DELB,   NL
     7            DELF,DLCL,NDEL,PSIF(50),TOF(50),TOF(50),TB,TC,TINCR,   NL
     8            XBDRY(10),YBDRY(10),ZGP(21,21),THG(21,21),PHIG(21,21),NL
     9            XB,XE,XINCR,NX,YB,YE,YINCR,NY,NBX,NBY,UVWMIN,PQRMIN    NL
      COMMON/INPT1/YC1P,YC2P,ZC2P,DELTC,PHIC1,PHIC2,AMUC,FIP(35),XIPS,   NL
     1            CPSP,OMGPS,AKPS,EPSPS,XPS,RWHJB,RWHJE,DRWHJ,INDCRB,    NL
     2            PSIFIO,PSIFDO                                          NL
      COMMON /INTG/NEQ,T,DT,VAR(50),DER(50)                              NL
      COMMON /DIMV/X1P,X2P,X3P,X4P,Y1P,Y2P,Y3P,Y4P,Z1P,Z2P,Z3P,Z4P,PHI1,NL
     1            PHI2,PHI3,PHI4,PSI1,PSI2,PSI3,PSI4,CAYW(4),CBYW(4),    NL
     2            CGYW(4),ZPGI(4),THGI(4),PHGI(4),CPG(4),SPG(4),CTG(4),NL
     3            STG(4),CAGZ(4),CBGZ(4),CGGZ(4),D1(4),D2(4),D3(4),      NL
     4            XLM1(4),XLM2(4),XLM3(4),AMTX(3,3),CMTX(3,4),XGPP(4),   NL
     5            YGPP(4),ZGPP(4),DMATX(10,11),DELTA(4),CAR(4),CBR(4),   NL
     6            CGR(4),FF(4),HI(4),FC(4),TI(4),AX(4),BX(4),CX(4),      NL
     7            CTXG(4),UG(4),STXG(4),AY(4),BY(4),CY(4),CPYG(4),       NL
     8            SPYG(4),VG(4),PSIIP(4),PHICI(4),CAC(4),CBC(4),CGC(4),NL
     9            FCXU(4),FCYU(4),FCZU(4),FS(4),CAXW(4),CBXW(4),CGXW(4)NL
      COMMON /DIMV/AS(4),BS(4),CS(4),CAS(4),CBS(4),CGS(4),BETP(4),       NL
     1            BETBP(4),FSXU(4),FSYU(4),FSZU(4),FRXU(4),FRYU(4),      NL
     2            FRZU(4),FXU(4),FYU(4),FZU(4),SI(4),F1FI(2),F1RI(2),    NL
     3            F2FI(2),F2RI(2),CAH(4),CBH(4),CGH(4)                   NL
      COMMON /COMP/SUMM,THETN,PHIN,PSIN,PI,RAD,GAM1,GAM2,GAM3,GAM4,GAM5,NL
     1            GAM6,GAM7,GAM8,GAM9,THETT,PHIT,PSIT,A12,A23,ZRO,TRO2,NL
     2            TFO2,TIZ,RHO2,RHOMUR,AMUF,BMUR,ZPR,TM4,RHMR2,AO2APB,   NL
     3            BO2APB,RFTF,TSC2,RRTS,RROMUR,XMUFO2,AXMFO2,XMTFO4,     NL
     4            XIZR,RTR,RHMR2I,XIXP,XIZP,XIXZP,XIYZP,D1PD2,D1MD2,     NL
     5            ZFD2,ZFD3R,ZFD3P,ZFD12,TIZ2,TG61,DD1P2,DD1M2,RPR,PHRPNL
     6           ,TANTP,SPHTP,CPHTP,SECTP,SFXS,SFYS,SFZS,SNPS,SNTS,      NL
     7            SNPSS,TPR,CAY,CBY,CGY,CAX,CBX,CGX,SFYU,SFXU,SFYUF,     NL
     8            SFYUR,SFZU,COSTH,SINTH,COSPS,SINPS,COSPH,SINPH,ANG1,   NL
     9            ANG2,CPHI,SPHI,CPSI,SPSI,P1,P2,P3,P4,P5,P6,TX,TY,TZ    NL
      COMMON /COMP/TBH,DISTX,DISTY,DISTD,DISTS,D21,ZETA4,ZETA4D,ZETA3,   NL
     1            ZETA3D,SFZ1,SNPU,SNTU,HCGH1,HCGH2,HCGH3,HCGH4,TERM1,   NL
     2            TERM2,SNPSU,SNPF,HCBH1,HCBH2,HCBH3,HCBH4,HCAH1,HCAH2,NL
     3            HCAH3,HCAH4,UQ,WP,UR,QR,VP,PR,P2,Q2,R2,VR,WQ,PQ,PHIR2NL
     4           ,PHIRD2,RPHRD,GCTH,GSTH,GCTSP,GCTCP,XXX,YYY,IX,IY,XX1,NL
     5            XX2,YY1,YY2,THG1,THG2,PHG1,PHG2,ZZ1,ZZ2,LLL            NL
      COMMON /COMPN/ CMT2M1,FRSP(4),FRCP(4),OMEGT,ICBHIT,JCBHIT,         NL
     1              DPSINT,TANPC1,TANPC2,PHIC1P,PHIC2P,AMUCMP,PHI1D,     NL
     2              PHI2D,LCB1(4),LCB2(4),IHIT,AJMTX(3,3),BMTX(3,3),     NL
     3              SFRX(4),SFRY(4),SFRZ(4),T1PSI,T2PSI,XMU              NL
      COMMON/ADTNL/U1,U2,U3,U4,V1,V2,V3,V4,W1,W2,W3,W4,XTRA(300)         NL
      DIMENSION XP(4),YP(4),ZP(4),PHII(4),PSII(4),UI(4),VI(4),WI(4)      NL
      EQUIVALENCE (XP,X1P),(YP,Y1P),(ZP,Z1P),(PHII,PHI1),(PSII,PSI1),    NL
     1            (UI,U1),(VI,V1),(WI,W1)                                NL
      EQUIVALENCE (U,VAR(1)),(V,VAR(2)),(W,VAR(3)),(P,VAR(4)),(Q,VAR(5))NL
     1           ,(R,VAR(6)),(DEL1,VAR(7)),(DEL1D,VAR(8)),(DEL2,VAR(9)),NL
     2            (DEL2D,VAR(10)),(DEL3,VAR(11)),(DEL3D,VAR(12)),        NL
     3            (PHIR,VAR(13)),(PHIRD,VAR(14)),(THETTP,VAR(15)),       NL
     4            (PHITP,VAR(16)),(PSITP,VAR(17)),(XCP,VAR(18)),         NL
```

FIGURE B2. LISTING OF AS-MODIFIED SUBROUTINE NLDFL

```
     5              (YCP,VAR(19)),(ZCP,VAR(20)),(PSIFI,VAR(21)),            NLDF   59
     6              (PSIFID,VAR(22))                                        NLDF   60
      EQUIVALENCE  (DU,DER(1)),(DV,DER(2)),(DW,DER(3)),(DP,DER(4)),         NLDF   61
     1              (DQ,DER(5)),(DR,DER(6)),(DDEL1,DER(7)),(DDEL1D,DER(8))NLDF     62
     2             ,(DDEL2,DER(9)),(DDEL2D,DER(10)),(DDEL3,DER(11)),        NLDF   63
     3              (DDEL3D,DER(12)),(DPHIR,DER(13)),(DPHIRD,DER(14)),      NLDF   64
     4              (DTHITP,DER(15)),(DPHITP,DER(16)),(DPSITP,DER(17)),     NLDF   65
     5              (DXCP,DER(18)),(DYCP,DER(19)),(DZCP,DER(20)),           NLDF   66
     6              (DPSIFI,DER(21)),(DDPSFI,DER(22))                       NLDF   67
      DIMENSION YCIP(2)                                                     NLDF   68
      EQUIVALENCE  (YCIP,YC1P)                                              NLDF   69
      EQUIVALENCE  (XIYP,XTRA(1)),(SPHIC,XTRA(2)),(CPHIC,XTRA(3))           NLDF   70
      EQUIVALENCE  (YBPTP,XTRA(7)),(PCAB,XTRA(8)),(PCBB,XTRA(9)),           NLDF   71
     1              (PCGB,XTRA(10)),(PPPB,XTRA(11)),(CAB1,XTRA(12)),        NLDF   72
     2              (CBB1,XTRA(13)),(CGB1,XTRA(14)),(RB1,XTRA(15))          NLDF   73
      EQUIVALENCE(NUMLD,XTRA(16))                                           NLDF   74
      EQUIVALENCE(NLDCTR,XTRA(17))                                          NLDF   75
      EQUIVALENCE  (VDEF,XTRA(18)),(PVDEF,XTRA(19))                         NLDF   76
      LOGICAL LCB1,LCB2                                                     NLDF   77
      COMMON/INPT2/A4,YBP0,ZBTP,ZBBP,XVF,XVR,YV,ZVT,ZVB,AKV,SIGR(11),SFTNLDF   78
     1              ,CONS,AMUB,EPSV,EPSB,XM,EPST,DDD,INDB,DELYBP,           NLDF   79
     2               DELTF, AO, DATDRV(9), XINPT(100)                       NLDF   80
      COMMON/BARITR/EN,IBHIT,JBHIT,XCPNP(3),YCPNP(3),ZCPNP(3),XCPN(3),      NLDF   81
     1                YCPN(3),ZCPN(3),AA1(17),BB1(17),CC1(17),RR1(17),      NLDF   82
     2                AA2(17),BB2(17),CC2(17),RR2(17),CAB,CBB,CGB,CABT,     NLDF   83
     3                CBBT,CGBT,RB,XBT,YBT,ZBT,XBB,YBB,ZBB,RR2P(17),        NLDF   84
     4                YBPT,XNN(17),YNN(17),ZNN(17),XMTX(3,4),IDPT(17),IPT   NLDF   85
     5               ,ININD,UNP(17),VNP(17),WNP(17),VMAX(4),I1,I2,I3,I4,    NLDF   86
     6                XCPTP,YCPTP,ZCPTP,XCPBP,YCPBP,ZCPBP,YCPMP,AINTI,      NLDF   87
     7                AINTP,SXR,SYR,SZR,SDEN,XRI,YRI,ZRI,FRICT,DELBB,VTAN,NLDF     88
     8                FNP,FB,URP,VRP,WRP,EPSL,XLDP,DFLX,VL,NCYC,EEE,ENRGY,NLDF     89
     9                SWORK,SPENGY,DISS,IPLN,ILOAD                          NLDF   90
      COMMON/HARDPT/ FRICF(4),UPT(4),VPT(4),WPT(4)
      DIMENSION INDXPT(4)                                                   NLDF   91
      EQUIVALENCE(INDXPT,I1)                                                NLDF   92
      REAL*8 ALIM1/'UPPER'/,ALIM2/'LOWER'/,XLIM                             NLDF   93
      EQUIVALENCE  (XF,XTRA(5)),(DELBBP,XTRA(6))                            NLDF   94
      WRITE(6,500) YBPT,YBPTP,DELBB                                         NLDF   95
  500 FORMAT(/,I3,'NLDFL',2X,7E13.6,/)                                      NLDF   96
    1 XLP = VMAX11                                                          NLDF   97
      VSIGN = 0.0                                                           NLDF   98
      VMAX11 = (YBPT-YBPTP)/DT                                              NLDF   99
      IF(ABS(VMAX11).LT.0.001) VMAX11 = 0.0                                 NLDF  99A
      VMAX(1) = VMAX11                                                      NLDF  100
  203 XL = DELBB                                                            NLDF  107
      EPSP = EPSL                                                           NLDF  108
      XVLP = VL                                                             NLDF  109
    2 VL = XL-EPSL                                                          NLDF  110
      FB = SIGR(1)                                                          NLDF  117
      XX = VL                                                               NLDF  118
      YY = VPT(1)                                                           NLDF  119
    4 DO 5  I=2,6                                                           NLDF  120
      J = I+5                                                               NLDF  121
      FB = FB+SIGR(I)*XX+SIGR(J)*YY                                         NLDF  122
      XX = XX*VL                                                            NLDF  123
      YY = YY*VPT(1)                                                        NLDF  124
    5 CONTINUE                                                              NLDF  125
      ILOAD = 0                                                             NLDF  126
      GO TO 13                                                              NLDF  127
   13 ENGY = (XF+FB)*(VL+EPSL-EPSP-XVLP)/2.0                                NLDF  179
```

FIGURE B2. CONTINUED

```
      ENRGY = ENRGY+ENGY                                                NLDF
      EPL = ENGY                                                        NLDF
      EMI = 0.0                                                         NLDF
      GO TO 15                                                          NLDF
   14 EMI = ENGY                                                        NLDF
      EPL = 0.0                                                         NLDF
   15 EEE = EEE+CONS*EPL+EMI                                            NLDF
  300 XF = FB                                                           NLDF
      WRITE(6,400) FB,EPSL,DELX,CD0,CD1,CD2,VSIGN,DELBB,ILOAD           NLDF1
  400 FORMAT(/,2X.8E12.4,2X,I2,/)                                       NLDF1
      RETURN                                                            NLDF
      ENTRY NLDFRC                                                      NLDF
   16 WL = DELBB-EPSL                                                   NLDF
      IF(ILOAD.NE.0)GO TO 19                                            NLDF
      XX = WL                                                           NLDF
      YY = VPT(1)                                                       NLDF
      FB = SIGR(1)                                                      NLDF
   17 DO 18 I=2,6                                                       NLDF
      J = I+5                                                           NLDF
      FB = FB+SIGR(I)*XX+SIGR(J)*YY                                     NLDF
      XX = XX*WL                                                        NLDF
      YY = YY*VPT(1)                                                    NLDF
   18 CONTINUE                                                          NLDF
      GO TO 20                                                          NLDF
   19 IF(WL-SET*DELX.GT.0.0)GO TO 100                                   NLDF
      FB = 0.0                                                          NLDF
      RETURN                                                            NLDF
  100 FB = CD0+CD1*WL+CD2*WL**2                                         NLDF
   20 FB = AMAX1(FB,0.0)                                                NLDF
      RETURN                                                            NLDF
      END                                                               NLDF
```

FIGURE B2. CONCLUDED

APPENDIX C. TEST VEHICLE DAMAGE COSTS

Jack Winslow Body Shop

COMPLETE BODY WORK ★ WRECKS RE-BUILT ★ WRECKER SERVICE

HIGHWAY 6 S. AT GRAHAM RD. — P. O. BOX 9085
COLLEGE STATION, TEXAS 77840

JACK WINSLOW, Sr.
JACK WINSLOW, Jr.
PHONE 846-1415

OWNER V15-1 DATE

ADDRESS PHONE

YEAR MAKE BODY STYLE

MILEAGE LICENSE NO IDENTIFICATION NO.

APPRAISED FOR: APPRAISER:

	FRONT	HRS.	PARTS	NET			HRS.	PARTS	NET
1	Bumper	1.0	24 5?			Battery			
	Arms					Aerial			
	Guard					Headlamp			
	Guard Rail				1	Door	2.2	78 25	
	Gravel Guard				1	Sealed Beam	0.3	3 25	
						Retainer			
	REAR								
	Bumper				1	Park'g Lamp	0.3	7 75	
	Arms					Side Lamp			
	Guard								
	Guard Rail				1	Tail Light [illegible]			
						License Lt.			
	Frame					Horn			
						Wheel			
1	Grill Panel	1.0	58 00			Hub Cap			
	Moulding					FRONT SUSP.			
						Hub & Drum			
1	Medallion	—	3 60			Knuckle			
	Extension					UpCont.Arm Shaft			
						Lr.Cont.Arm Shaft			
	Radiat'r Core					Ball Joints			
	Core Supp'rt								
	Core Baffle					Frt. System			
	Fan					Tie Rod			
	Water Pump					Drag Link			
	Hose					Steer'g Gear			
						Steer'g Wheel			
	Air Cond.					Horn Ring			
	Condenser					Tire			
	Receiver								
	Line					REAR SUSP.			
A	Hood	2.0							
	Hood Mould'g					Eng.Trans.& Fuel			
	Hood Lock Plt.								
	Hood Hinges								
	Medallion					Motor Supp't			
						Tail Pipe			
1	Fender	3.0	76 00			Gas Tank			
	Moulding								
	Name Plate								
1	Skirt [illegible]	1.0	15 60			Windsh'ld			
						Moulding			
	Fender					Moulding			
	Moulding								
	Name Plate					Top			
	Skirt								

		HRS.	PARTS	NET
	Quarter R. INNER OUTER			
5	Quarter L. INNER OUTER	2.0		
	Quarter Ext.			
	Moulding			
2	Ornaments		11 20	
	Rocker Pnl			
	Moulding			
	Cent'r Post			
5	Door		4.0	
	Glass TINT CLEAR			
	Door Handle			
	Moulding			
	Door			
	Glass TINT CLEAR			
	Door Handle			
	Moulding			
	Trunk Lid			
	Hinge			
	Medallion			
	Lower Panel			
	Floor			
	Seat			
	Seat Adj.			
V	Painting	7.3		21 00
	Under Coat			
	GROSS TOTAL			

LABOR 27.1 HRS.	9.00	243	90
PARTS LESS %	$	211	25
NET		21	00
TAX		11	61
WRECKER			
TOTAL		482	76
LESS DEPRECIATION			
NET TOTAL			

ON AUTHORIZATION BY OWNER, WE AGREE TO COMPLETE AND GUARANTEE REPAIRS AS PER APPRAISAL.

GARAGE

ACCEPTED BY

Code: A-Align; 1-2-New; OH-Overhaul; S-Straighten; R-Repair

THIS IS NOT AN AUTHORIZATION FOR REPAIRS

FIGURE C1. REPAIR COSTS, MB-1 AUTOMOBILE
(60 MPH/8 DEGREES)

Jack Winslow Body Shop

COMPLETE BODY WORK ★ WRECKS RE-BUILT ★ WRECKER SERVICE

HIGHWAY 6 S. AT GRAHAM RD. — P. O. BOX 9085

COLLEGE STATION, TEXAS 77840

JACK WINSLOW, Sr.
JACK WINSLOW, Jr.

PHONE 846-1415

OWNER MB-2 DATE

ADDRESS PHONE

YEAR MAKE BODY STYLE

MILEAGE LICENSE NO. IDENTIFICATION NO.

APPRAISED FOR: APPRAISER:

	FRONT	HRS	PARTS	NET			HRS.	PARTS	NET
1	Bumper	1.0	70.60			Battery			
2	Arms Rt		10.50			Aerial			
	Guard				1	Headlamp Cov	3	32.00	
	Guard Rail				1	Door	2	9.60	
1	Gravel Guard	1.0	14.00			Sealed Beam			
						Retainer			
	REAR								
	Bumper				1	Park'g Lamp	.2	7.85	
	Arms					Side Lamp			
	Guard								
	Guard Rail					Tail Light			
						License Lt.			
S	Frame	4.0				Horn			
					1	Wheel	.3	22.60	
	Grill Panel					Hub Cap			
	Moulding					FRONT SUSP.			
					1	Hub & Drum		40.00	
	Medallion				1	Knuckle	4.5	59.46	
	Extension				1	UpCont.Arm-Shaft		31.50	
					1	Lr.Cont.Arm-Shaft		22.00	
	Radiat'r Core					Ball Joints			
	Core Supp'rt								
	Core Baffle				A	Frt. System			15.50
	Fan				1	Tie Rod			
	Water Pump				1	Drag Link			
	Hose					Steer'g Gear			
						Steer'g Wheel			
	Air Cond.					Horn Ring			
	Condenser				1	Tire		42.00	
	Receiver				1	Valve Stem		2.00	
	Line					REAR SUSP.			
	Hood								
	Hood Mould'g					Eng.Trans.& Fuel			
	Hood Lock Plt.								
	Hood Hinges								
	Medallion					Motor Supp't			
						Tail Pipe			
1	Fender Rt	3.0	77.00			Gas Tank			
1	Moulding	.5	12.70						
	Name Plate				S	Rt Cowl	8.0		
1	Skirt Rt	.3	6.90		1	Windsh'ld	3.3	64.00	
						Moulding			
	Fender					Moulding			
	Moulding								
	Name Plate					Top			
	Skirt								

		HRS.	PARTS	NET
	Quarter R. INNER / OUTER			
1	Quarter L. INNER / OUTER	13.5	120.00	
	Quarter Ext.			
	Moulding			
S	Rt Lock Pillar	2.0		
	Rocker Pnl.			
	Moulding			
	Cent'r Post			
1	Door Rt	2.5	129.00	
	Glass TINT / CLEAR			
	Door Handle			
	Moulding			
1	Hinge		15.60	
	Door			
	Glass TINT / CLEAR			
	Door Handle			
	Moulding			
	Trunk Lid			
	Hinge			
	Medallion			
	Lower Panel			
	Floor			
	Seat			
	Seat Adj.			
	Painting	7.5		22.50
	Under Coat			
	GROSS TOTAL			

LABOR 47.9 HRS. @ 9.00	431.10
PARTS LESS 817.81 % $	817.81
NET	38.45
TAX	42.81
WRECKER	
TOTAL	1330.17
LESS DEPRECIATION	
NET TOTAL	

ON AUTHORIZATION BY OWNER, WE AGREE TO COMPLETE AND GUARANTEE REPAIRS AS PER APPRAISAL.

GARAGE ______________

ACCEPTED BY ______________

Code: A-Align 1-2-New
OH-Overhaul S-Straighten
R-Repair

THIS IS NOT AN AUTHORIZATION FOR REPAIRS

FIGURE C2. REPAIR COSTS, MB-2 AUTOMOBILE
(63.4 MPH/14.7 DEGREES)

Jack Winslow Body Shop

COMPLETE BODY WORK ★ WRECKS RE-BUILT ★ WRECKER SERVICE

HIGHWAY 6 S. AT GRAHAM RD. — P. O. BOX 9085
COLLEGE STATION, TEXAS 77840

JACK WINSLOW, Sr.
JACK WINSLOW, Jr.
PHONE 846-1415

OWNER T4-1 DATE
ADDRESS PHONE
YEAR MAKE BODY STYLE
MILEAGE LICENSE NO IDENTIFICATION NO.
APPRAISED FOR: APPRAISER:

	FRONT	HRS.	PARTS	NET
1	Bumper	1.0	56.00	
1	Arms		12.00	
	Guard			
	Guard Rail			
	Gravel Guard			
1	[illegible]	.5	16.20	
	REAR			
	Bumper			
	Arms			
	Guard			
	Guard Rail			
1	Valance		50.00	
1	Frame [illegible]	7.5	15.00	
1	[illegible]	.5	22.00	
1	[illegible] 13.		14.63	
1	Grill Panel		35.60	
	Moulding			
	Medallion			
	Extension			
1	Radiat'r Core	.5	35.00	
5	Core Supp'rt	2.0		
	Core Baffle			
1	Fan	.3	14.40	
	Water Pump			
	Hose			
	Air Cond.			
	Condenser			
	Receiver			
	Line			
1	Hood	1.1	90.00	
	Hood Mould'g			
	Hood Lock Plt.			
	Hood Hinges			
	Medallion			
1	Fender	3.0	74.00	
	Moulding			
	Name Plate			
1	Skirt [illegible]	.3	57.10	
1	[illegible]	3.0	50.00	
	Fender			
	Moulding			
	Name Plate			
	Skirt			

		HRS.	PARTS	NET
	Battery			
	Aerial			
1	Headlamp	.3	31.00	
1	Door	.2	11.00	
	Sealed Beam			
	Retainer			
1	Park'g Lamp	.3	22.00	
	Side Lamp			
	Tail Light			
	License Lt.			
	Horn			
1	[illegible]	—	2.00	
1	Wheel	.3	22.00	
1	Hub Cap	—	6.70	
	FRONT SUSP.			
1	Hub & Drum		40.00	
1	Knuckle	4.5	59.46	
1	UpCont.Arm-Shaft		32.50	
1	Lr.Cont.Arm-Shaft		22.02	
	Ball Joints			
A	Frt. System			13.95
1	Tie Rod			
1	Drag Link			
	Steer'g Gear			
	Steer'g Wheel			
	Horn Ring			
1	Tire		42.00	
	REAR SUSP.			
	Eng.Trans.&Fuel			
1	Motor Supp't	2.5	14.60	
	Tail Pipe			
	Gas Tank			
	Windsh'ld			
	Moulding			
	Moulding			
	Top			

		HRS.	PARTS	NET
	Quarter R. INNER / OUTER			
✓	Quarter L. INNER / OUTER	8.0		
	Quarter Ext.			
	Moulding			
	Rocker Pnl			
	Moulding			
	Cent'r Post			
5	Door RH	4.5		
	Glass TINT / CLEAR			
	Door Handle			
	Moulding			
S	Door LH	1.5		
	Glass TINT / CLEAR			
	Door Handle			
	Moulding			
	Trunk Lid			
	Hinge			
	Medallion			
	Lower Panel			
	Floor			
	Seat			
	Seat Adj.			
✓	Painting	9.5		27.00
	Under Coat			
	GROSS TOTAL			

LABOR 54.5 HRS.	9.00	488.70
PARTS LESS % $		856.69
NET		42.95
TAX		44.98
WRECKER		
TOTAL		1433.32
LESS DEPRECIATION		
NET TOTAL		

ON AUTHORIZATION BY OWNER, WE AGREE TO COMPLETE AND GUARANTEE REPAIRS AS PER APPRAISAL.

GARAGE ______________

ACCEPTED BY ______________

Code: A-Align 1-2-New
OH-Overhaul S-Straighten
R-Repair

THIS IS NOT AN AUTHORIZATION FOR REPAIRS

FIGURE C3. REPAIR COSTS, T4-1 AUTOMOBILE
(57.3 MPH/25 DEGREES)

Jack Winslow Body Shop

COMPLETE BODY WORK ★ WRECKS RE-BUILT ★ WRECKER SERVICE

HIGHWAY 6 S. AT GRAHAM RD. — P. O. BOX 9085

COLLEGE STATION, TEXAS 77840

JACK WINSLOW, Sr.
JACK WINSLOW, Jr.

PHONE 846-1415

OWNER ________ DATE ________

ADDRESS ________ PHONE ________

YEAR 63 MAKE Chev. BODY STYLE 4 dr.

MILEAGE ________ LICENSE NO. ________ IDENTIFICATION NO. CMB3

APPRAISED FOR: ________ APPRAISER ________

	FRONT	HRS.	PARTS	NET			HRS.	PARTS	NET
1	Bumper R	2.0	32 00			Battery			
2	Arms R		6 00			Aerial			
	Guard					Headlamp			
	Guard Rail					Door			
	Gravel Guard					Sealed Beam			
1	Bumper reinforc.		16 00			Retainer			
	REAR								
	Bumper					Park'g Lamp			
	Arms					Side Lamp			
	Guard								
	Guard Rail					Tail Light			
						License Lt.			
5	Frame ends	4.0				Horn			
					2	Wheel R		64 00	
	Grill Panel					Hub Cap			
	Moulding					FRONT SUSP.			
						Hub & Drum			
	Medallion					Knuckle			
	Extension					UpCont.Arm Shaft			
						Lr.Cont.Arm Shaft			
	Radiat'r Core					Ball Joints			
5	Core Supp'rt	2.0							
	Core Baffle				A	Frt. System			NC
	Fan					Tie Rod			
	Water Pump					Drag Link			
	Hose					Steer'g Gear			
						Steer'g Wheel			
	Air Cond.					Horn Ring			
	Condenser					Tire			
	Receiver								
	Line					REAR SUSP.			
5	Hood	3.0							
	Hood Mould'g					Eng.Trans.& Fuel			
	Hood Lock Plt.								
1	Hood Hinges R	.5	7 60						
	Medallion					Motor Supp't			
						Tail Pipe			
1	Fender R	2.5	25 00			Gas Tank			
	Moulding								
	Name Plate								
1	Skirt R	1	12 60			Windsh'ld			
						Moulding			
	Fender					Moulding			
	Moulding								
	Name Plate					Top			
	Skirt								

		HRS.	PARTS	NET
	Quarter R. INNER OUTER			
5	Quarter L. INNER OUTER	5.0		
	Quarter Ext.			
1	Moulding R	.3	12 60	
	Rocker Pnl.			
	Moulding			
	Cent'r Post			
5	Door R F	2.5		
	Glass TINT CLEAR			
	Door Handle			
	Moulding			
5	Door R R	1.5		
	Glass TINT CLEAR			
	Door Handle			
	Moulding			
	Trunk Lid			
	Hinge			
	Medallion			
	Lower Panel			
	Floor			
	Seat			
	Seat Adj.			
	Painting	4.0		44 00
	Under Coat			
	GROSS TOTAL			

LABOR 35.6 HRS.	9.00	320 40
PARTS LESS % $		214 20
NET		599 5
TAX		13 96
WRECKER		
TOTAL		613.71
LESS DEPRECIATION		
NET TOTAL		

ON AUTHORIZATION BY OWNER, WE AGREE TO COMPLETE AND GUARANTEE REPAIRS AS PER APPRAISAL.

GARAGE ________

ACCEPTED BY ________

Code: A-Align 1-2-New
OH-Overhaul S-Straighten
R-Repair

THIS IS NOT AN AUTHORIZATION FOR REPAIRS

FIGURE C4. REPAIR COSTS, CMB-3 AUTOMOBILE (60.9 MPH/7 DEGREES)

Jack Winslow Body Shop

COMPLETE BODY WORK ★ WRECKS RE-BUILT ★ WRECKER SERVICE

HIGHWAY 6 S. AT GRAHAM RD. — P. O. BOX 9085
COLLEGE STATION, TEXAS 77840

JACK WINSLOW, Sr.
JACK WINSLOW, Jr.
PHONE 846-1415

OWNER	DATE
ADDRESS 63 Chev of Sl	PHONE
YEAR	MAKE
BODY STYLE C M B 4	
MILEAGE	LICENSE NO.
IDENTIFICATION NO.	
APPRAISED FOR	APPRAISER

	FRONT	HRS.	PARTS	NET			HRS.	PARTS	NET
2	Bumper Frame	2.0	4500			Battery			
2	Arms		600			Aerial			
	Guard				1	Headlamp	1.0	3400	
	Guard Rail				2	Door		1200	
1	Gravel Guard		1400			Sealed Beam			
1	reinforcement		1600			Retainer			
	REAR								
	Bumper					Park'g Lamp	.3	720	
	Arms					Side Lamp			
	Guard								
	Guard Rail					Tail Light			
						License Lt.			
5	Frame	15.0				Horn			
					1	Shroud		1300	
					1	Wheel		2200	
1	Grill Panel		3300			Hub Cap			
	Moulding					FRONT SUSP.			
					1	Hub & Drum		3400	
	Medallion				1	Knuckle		3300	
	Extension				1	UpCont.Arm Shaft	4.0	2500	
					1	Lr.Cont.Arm Shaft		3000	
1	Radiat'r Core	1.0	9200		2	Ball Joints		2400	
1	Core Supp'rt	2.0	3700		1	Spring		1200	
	Core Baffle				A	Frt. System			895
1	Fan	.3	440		1	Tie Rod		1125	
	Water Pump					Drag Link			
	Hose					Steer'g Gear			
						Steer'g Wheel			
	Air Cond.					Horn Ring			
	Condenser					Tire			
	Receiver								
	Line					REAR SUSP.			
	Hood								
	Hood Mould'g					Eng.Trans.& Fuel			
	Hood Lock Plt.								
2	Hood Hinges	1.0	1520						
	Medallion				2	Motor Supp't	5.0	1400	
						Tail Pipe			
1	Fender	2.5	2510			Gas Tank			
1	Moulding								
	Name Plate				5	Cowling	6.0		
1	Skirt	1.0	1600		1	Windsh'ld	5.0		14700
1	Left		600			Moulding			
5	Fender RH	3.0				Moulding			
	Moulding								
	Name Plate					Top			
	Skirt								

		HRS.	PARTS
	Quarter R. INNER / OUTER		
5	Quarter L. INNER / OUTER	5.0	
	Quarter Ext.		
1	Moulding	.3	260
5	Rocker Pnl	3.5	
	Moulding		
	Cent'r Post		
5	Door LH, Glass TINT CLEAR	6.0	
	Door Handle		
	Moulding		
5	Door RH, Glass TINT CLEAR	1.5	
	Door Handle		
	Moulding		
	Trunk Lid		
	Hinge		
	Medallion		
	Lower Panel		
	Floor		
	Seat		
	Seat Adj.		
	Painting	12.0	
	Under Coat		
	GROSS TOTAL		

LABOR 72.4 HRS. @ 9.00	651
PARTS LESS % $	643
NET	2,10[illegible]
TAX	42[illegible]
WRECKER	
TOTAL	15[illegible]8
LESS DEPRECIATION	
NET TOTAL	

ON AUTHORIZATION BY OWNER, WE [illegible] TO COMPLETE AND GUARANTEE R[illegible] AS PER APPRAISAL.

GARAGE

ACCEPTED BY

Code: A-Align, 1-2-New, OH-Overhaul, S-Straighten, R-Repair

THIS IS NOT AN AUTHORIZATION FOR REPAIRS

FIGURE C5. REPAIR COSTS, CMB-4 AUTOMOBILE
(60.7 MPH/15 DEGREES)

Jack Winslow Body Shop

COMPLETE BODY WORK ★ WRECKS RE-BUILT ★ WRECKER SERVICE

HIGHWAY 6 S. AT GRAHAM RD. — P. O. BOX 9085
COLLEGE STATION, TEXAS 77840

JACK WINSLOW, Sr.
JACK WINSLOW, Jr.
PHONE 846-1415

OWNER ____ DATE ____
ADDRESS ____ PHONE ____
YEAR 73 MAKE [illegible] BODY STYLE C-MB 1
MILEAGE ____ LICENSE NO. ____ IDENTIFICATION NO. ____
APPRAISED FOR: ____ APPRAISER: ____

	FRONT	HRS.	PARTS	NET			HRS.	PARTS	NET
	Bumper	1.0	60.00			Battery			
2	Arms		9.10			Aerial			
1	~~Guard~~ [illegible]	.5	12.20		1	Headlamp	1.0	22.65	
	Guard Rail				1	Door		36.0	
1	Gravel Guard	1.0	22.00			Sealed Beam			
						Retainer			
	REAR								
	Bumper				1	Park'g Lamp		7.20	
	Arms					Side Lamp			
	Guard								
	Guard Rail					Tail Light			
5	[illegible]	10.0				License Lt			
1	Frame	5.0	233.00			Horn			
						Wheel		31.62	
	Grill Panel	1.0	35.00			Hub Cap			
	Moulding					FRONT SUSP.			
						Hub & Drum		7.00	
	Medallion				1	Knuckle	4.0	37.97	
	Extension				1	UpCont.Arm-Shaft		6.82	
					1	Lr.Cont.Arm Shaft		21.73	
1	Radiat'r Core	1.0	88.52		1	Ball Joints		18.31	
1	Core Supp'rt	5.2	35.40						
	Core Baffle				1	Frt. System			15.95
1	Fan	.3	4.60			Tie Rod			
1	Water Pump	1.0	23.17			Drag Link			
	Hose					Steer'g Gear			
						Steer'g Wheel			
	Air Cond.					Horn Ring			
	Condenser					Tire			
	Receiver								
	Line					REAR SUSP.			
1	Hood	1.0	88.20						
	Hood Mould'g					Eng. Trans. & Fuel			
	Hood Lock Plt.								
	Hood Hinges								
	Medallion					Motor Supp't			
						Tail Pipe			
1	Fender	2.5	72.00			Gas Tank			
	Moulding								
	Name Plate				5	[illegible]	8.0		
1	Skirt		18.57			Windsh'ld	2.1		130.00
3	[illegible]	1.0	23.57			Moulding			
	Fender					Moulding			
	Moulding								
	Name Plate					Top			
	Skirt								

		HRS.	PARTS	NET
	Quarter R. INNER/OUTER			
	Quarter L. INNER/OUTER			
	Quarter Ext.			
	Moulding			
	Rocker Pnl.			
	Moulding			
5	Cent'r Post	2.0		
5	Door	2.0		
	Glass TINT/CLEAR			
	Door Handle			
	Moulding			
	Door			
	Glass TINT/CLEAR			
	Door Handle			
	Moulding			
	Trunk Lid			
	Hinge			
	Medallion			
	Lower Panel			
	Floor			
	Seat			
	Seat Adj.			
	Painting	7.0		280.00
	Under Coat			
	GROSS TOTAL			

LABOR 60.0 HRS. 9.00		540.00
PARTS LESS % $		739.13
NET		173.95
TAX		45.65
WRECKER		
TOTAL		1,498.73
LESS DEPRECIATION		
NET TOTAL		

ON AUTHORIZATION BY OWNER, WE AGREE TO COMPLETE AND GUARANTEE REPAIRS AS PER APPRAISAL.

GARAGE ____

ACCEPTED BY: ____

Code: A-Align 1-2-New
OH-Overhaul S-Straighten
R-Repair

THIS IS NOT AN AUTHORIZATION FOR REPAIRS

FIGURE C6. REPAIR COSTS, CMB-1 AUTOMOBILE (62.4 MPH/25 DEGREES)

APPENDIX D. PATH AND ENCROACHMENT ANGLE PLOTS

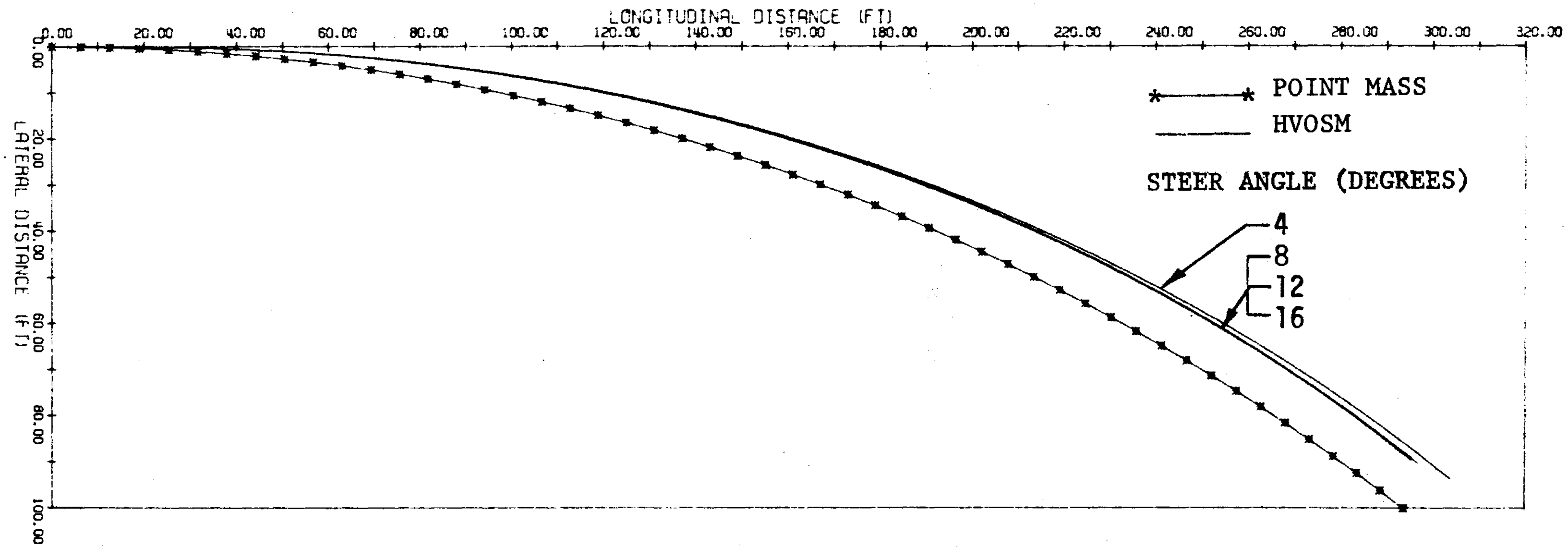

FIGURE D1. VEHICLE PATH, μ = 0.5

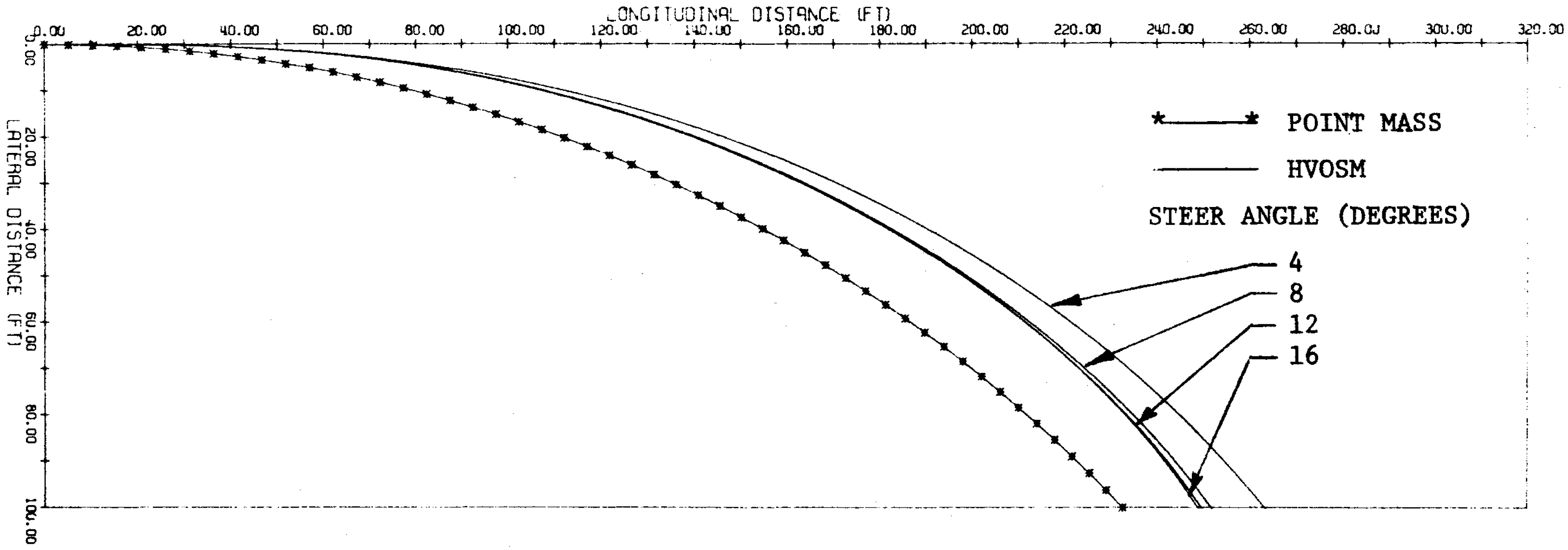

FIGURE D2. VEHICLE PATH, $\mu = 0.75$

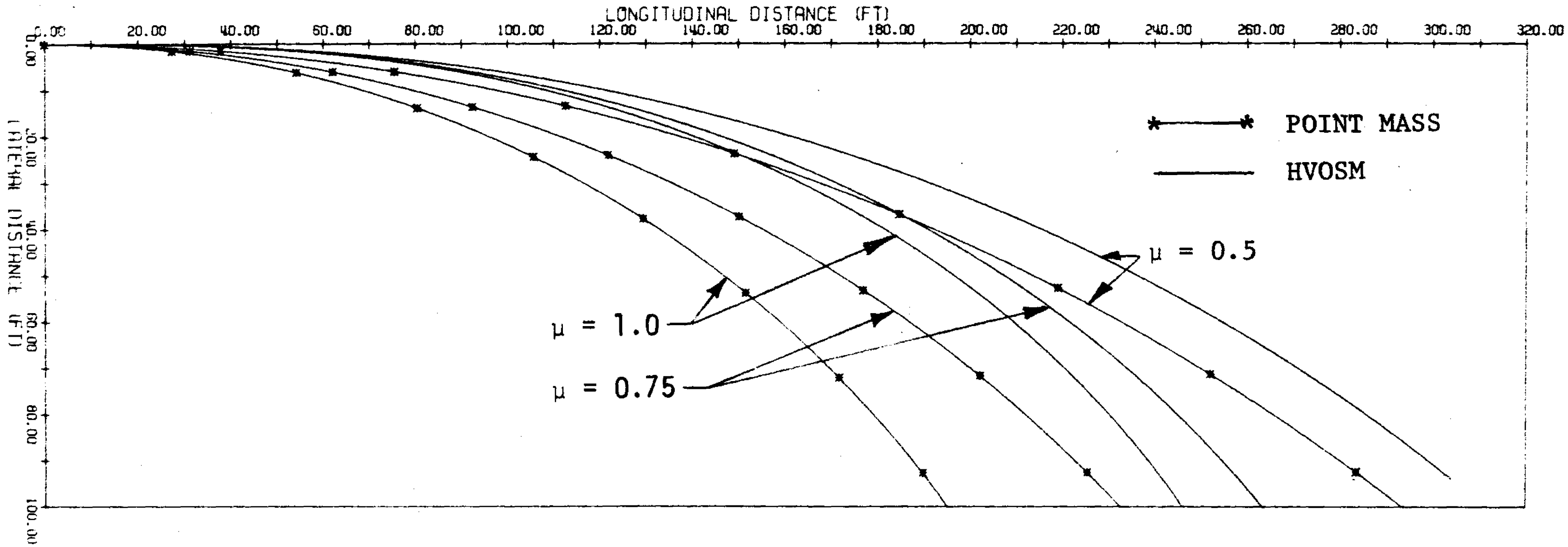

FIGURE D3. VEHICLE PATH, STEER ANGLE = 4 DEGREES

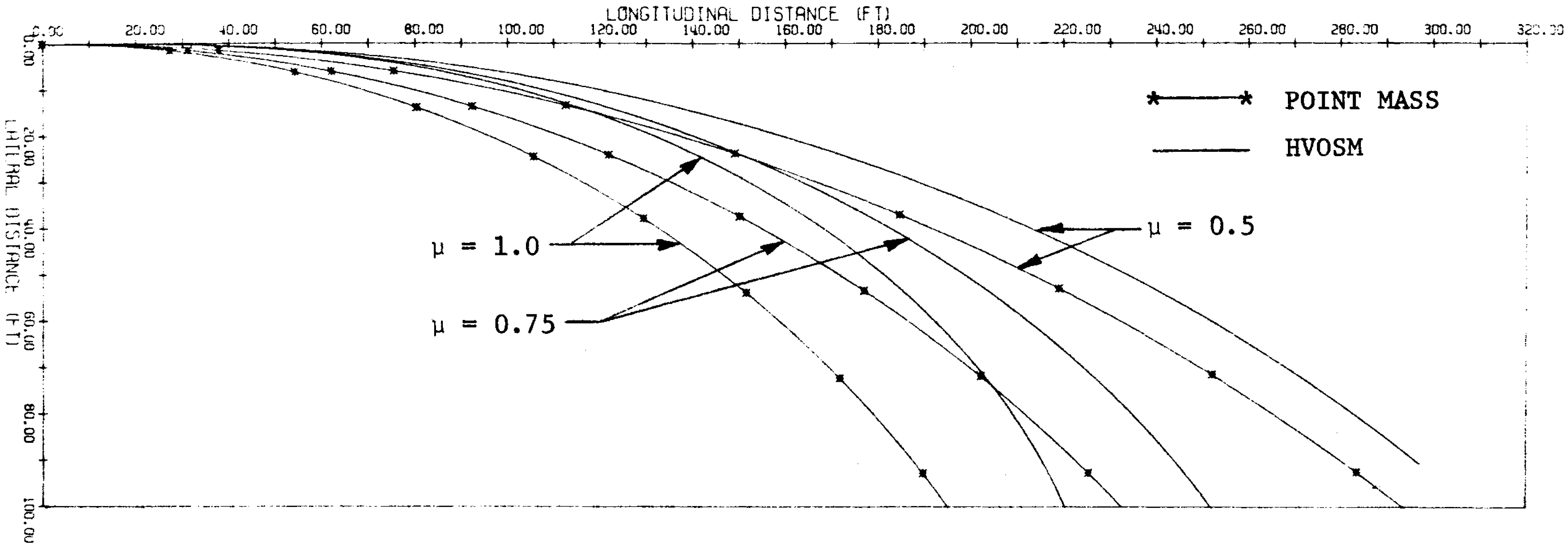

FIGURE D4. VEHICLE PATH, STEER ANGLE = 8 DEGREES

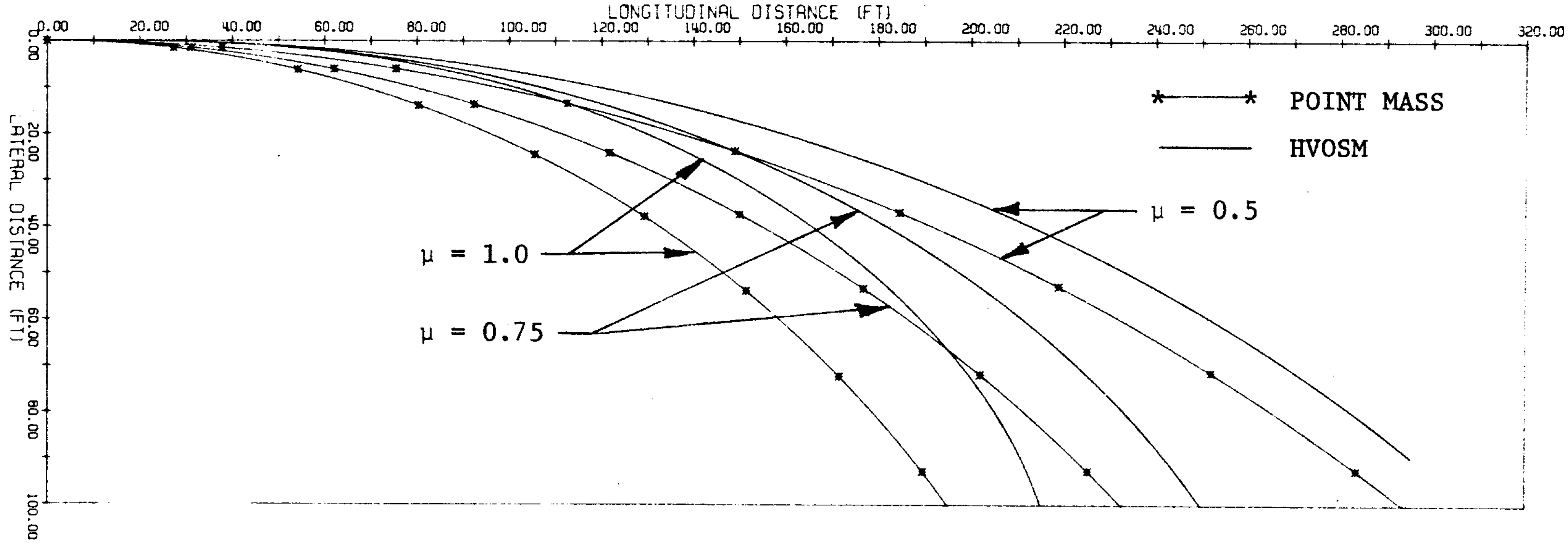

FIGURE D5. VEHICLE PATH, STEER ANGLE = 12 DEGREES

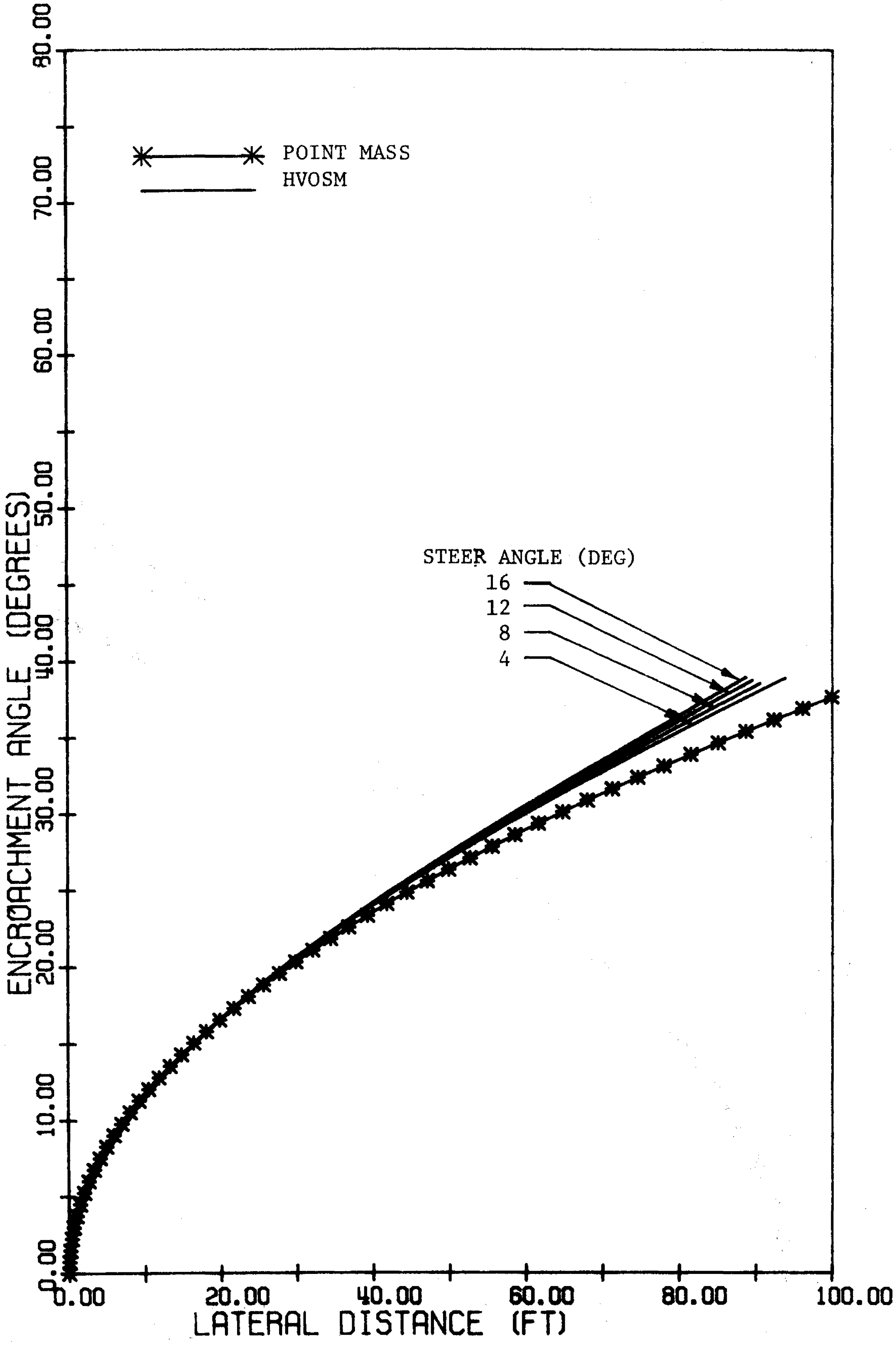

FIGURE D6. ENCROACHMENT ANGLES, $\mu = 0.5$

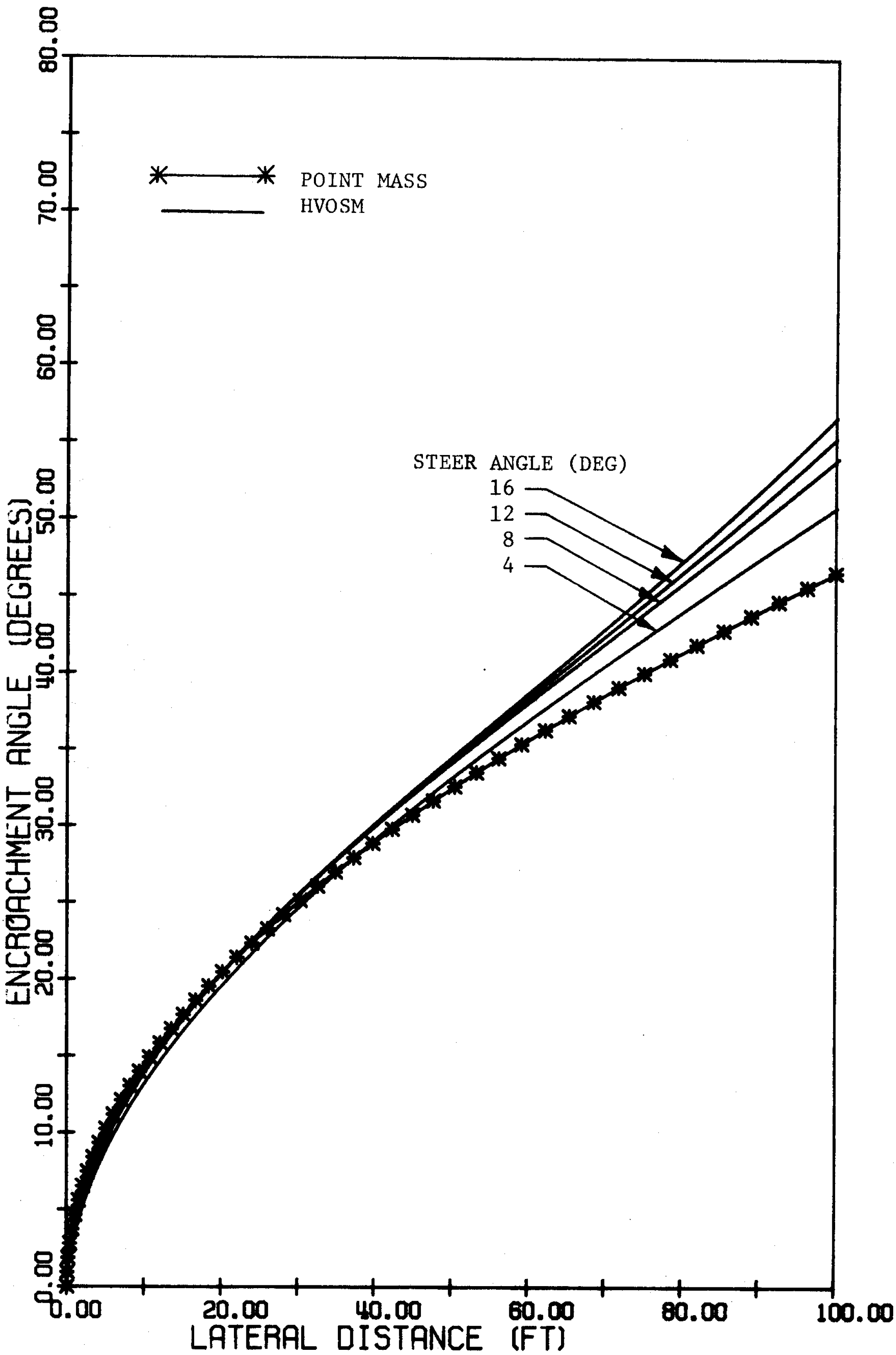

FIGURE D7. ENCROACHMENT ANGLES, $\mu = 0.75$

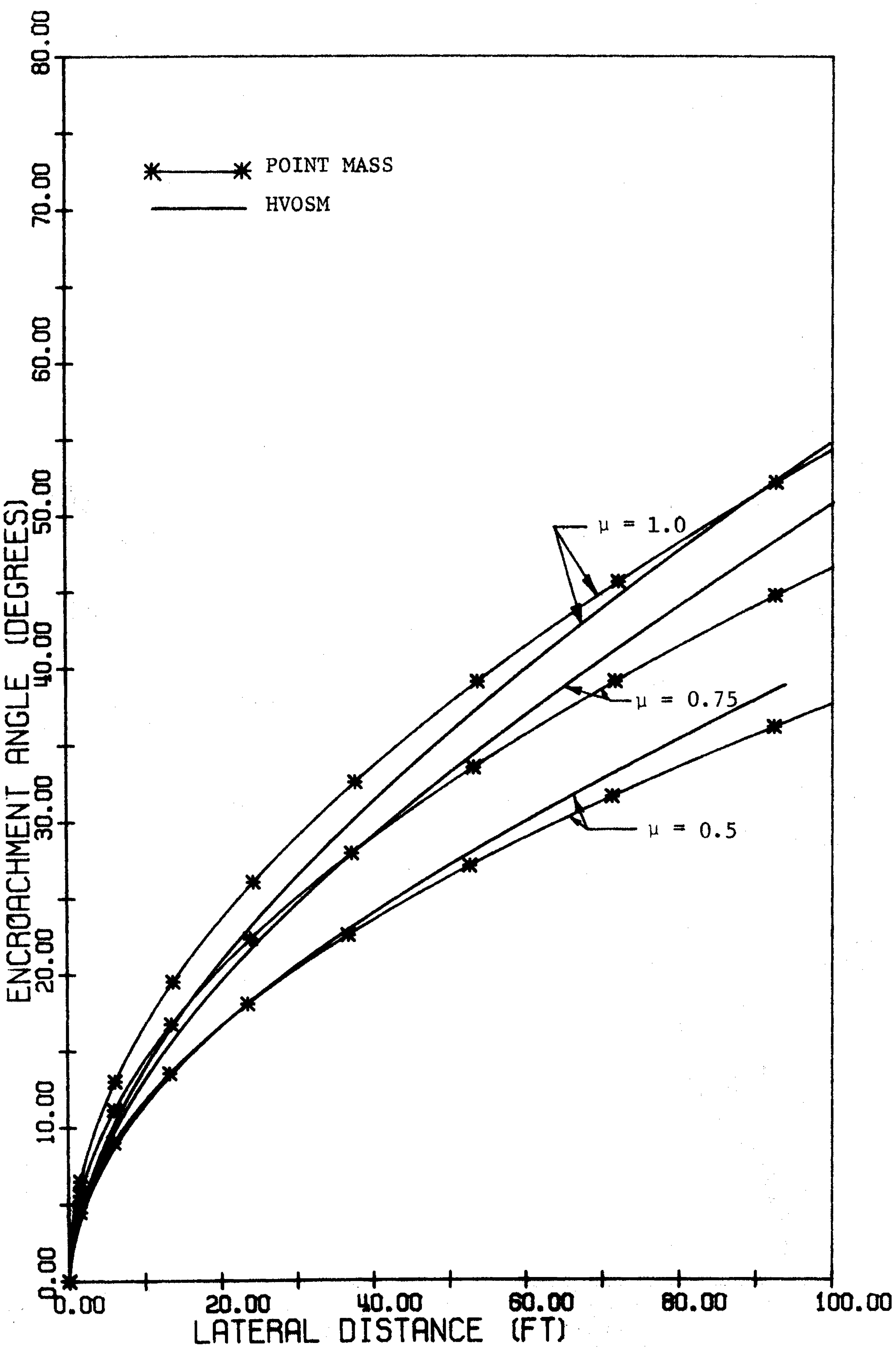

FIGURE D8. ENCROACHMENT ANGLES, STEER ANGLE = 4 DEGREES

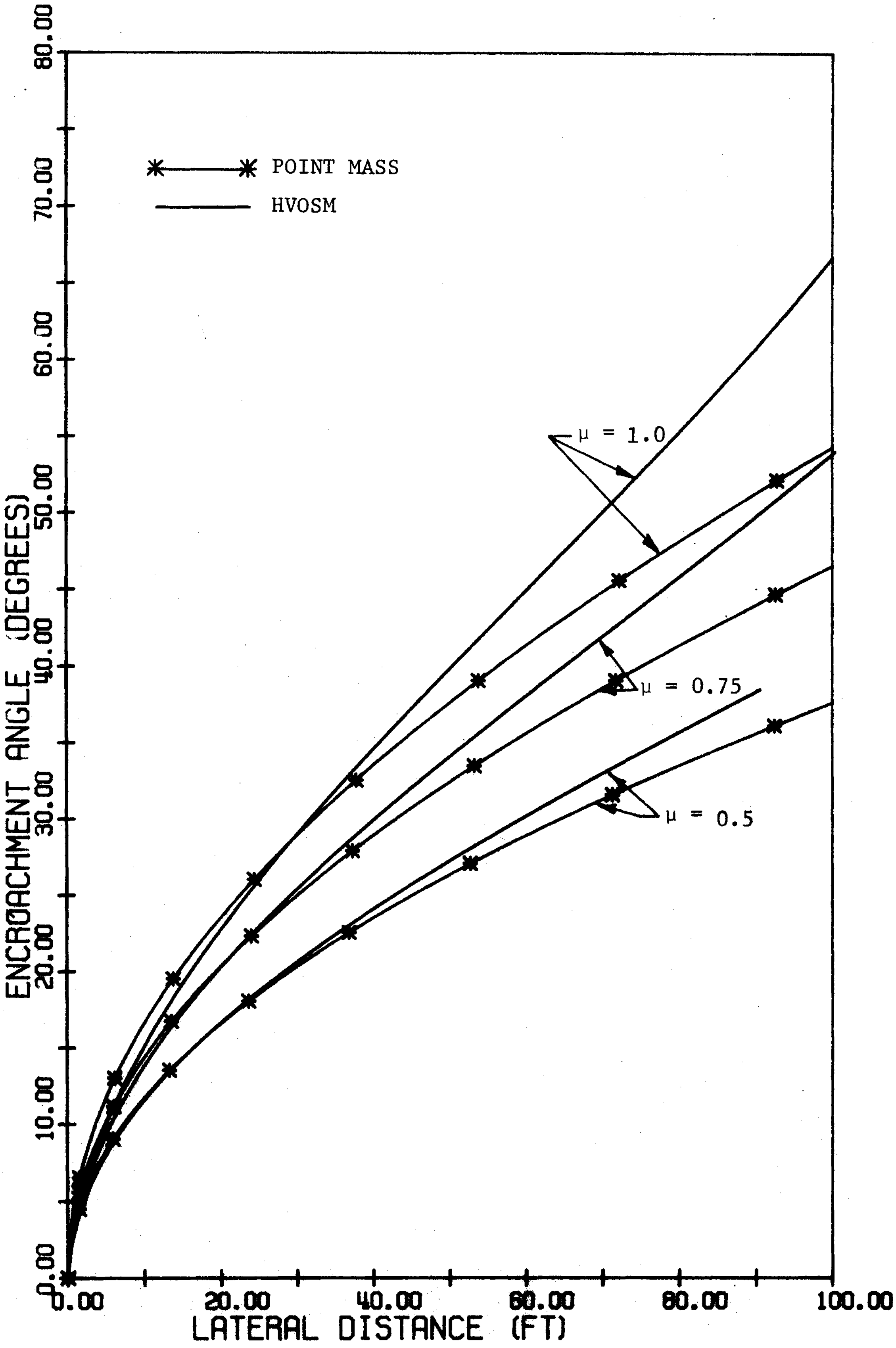

FIGURE D9. ENCROACHMENT ANGLES, STEER ANGLE = 8 DEGREES

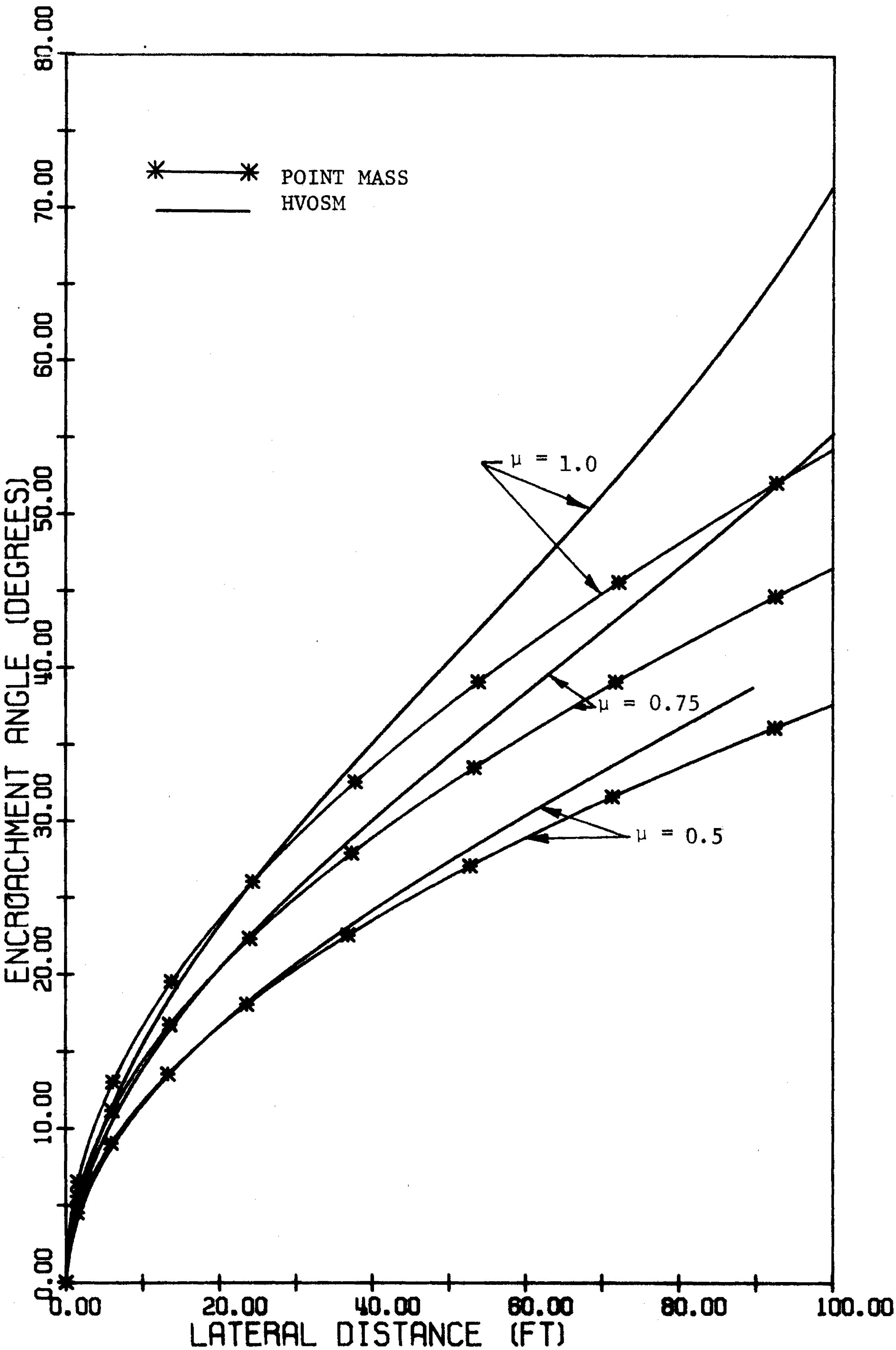

FIGURE D10. ENCROACHMENT ANGLES, STEER ANGLE = 12 DEGREES